Biomimetic matrices for pelvic floor repair

Vashaghian, M.

Publication date
2017
Document Version
Final published version
License
Other

Biomimetic Matrices for Pelvic Floor Repair

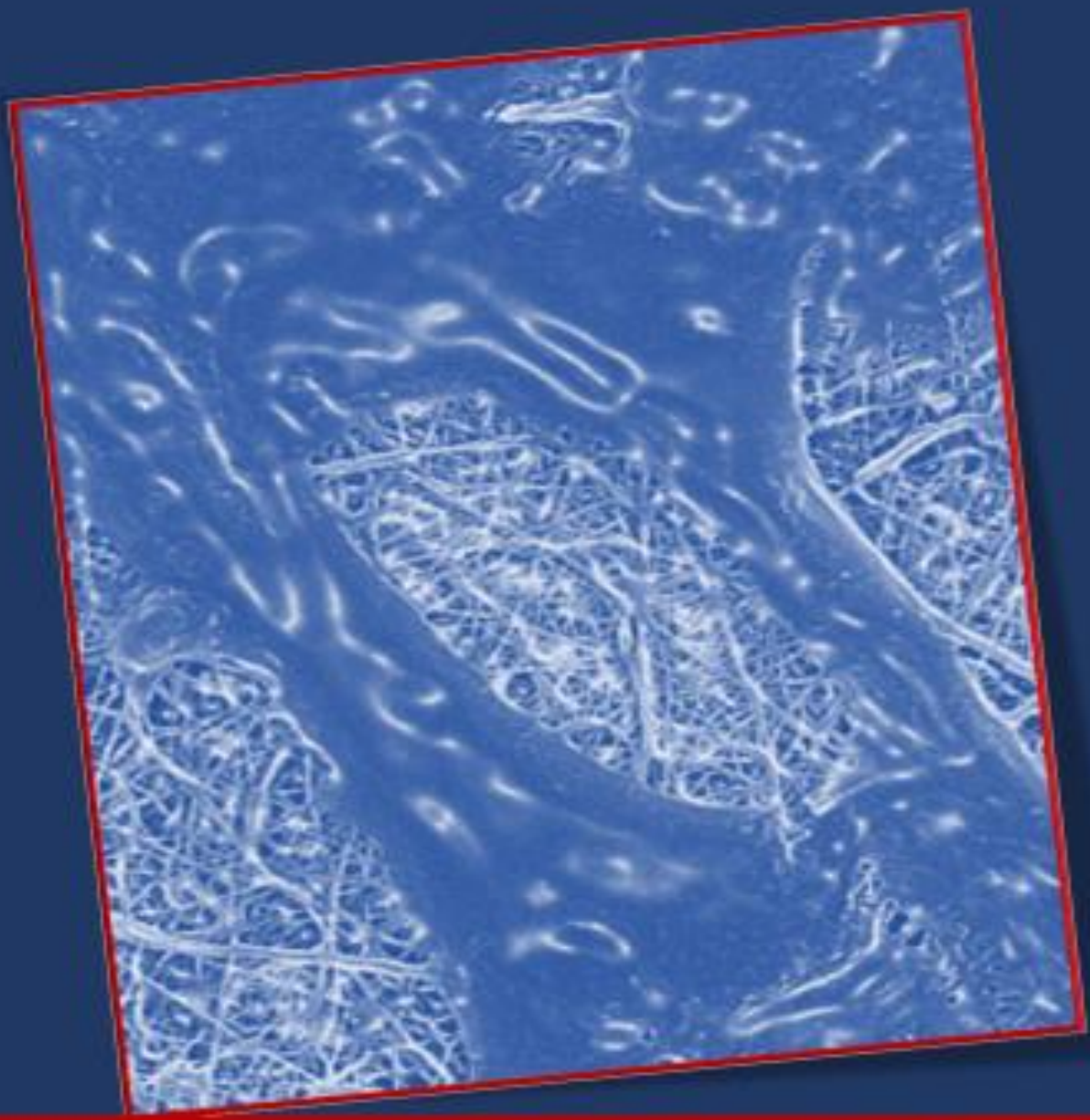

Mahshid Vashaghian

Biomimetic Matrices for Pelvic Floor Repair

Mahshid Vashaghian

Biomimetic matrices for pelvic floor repair

Financial support for printing this thesis was kindly provided by AMR-Academic Medical Center of Amsterdam, Amsterdam, the Netherlands

Cover design & lay-out: Mahshid Vashaghian

Printed by: GVO drukkers & vormgevers B.V.

ISBN: 978-94-6332-162-4

Biomimetic Matrices for Pelvic Floor Repair

ACADEMISCH PROEFSCHRIFT

ter verkrijging van de graad van doctor

aan de Universiteit van Amsterdam

op gezag van de Rector Magnificus

prof. dr. ir. K.I.J. Maex

ten overstaan van een door het College voor Promoties ingestelde commissie,

in het openbaar te verdedigen in de Agnietenkapel

op woensdag 31 mei 2017, te 10.00 uur

door Mahshid Vashaghian

geboren te Teheran, Iran

PROMOTIECOMMISSIE

Promotores:

Prof. dr. ir. T.H. Smit,	Vrije Universiteit Amsterdam
Prof. dr. J.P. W. Roovers,	AMC-Universiteit van Amsterdam

Overige leden:

Prof. dr. J. A. M. Deprest,	Katholieke Universiteit van Leuven
Prof. dr. C.V.C. Bouten,	Technische Universiteit van Eindhoven
Prof. dr. C.H. Van der Vaart,	Universiteit van Utrecht
Prof. dr. M.A. Boermeester,	AMC-Universiteit van Amsterdam
Prof. dr. A.A.B. Bergen,	AMC-Universiteit van Amsterdam
Dr. C. Ris-Stalpers,	AMC-Universiteit van Amsterdam

Faculteit: der Geneeskunde

The future belongs to those who believe in the beauty of their dreams!

Anne Eleanor Roosevelt

To my parents... Farideh & Morteza

Table of contents:

Chapter I

General Introduction and Thesis Overview

1. Pelvic floor health issues

Pelvic floor consists of ligaments and fascia-like tissues that provide mechanical support to the pelvic organs and withstand the Intra-Abdominal Pressure (IAP). Thus, mechanical properties like stiffness and strength are vital for their well-being and functioning. Overstretching results in tissue damage and the development of pelvic floor conditions like pelvic organ prolapse (POP) and stress urinary incontinence (SUI)[1]. Such disorders affect more than 50% of women worldwide. The life time risk to undergo a reconstructive surgery for POP is 11%.[2,3] POP (fig.I.1) is defined as "the descent of one or more of the anterior vaginal wall, posterior vaginal wall, the uterus (cervix), or the apex of the vagina (vaginal vault or cuff scar after hysterectomy)".[4] SUI (fig.I.2) is defined as the "involuntary leakage of urine on exertion, sneezing or coughing".[5] In the USA alone, about 135,000 women have surgery for incontinence, and 200,000 for prolapse each year [6,7]. In the Netherlands, one out of ten women is predicted to undergo a reconstructive pelvic surgery in their life time.[8] The pathogenesis of both, SUI and POP, is due to the damage of the muscular and connective tissues of the pelvic floor and are both thought to be multifactorially affected by ageing, obesity, pregnancy, and childbirth, as well as genetic factors and menopause.[9]

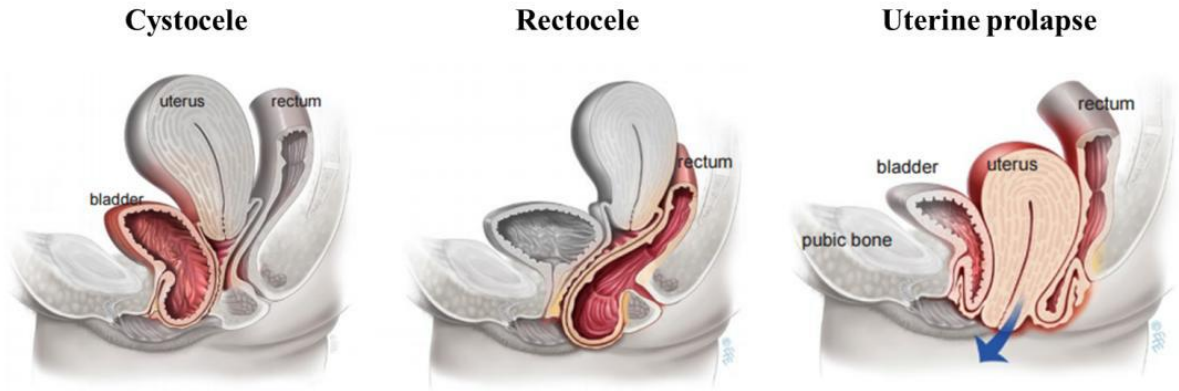

Figure I.1 Types of pelvic organ prolapse (POP) from left to right: prolapse of bladder (cystocele), rectum (rectocele) and uterus. Source: International urogynecology association (IUGA).

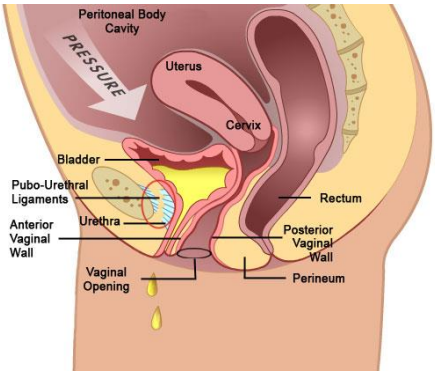

Figure I.2 Stress urinary incontinence (SUI). Due to weakness of the ligaments, an unwanted leakage of urine occurs under pressure. Source: International urogynecology association (IUGA).

Women with pelvic floor dysfunctions are often operated through a reconstructive surgery in which a native tissue or an implant is placed. The aim of vaginal mesh surgery is to provide an additional mechanical support for the pelvic organs, and to induce a host response that results in formation of new matrix (e.g. collagen and elastin), hence holding up the visceral organs of the pelvic cavity. The first attempts are often made with a native tissue harvested from the patient herself ("autograft", e.g. rectus fascia or dermis), or from another species ("xenograft", e.g. porcine/bovine dermis, or small intestine mucosa). These grafts may lose their integrity after several weeks-months, because they lack the mechanical strength required for load-bearing areas such as pelvic floor.[10,11] A synthetic implant can be used to reinforce the pelvic floor if the native tissue fails. Synthetic implants are often knitted polypropylene meshes,[12] with different knitting textures and styles;[13,14] these are stronger and so more suitable for longer-term use because they better maintain their mechanical properties. The meshes proved satisfactory in many patients, but have caused severe complications in some others, from which about 30% need a revision surgery within 3-4 years [15]. Chronic inflammation and pain, vaginal erosion (exposure) (15.6-24%),[16] dyspareunia[17] (9%) (difficult or painful sexual intercourse) and bleeding are the most frequent problems associated with the use of transvaginal knitted meshes in about 17% of the patients within 10-years[18,19]. Due to the repeatedly reported complications, the US Food and Drug Administration (FDA) released a safety warning in 2011 associated with the use of meshes.[20–23] Currently, there is no standard surgical approach to improve the outcome of surgery or for treatment of recurrences. The high number of patients and complications with the current surgical meshes draws our attention to a serious unmet demand for the development of new solutions.

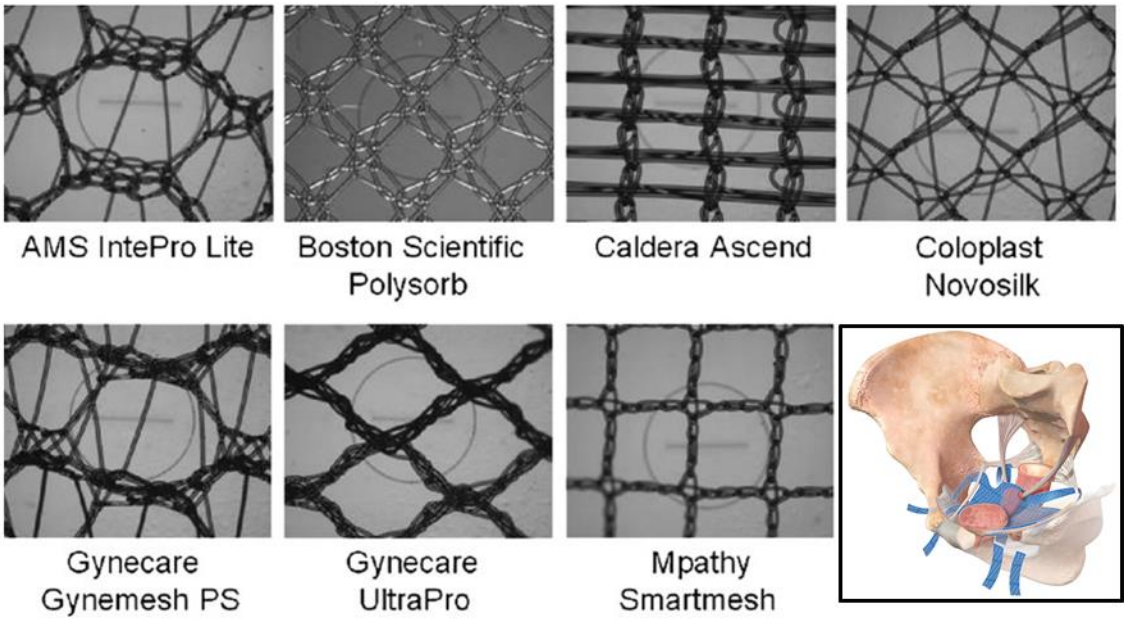

Figure I.3 Different knitting patterns of common vaginal meshes and (bottom right) a lateral cross section of a trans-vaginally implanted polypropylene knitted mesh in Cystocele repair [24,25].

The idea of using a polypropylene mesh for prolapse surgery was first derived from hernia meshes for the abdominal wall (where they also create complications[26,27]). The function of the implants as a scaffold for wound repair are comparable, but the anatomy of the pelvic floor and the wound healing process are different[28,29]. Thus, biomaterials and findings of the abdominal wall reconstruction models may not be simply extrapolated to the outcomes of vaginal surgery. Therefore, understanding and evaluating the cause of complications in the vaginal meshes are required to prevent complications in the next generation of the implants.

2. Poor interactions at cell-implant interface can cause clinical complications

An ideal biomaterial for repair of the weakened tissues of the pelvic floor should be like a hammock: mechanically strong, relatively stiff under tension, and flexible under bending with good pliability. As an implant, it also should be biocompatible, able to induce host a response (bioactive rather than bio-inert) and provide a proper environment for tissue cells to interact with each other. Characteristics of such an implant are determined by its chemical composition (material type) and its microstructure; both characteristics should be carefully designed to bring good clinical outcomes.

Microstructure is predominantly dictated by the fabrication method. Among the available techniques for fabricating pelvic floor meshes, knitting is the most common one. Polypropylene knitted meshes are non-degradable, inert, nontoxic, antigenic and macro-porous, according to Amid's classifications[30]. There are different knitted polypropylene meshes with different microstructures available (fig.I.3) [31]. The importance of the microstructure becomes more relevant as it plays a significant role in the pathology of mesh-related complications[32–34]. Amid classification identifies the two most determinant parameters in the mesh microstructure: porosity (which is relevant to weight as well) and filaments type [30] . Each of these microstructural factors affects the host tissue response and the remodeling process upon receiving a foreign material, and eventually the clinical outcome.

Porosity, weight and filaments type are all factors of the mesh knitting style [35]. Porosity should be large enough (> 75 µm) for proper integration of the mesh, otherwise the mesh is encapsulated and therefore painful and non-functional[36]. Also, porosity and pore shape are important for mesh pliability that is required for good handling at surgery [35,37,38]. Different porosities alter the mesh pliability as well as its integration capacity [31,39,40]. Mesh weight (expressed in g/m^2) depends on material density (g/m^3) and the overall porosity of the structure[41]. The clinical experience is that relatively heavy meshes cause more complications than the lighter ones [42–46], thus thinner meshes should be beneficial if they are mechanically strong enough. Meshes currently on the market are knitted into mono- or multi- filaments. In line with the findings on mesh weight, multifilament meshes seem to cause more complications (inflammatory response and infection)[47,48], because they may induce more foreign body reactions and prevent proper integration [36,44]. In conclusion, a mesh should preferably be highly porous, light-weight and monofilament. According to literature, current meshes have large porosities for integration and many of them are light-to-medium weight and monofilament. Still, the nature of interaction between cells and the mesh structure is suboptimal because implantation of the mesh sometimes leads to encapsulation and fibrosis instead of functional integration.

Meshes for vaginal prolapse surgery are generally stiffer than the soft tissues they support, partly because of their material and partly because of the knitting microstructure [31,49,50]. When a stiff mesh slides along the soft tissue upon loading, shear stresses are created at the tissue-implant interface, particularly at the hinge-like areas where the filaments are knitted into each other. These

interfacial stresses, cause problems in different ways. First, the remodeling capacity of the local fibroblasts declines [34,51]. Cells respond to mechanical stimuli by producing catabolic and inflammatory markers which degrade the matrix, leading to exposure of the mesh through the vaginal tissue [52,53]. Second, because of large interfacial shear stress, fibroblasts may differentiate into myofibroblasts [54]. These are intermediate mechano-responsive cells in the wound healing process responsible for closing of the wound by contraction [55–57]. Myofibroblasts produce excessive matrix (mainly collagen) under mechanical loading [56,57]. This newly-made matrix accumulates and develops into a stiff, fibrotic scar tissue which may show severe contractions.

Thus, pelvic floor meshes are more than just inert mechanical supports: they evoke a host reaction which is regulated by surface texture and mechanical forces. Clinical experience shows that the polypropylene knitted mesh is suboptimal. One way to improve the existing mesh-based treatments is to introduce a different level of microstructure with cell-scale fibers that cells can better adhere and respond to. Such microstructure, which may be a beneficial alternative to regulate cell-biomaterial interactions, can be created by electrospinning. Electrospinning is a technique to produce a different class of implants with nano-to-micro fibers and versatile variety of parameters.

3. Electrospun biomimetic matrices: alternative biomaterials for pelvic floor repair

3.1. Technique

Electrospinning (fig.I.4) is a method for fabrication of ultrathin polymeric fibers using an electrical potential. A high voltage is applied to a grounded (zero-potential) collector on one side and the negatively-charge nozzle of a polymer container on the other side. This creates an electric potential between the collector and the nozzle. By ejecting the polymer solution from the nozzle, a polymer jet is drawn towards the collector that ends up in forming fibers the further it gets from the nozzle. Continuous deposition of fibers on the collector, results in fabrication of a nanofibrous nonwoven matrix on the collector.

Although the main process of electrospinning is simple, there are different variables to be considered and it is a challenge to control all of them in a reproducible way. On the other hand, having these variables to play with allows controlling the microstructural properties of the end-products. Relevant technical parameters include polymer concentration, applied voltage, flow rate, solution properties, and ambient conditions like temperature and humidity. These parameters affect

microstructure by fiber size and morphology, or the overall porosity through which the properties of the products are determined. Table I.1 provides an overview of how each parameter impacts the product microstructure.

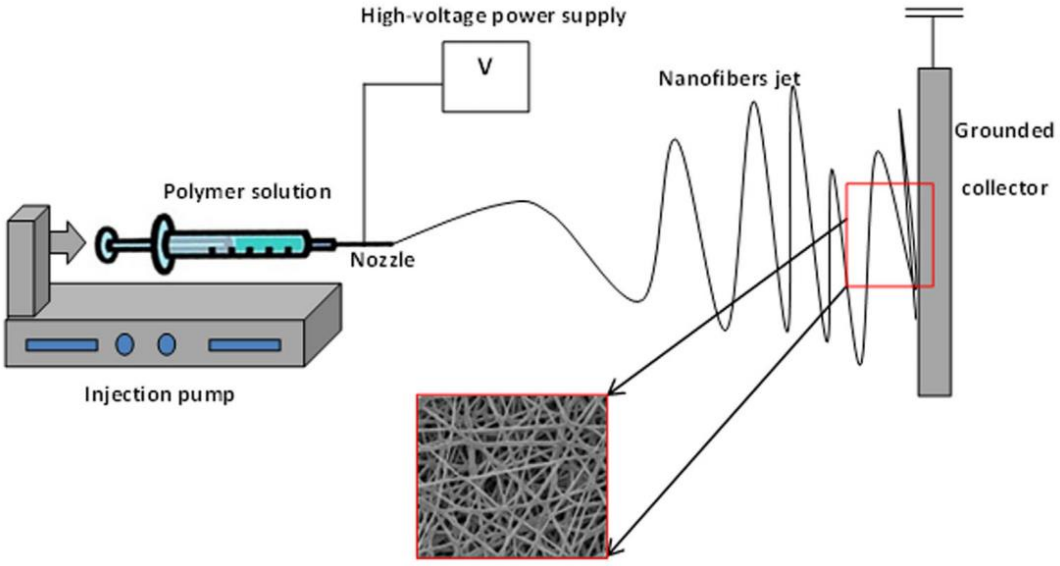

Figure I.4 Schematic of the electrospinning set-up used in this thesis. A polymer solution is injected from the nozzle toward a grounded collector once a high voltage is applied to the nozzle. This creates an ultrathin fiber jet which deposits on the collector in form of a randomly oriented non-woven mesh.

Table I.1 Effect of different parameters on electrospun fibers.

Parameter (increased)	**Effect on fibre size**	**Effect on porosity**	**Outcome**	**Ref.**
Polymer concentration	Increased	Not directly affected	Increased cellular activity, increased strength	[58,59]
Applied voltage	Decreased	Not directly affected		[60,61]
Distance to collector	Decreased	Not directly affected	Tensile property, Increased cell proliferation	[62]
Flow rate	Increased	Not directly affected		[61]
Temperature	Increased	Less porosity	Less infiltration, Higher tensile strength and strain,	[63,64]
Humidity	Increased	Less porosity		[65]

3.2. Electrospun fibers

Electrospun fibers can be produced in the same scale of cells and natural ECM proteins. For example, collagen fibrils are around 300-375 nm while electrospun fibers can be typically around 10 nm to 10 μm. Electrospun architecture, can improve cell-biomaterial interactions and therefore their mechano-biology in different ways. First, cell-biomaterial integrin-mediated bindings are increased in the electrospun microstructure (fig.I.5), owing to the high surface area-to-volume ratio provided by thin fibers. This leads to enhanced adhesion of cells to the biomaterial. Apart from fibers size, high porosity (>80%), pore geometry and interconnectivity of the electrospun matrices are favorable for cell nutrition and signaling. Furthermore, electrospun matrices show reduced inflammatory response as compared to conventional biomaterials [66,67]. As a result of improved cell-biomaterial interaction, cells show better proliferation and enhanced matrix deposition, contributing to new tissue generation. [68]

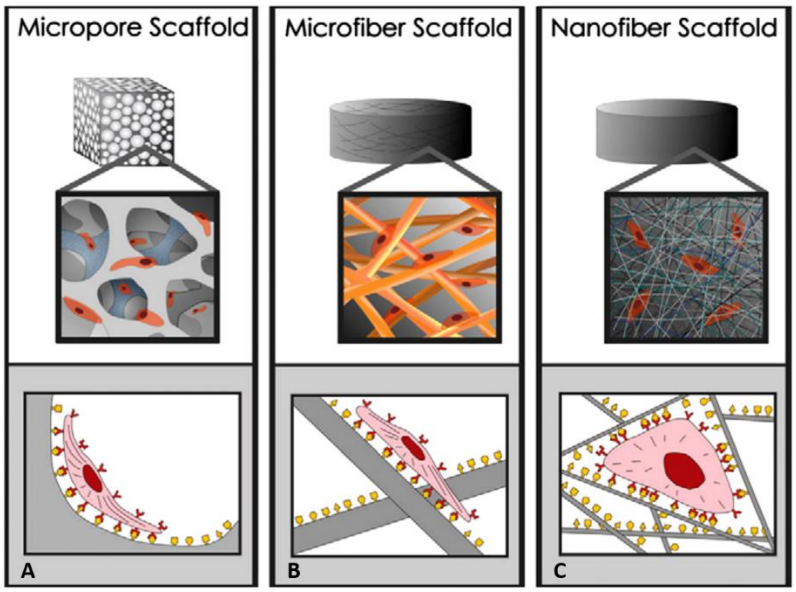

Figure I.5 Scaffold architecture affects cell binding and spreading. (A and B) Cells binding to scaffolds with microscale architectures flatten and spread as if cultured on flat surfaces. (C) Scaffolds with nanoscale architectures have larger surface areas to adsorb proteins, presenting many more binding sites to cell membrane receptors. The adsorbed proteins may also change conformation, exposing additional cryptic binding sites [66].

A large number of polymers, degradable or non-degradable, biological or synthetic, can be processed by electrospinning. From a material point of view, biological biomaterials are beneficial over synthetic, because their chemical composition is similar to that of found in our tissue matrix and thus facilitates the adhesion of cells and their capacity for protein synthesis. However, there are some deficiencies with biological materials including the risk of disease transmission, deterioration and loss of mechanical integrity before the new tissue matures. Synthetics, on the other hand, (degradable or non-degradable) have better defined properties, mechanical strength and integrity over longer-term. Degradable synthetic polymers have molecular bindings which are susceptible to (enzymatic) hydrolysis and thus are decomposed in the aqueous environment of the body. The most common family of this group are polyesters such as polylactide (PLA), polyglycolyide (PGA), co-polymers of these (e.g. PLGA) and polycaprolactone (PCL). These degrade by hydrolysis and are absorbed through the metabolic activity of the body as the de-composed acids are carried away through urine or blood. It is important that the degradation rate of the biomaterial is low enough to allows it to remain intact and stable until the new tissue regenerates. Due to the challenge of fine-tuning the degradation profile, non-degradable synthetic polymers are often preferred. This is particularly interesting for patients whose regenerative

capacity is lower due to aging, menopause, or genetic diseases in their connective tissues. In general, the use of strong, ductile and light (low molecular density) martials is recommended.

Electrospinning is a versatile technique. It is easy, in-expensive, possible to scale-up for mass production of textile medical devices. Changing the spinning parameters change the microstructure and therefore the properties of the biomaterial, so one can play with these parameters to design an appropriate implant.

4. Towards a new generation of implants

Electrospun biomaterials have a surface that is more gentle to cells in comparison with the knitted meshes, because thin fibers generally have a more homogenous structure and relevantly small surface roughness; this is suitable for cells anchorage but not too rough in surface to harm them. However, an optimal design needs to be found yet. If we want to have a proper implant for repair of a particular tissue, we need to tackle cell-(tissue)-implant responses which are specific to the anatomy, condition and disease status of that target tissue. This led us to our goals in this thesis; i) to identify the of microstructural characteristics of electrospun biomaterials, ii) to study biologic responses of the relevant cells for a close mimic of the biological -damaged- environment, iii) to evaluate the behavior of cell-biomaterial under mechanical loading conditions with regard to the mechano-biological role of the implant.

5. Aims and outlie of this thesis

In order to find an alternative scaffold for pelvic floor repair, the goal of this thesis is: to investigate some of the functional characteristics of electrospun biomaterials and their potential for regeneration of pelvic floor soft tissues.

Following this aim, we defined several questions which we addressed in chapters 2-5 of this thesis:

1- How are different electrospun biomaterials characterized for structural and mechanical properties? (what characteristics are relevant?) (**chapter 2**) ow do unhealthy cells (those affected by disease) respond to electrospun fibers? (**chapter 2**)
2- What are the effects of fiber size on the mechanical properties and cellular response on an electrospun biomaterial? (**chapter 3)**
3- How would unhealthy cells react to fibers under cyclic mechanical loading? (**chapter 4**)

4- What is in the literature: applications of biomimetic nanofibrous matrices for pelvic floor (**chapter 5**).

In **chapter6**, we provide a general discussion of all the information obtained through chapter 2-5.

Chapter II

Toward a New Generation of Pelvic Floor Implants With Electrospun Nanofibrous Matrices: A Feasibility Study

Mahshid Vashaghian, Alejandra M. Ruiz-Zapata, Manon H. Kerkhof, Behrouz Zandieh-Doulabi, Arie Werner, Jan Paul Roovers, and Theo H. Smit

Neurourology and Urodynamics 2016; 34(3): 224-230.

Abstract:

Objective: The use of knitted, polypropylene meshes for the surgical treatment of pelvic organ prolapse (POP) is frequently accompanied by severe complications. Looking for alternatives, we studied the potential of three different electrospun matrices in supporting the adhesion, proliferation and matrix deposition of POP and non-POP fibroblasts, the most important cells to produce extracellular matrix (ECM), *in-vitro*. ***Study design:*** We electrospun three commonly used medical materials: nylon; poly (lactide-*co*-glycolide) blended with poly-caprolactone (PLGA/PCL); and poly-caprolactone blended with gelatin (PCL/Gelatin). The matrices were characterized for their microstructure, hydrophilicity and mechanical properties. We seeded POP and non-POP fibroblasts from patients with pelvic organ prolapse and we determined cellular responses and ECM deposition. ***Results***: All matrices had >65% porosity, homogenous microstructures and close to sufficient tensile strength for pelvic floor repair: 15.4 ±3.3 MPa for Nylon; 12.4 ±1.6 MPa for PLGA/PCL; and 3.5 ±0.9 MPa for PCL/Gelatin. Both the POP and non-POP cells adhered to the electrospun matrices; they proliferated well and produced ample extracellular matrix. Overall, the best *in-vitro* performance appeared to be on nylon, presumably because this was the most hydrophilic material with the thinnest fibers. ***Conclusion*** Electrospun nanofibrous matrices show feasible mechanical strength and great biocompatibility for POP and non-POP fibroblasts to produce their ECM *in-vitro* and thus may be candidates for a new generation of implants for pelvic floor repair. Further studies on electrospun nanofibrous matrices should focus on mechanical and immunological conditions that would be presented *in-vivo*.

Introduction:

Pelvic organ prolapse (POP) is a serious health problem affecting almost half of the women over 50 worldwide[69]. Vaginal prolapse surgery aims to restore pelvic-floor function by providing a mechanical support. Randomized controlled trials have shown that both objective and subjective cure are improved if vaginal surgery is performed with the use of an implant. However, about 3 to 4% of patients need to undergo a re-operation because of adverse events that are specific for such implant. These so-called mesh-specific complications involve vaginal exposure, erosion and chronic pain due to scarring of the vagina[70,71,22]. Apparently, in some women the knitted meshes result in chronic inflammatory response and contractile scar formation. One suggested explanation is that the texture of knitted implants create shear stresses upon mechanical loading and affects cell behavior at implant-tissue interface, resulting in fibrous tissue formation[19,24,32,34,72]. With an increasing number of women suffering from POP, there is an urgent need for a new solution.

An alternative could be provided by electrospinning; a technology that uses an electric potential to create ultrathin fibers from a polymer solution [73]. Nanofibrous electrospun matrices are porous with highly interconnected pores which mimic the geometrical structure of the natural extracellular matrix (ECM). This structure has shown to favor cell attachment and growth[66], and reduce the inflammatory response compared with conventional biomaterials [67]. Given the cell-cell binding and cell-matrix attachments onto the fibers through which cell functions are regulated, besides their lightweight characteristics, electrospun matrices may provide a good interaction with host cells [74] and reduce shear stresses at the implant-tissue interface *in-vivo*.

Fibroblasts are the cells responsible for production, remodeling and maintenance of the ECM. In POP condition the remodeling capacity of vaginal fibroblasts changes [75,76], which might have an impact on the mesh-based treatments and should be taken into account. Therefore, as an initial step

towards a new generation of pelvic implants, we found it worthwhile to explore how both POP and non-POP cells function in response to electrospun nanofibrous matrices *in-vitro*. Thus, in the present study we investigated the mechanical and biological potential of three different electrospun matrices. Nylon (polyamide 6) is a well-known non-degradable material used in urinary tapes and heart valves[77,78]and can be useful for older POP-patients with less regenerative capacity, who may require a permanent support. To avoid complications on the long term, degradable poly(glycolide-co-lactide acid) blended with poly-caprolactone (PLGA/PCL) was investigated. Both polymers are FDA-approved with an old history of biomedical applications[79] and were blended to improve strength and hydrophilicity[80]. A blend of polycaprolactone and gelatin was chosen as a degradable semi-synthetic material. Gelatin is a natural polymer that increases cell attachment, while PCL provides the mechanical strength[81]. Nanofibrous matrices of each material were characterized for microstructure, hydrophilicity and mechanical properties. Human vaginal fibroblasts from POP and non-POP (as healthy control) sites of POP patients were seeded on the matrices and cell viability, adhesion, proliferation and matrix production were assessed.

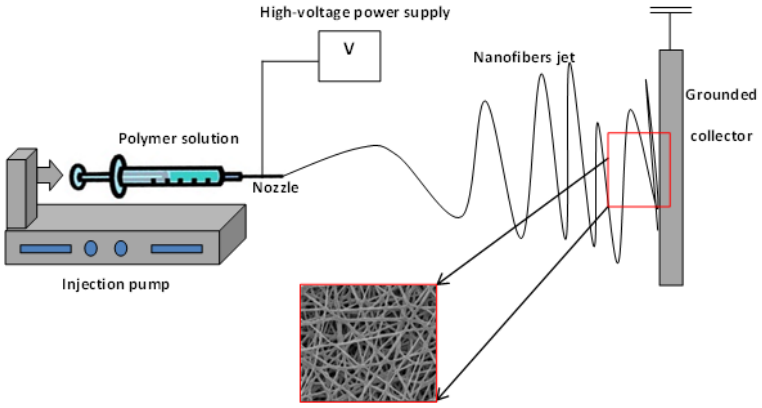

Figure II.1 Schematic of electrospinning set-up

Materials and Methods

2.1. Materials

Nylon-6 (10 kD pellets), Gelatin type-A (bovine skin), formic-acid, tetra-fluoro-ethylene (TFE), chloroform (CHCL3), methanol (MeOH), ethanol (EtOH) were purchased from Sigma, Netherlands. Fetal bovine serum (FBS), streptomycin, penicillin, amphotericin-B, vitamin C were purchased from Sigma, USA. Cell culture medium Dulbecco's-modified-Eagle's-medium-DMEM was purchased from Gibco-Life technologies, UK. Poly-caprolactone (PCL), 124 kD, and poly(lactic-co-glycolic acid) (PLGA), 95 kD, were purchased from Purac, Netherlands. Teflon tubes were bought from Instrulab, Netherlands. Blunt-end needles and 2-3 ml syringes were provided by VWR, Netherlands. Live/dead staining kit and CyQuant cell proliferation assay were purchased from Molecular Probes Inc. Invitrogen USA. SynergyTMHT multi-mode microplate reader was bought from Biotek Instruments Inc. Vermont USA.

2.2. Preparation of electrospun matrices

Polymer solutions were prepared of Nylon 20% (w/v) in Formic Acid; PLGA/PCL (75/25) 15% (w/v) in CHCl3/MeOH (3/1); and PCL/Gelatin (70/30) 15% (w/v) in TFE. An electrospinning device (IME Technologies, Netherlands) was used for fabrication of matrices (fig.II.1). A grounded collector was placed horizontally at a distance of 15 cm from the needle. With a syringe pump (Harvard apparatus, PHD 2000, USA) 0.8 ml of each polymer solution was extruded at flow rates between 0.5-1 ml/h, under an applied voltage of 20 kV. Fibers were collected on aluminum foil at room temperature and humidity. Circular samples with 5 cm diameter were separated from the foil and vacuumed overnight to remove residual solvent. Samples were disinfected with two changes of 70% ethanol, and overnight incubation in 1% antimicrobial culture medium at 37°C.

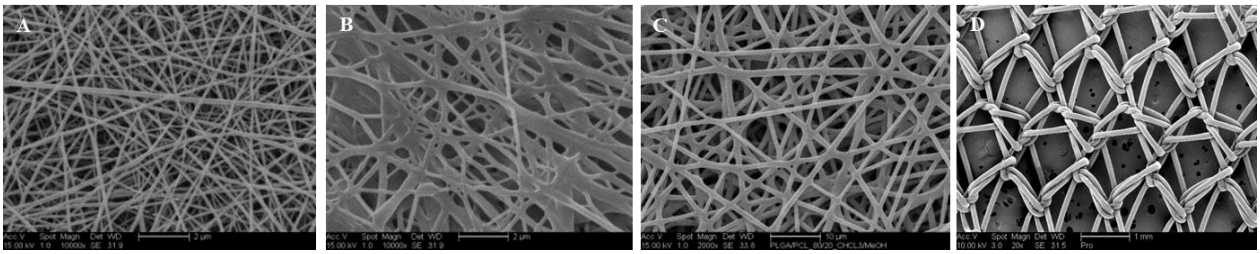

Figure II.2. Representative SEM pictures of the electrospun matrices showing microstructure morphology of A) Nylon, B) PCL/Gelatin and C) PLGA/PCL, in comparison with D) conventional knitted polypropylene mesh. Scale bar is 2 µm (A and B), 10 µm (C) and 1 mm (D).

Table II.1. Microstructural Characteristics of the Electrospun Matrices Sample

Sample (1 cm²)	**Filament structure**	**Water contact angle (°)**	**Thickness (µm)**	**Porosity (%)**	**Pore area (µm²)**	**Fibers diameter (nm)**	**Weight (gr/m²)**
Nylon	Mono	40 ±10*	50 ±4.5*	69 ±4	1.3 ±0.1*	117 ±7.81*	35 ±6
PCL/Gelatin	Mono	70 ±7.5	80 ±6	78 ±10	1.9 ±0.8*	204 ±37.5	44 ±3.7
PLGA/PCL	Mono	130 ±2.3	136 ±27	81 ±6	8.8± 0.6	994 ±115	55 ±3.2

*Data are presented as mean ±standard deviation (*P<0.05, analyzed with one-way ANOVA, comparisons were made between the three matrices, n=3)*

2.3. Matrices characterizations

2.3.1. Microstructure

The morphology of the matrices was visualized using a Scanning Electron Microcopy (SEM; Philips, XL20, Fei, Netherlands). Samples of 1 cm^2 were sputter-coated with gold and visualized under a high vacuum and 15 kV. Fiber diameter, pore area and distribution were calculated using pictures of five random spots per sample. About 50 measurements were made per picture using ImageJ 1.44p software (NIH, USA). The thickness of matrices was measured on cross-sectional SEM images at three different areas. The dry-weight of electrospun matrices were also obtained (n=3).

2.3.2. Porosity

Porosity here refers to the amount of void space between the fibers, that is: the sample volume not occupied by the material. The volume (V_s) of each sample (n=3) was obtained by measuring its apparent dimensions. Samples were dry-weighed (W_d) and soaked in 100% ethanol for 45 min under low pressure[82] . Samples were removed from ethanol and immediately weighed (W_w). The weight of entrapped ethanol (W_{Eth}) was the difference. Knowing the density of ethanol (ρ_{Eth}), the volume of entrapped ethanol is $V_{Eth} = \rho_{Eth}/W_{Eth}$. Then porosity is calculated as $P = V_{eth}/V_s * 100\%$.

2.3.3. Contact angle

The contact angle between a deionized water drop and the material surface was used as an indication of matrices hydrophilicity (n=3). 10 µl of deionized water was dropped on each sample and pictures were taken after 20s, with a high-resolution camera (SONY, NEX 5N, 55mm micro-Nikkor, Japan). The contact angle was measured using the automated "drop analysis" plugin from ImageJ software (NIH).

2.3.4. Mechanical properties

Mechanical properties of the samples were evaluated with uniaxial tensile and indentation tests according to ASTM standards (F2150). Tensile tests (n=4) were performed with a universal Instron device (Netherlands) [80]. Bone-shaped samples of 60x20 mm were tightly clamped between two vertical sand-paper-glued clips to create maximum friction, leaving a length of 40 mm between the clamps. Samples were preloaded at a rate of 0.2 mm/min to ensure that the matrices start from the same reference point, and then stretched at the rate of 1 mm/min until rupture. Stress-strain curves were generated from which the mechanical properties were derived (tableII.2). The ultimate tensile strength of the material is the rupture force divided by the original cross-sectional area.

The micro-stiffness of the samples was measured using a micro-indenter with a spherical probe of 80 µm radius [83–85](Piuma, Optics11, Netherlands). Matrices were wetted with basic culture medium for one hour prior to the test. A total of 36 indentations were performed per sample with an average distance of 500 µm between the indentation points. Indentation speed and depth were 8.5µm/s and 17 µm, respectively.

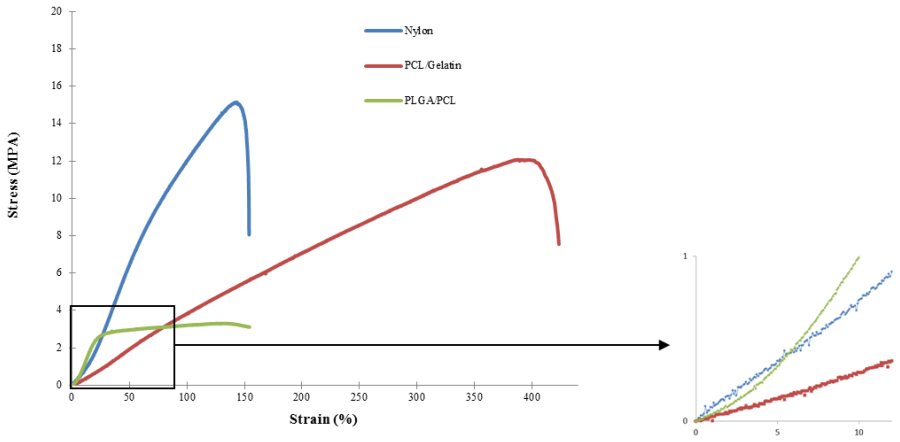

Figure II.3. Representative stress-strain curve of three electrospun matrices: Nylon (blue), PCL/Gelatin (red) and PLGA/PCL (green), determined by uniaxial tensile test (n=4). The insert is the toe region of the curve at higher magnification.

2.4. Assessment of cellular responses

2.4.1 Tissue collection and cell isolation

Approval for tissue collection and patient informed consent was obtained from the medical ethical committees of VU University Medical Centre (Amsterdam) and Kennemer Gasthuis Hospital (Haarlem). Full-thickness 1 cm^2 anterior vaginal wall biopsies were taken from two patients undergoing reconstructive surgery of the anterior vaginal compartment. Both patients, one pre- (POP-pre) and one post-menopausal woman (POP-post), had cystocele (POP-Q ≥ 2). A woman

operated for benign gynecological reasons was selected as a healthy control (non-POP), and for ethical reasons, a full-thickness biopsy was taken from the anterior pre-cervical region. Within 24h, cells were isolated and cultured as described previously [86]. Prior to the experiments, cells were grown until passage 3 or 6 in an incubator at 37°C, 95% humidity and 5% CO_2, with culture medium: DMEM supplemented with 10% FBS, 100µg/ml streptomycin, 100U/ml penicillin, and 250µg/ml amphotericin-B. The authors are aware that cells from different locations might have slightly different behavior. However, due to limited access to vaginal fibroblasts of the very same locations, such differences were neglected here.

2.4.2 Cell viability

Cells were cultured on disinfected electrospun matrices of Nylon, PLGA/PCL and PCL/Gelatin in culture medium, at a density of 150,000 cells/cm^2. After three days, cell viability was assessed by LIVE/DEAD viability/cytotoxicity kit for mammalian cells according to the manufacturer's protocol. Briefly, cells were washed with D-PBS and incubated for 5–10 min at room temperature in a mixture of the probes: calcein AM for esterase activity in living cells (green), and ethidium homodimer-1 which penetrates dead cells (red). Live and dead cells were visualized with an inverted Leica DMIL microscope (Microsystems, Germany).

2.4.3 In-vitro matrix production on electrospun matrices

New matrix produced on the electrospun matrices was evaluated after 3 and 24 days. Fibroblasts from controls, POP-pre and POP-post tissues subjected to a Count and Viability assay using a Muse Cell Analyzer (Merck Millipore, Darmstadt, Germany). Cells were cultured at a density of 150,000 cells/cm^2on the electrospun matrices with 10%-culture medium. After three days, cells

were synchronized for 1hour at 5°C and refreshed with culture media supplemented with 50 µg/ml vitamin C and thereafter every 3-4 days.

2.4.4 Cell morphology on the matrices

Cell morphology was qualitatively evaluated with SEM. Cell-seeded samples at each time point were fixed in 4% formaldehyde (pH 7.2) and underwent serial dehydration with ethanol and then sputter-coated with gold. Different magnification pictures were obtained from random spots on each sample.

2.4.5 Histology

To visualize the cells, samples were fixated in 4% formaldehyde, washed with PBS, dehydrated in ethanol gradient, stained with hematoxylin-eosin (H&E), and washed under running tap water. After drying, they were mounted on glass slides with aqueous mounting medium. To visualize the total collagen deposition, dehydrated samples were transversally stained in picrosirius red at room temperature. After one hour, samples were washed in two changes of acidified water, dried and mounted with aqueous mounting medium onto glass slides. All stained samples were imaged using the bright field of an inverted Leica DMIL microscope with a DFC320 digital camera (Leica Microsystems, Germany) at 20x magnification, and illustrated in black and white to limit data-misinterpretations of the background colors.

2.4.6 Total DNA assay

At each end point samples were washed with PBS, carefully transferred to a new well and 300µl/well of milliQ water was added. Samples were frozen and thawed three times and the total

DNA of duplicate samples was measured with the CyQuant kit and following the supplier's specifications. Fluorescence was measured using SynergyTMHT multi-mode microplate reader.

2.5. Statistical analysis

For all normally-distributed data, the mean ±standard deviation (SD) was reported. One-way analysis of variance (ANOVA) was used to test differences between all the groups. Where a group of effects appeared statistically significant, Bonferroni post- hoc test was used to determine whether the differences were statistically significant (SPSS v20 software, Chicago, IL). All statistical tests were two-sided and differences were considered statistically significant at 5% level ($p<0.05$).

Table II.2. Micro-stiffness of the electrospun matrices obtained by indentation test

Sample (1 cm^2)	**Dry micro-stiffness (MPa)**	**Wet micro-stiffness (MPa)[a]**
Nylon	0.5 ±0.01	0.48 ±0.02
PCL/Gelatin	0.31 ±0.01	0.24 ±0.03
PLGA/PCL	0.36 ± 0	0.17 ±0.02*

*Data are presented as mean ±standard deviation (*P<0.05, analyzed with one-way ANOVA, comparisons were made between the dry and wet condition for each type of material, n¼4). [a] Wet: 1hr immersion in DMEM.*

Table II.3. Mechanical Properties of the Electrospun Matrices Obtained by Uniaxial Tensile Test

Sample

Sample (1 cm^2)	**Force at rupture (N)**	**Toe stress (MPa)**	**Toe strain (%)**	**Toe stiffness (MPa)**	**Yield stress (MPa)**	**Yield strain (%)**	**Linear stiffness (MPa)**	**Ultimate stress (MPa)**	**Ultimate strain (%)**
Nylon	7.7 ±0.4	0.82 ±0.1	11.2* ±0.8	7.32 ±1	8 ±1.1	58.2 ±8.3	13.74 ±0.8	15.4 ±3.3*	100 ±2
PCL/Gelatin	9.7 ±0.6	0.3 ±0.0	9.5 ±1.0	2.9 ±0.5	3.8 ±0.3	100 ±5.3	3.8 ±0.14	12.4 ±1.6	382 ±23.5*
PLGA/PCL	4.3 ±0.6	0.1 ±0.0	2.17 ±0.0	4.8 ±1.5	2.5* ±0.0	18 ±1.5	13.8 ±2	3.5 ±0.9	140 ±14.6

*Data are presented as mean ±standard deviation (*P<0.05, analyzed with one-way ANOVA, comparisons were made between the three matrices, n=4)*

3. Results

3.1 Microstructure and porosity

Table II.1 summarizes the microstructural properties of electrospun matrices. The histograms of fiber and pore distribution are presented in fig.II.1 supplementary files. Fibers were homogenously distributed in each sample and the distribution of pores seems more even in PLGA/PCL and Nylon than in PCL/Gelatin. All the matrices were >65% porous and weighed <30 g/m^2.

3.2 Contact angle

With a contact angle of 40 ±7˚, Nylon was significantly more hydrophilic than PCL/Gelatin (70±7.5˚) and PLGA/PCL (130±2.3˚) (tableII.1).

3.3 Mechanical properties

The mechanical properties of the electrospun matrices are summarized in tableII.2& tableII.3, and a representative stress-strain curve of electrospun matrices is shown in fig.II.3. Nylon had the highest yield and ultimate strength among the three matrices, while PCL/Gel had highest strain at yield and ultimate strength. During the test, it was observed that PLGA/PCL depicted a necking plastic deformation at yield stress of 2 N, while Nylon and PCL/Gel were more brittle with no necking. On indentation, Nylon also had the highest micro-stiffness and one-hour wetting caused a reduction in the micro-stiffness of all specimens (tableII.2).

3.4 Cell viability

POP and non-POP (considered as heathy control) human vaginal fibroblasts showed good survival and attachment to all matrices with no signs of toxicity after 3 days (fig.II.4 and supplementary fig.II.2). Only on one of the PCL/Gelatin matrices (fig.II.4B) some dead cells were observed.

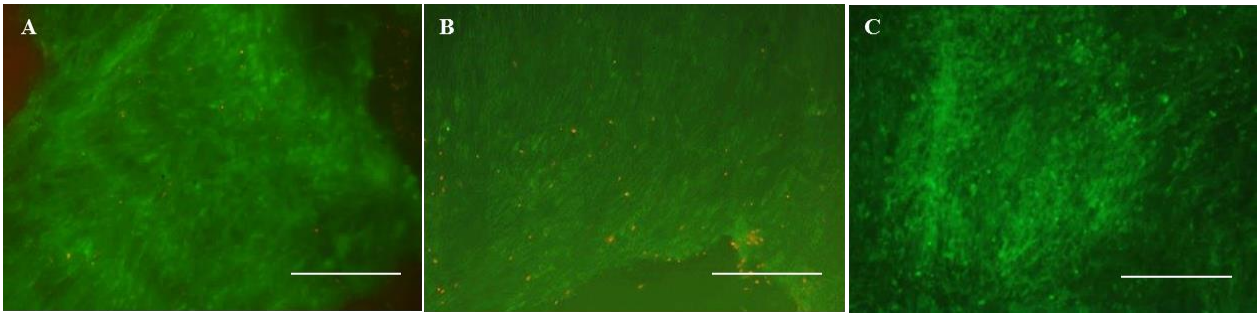

Figure II.4. Live/Dead staining of healthy vaginal fibroblasts (from non-POP site) on different electrospun matrices of A) Nylon, B) PCL/Gelatin and C) PLGA/PCL after 3 days. Alive cells are green and red cells are dead. Scale bar is 200 µm.

3.5 Cell-matrices interaction

We observed that cells attached well to the electrospun matrices at day 3 (fig.II.5 and supplementary fig.II.3), and best on Nylon. Both POP and non-POP cells produced abundant matrix on the nanofibrous matrices after 24 days, and maintained their fibroblast-like morphology. Micro-vesicle-like organelles formed after 3 days on Nylon while they were still immature on the other ones. Cells seemed to be aggregated on PCL/Gelatin samples.

3.6. Histology (H&E and Picrosirius red)

POP and non-POP cells were found on the matrices by H&E staining (fig.II.6 and supplementary fig.II.4). We saw an increase in the number of cells, which was confirmed by DNA assay (fig.II.6, chart). Cells on PCL/Gelatin often formed aggregates (black arrow in fig.II.6-B) especially at early time points, while they were more elongated on Nylon and PLGA/PCL. Based on qualitative observation from total collagen staining, all cell groups started producing matrix after 3 days, increasingly up to 24th day (fig.II.7 and supplementary fig.II.5). More amount of matrix was observed on Nylon. No major differences were seen in the amount of matrix made by cells from different patients.

3.7. Cell counting (DNA assay)

Cell numbers increased over time on all matrices (fig.II.6). Overall, proliferation rate was highest on Nylon, and lowest on PCL/Gelatin. Proliferation of post-menopausal cells (POP-post), however, decreased from day 13 to 24 on PLGA/PCL.

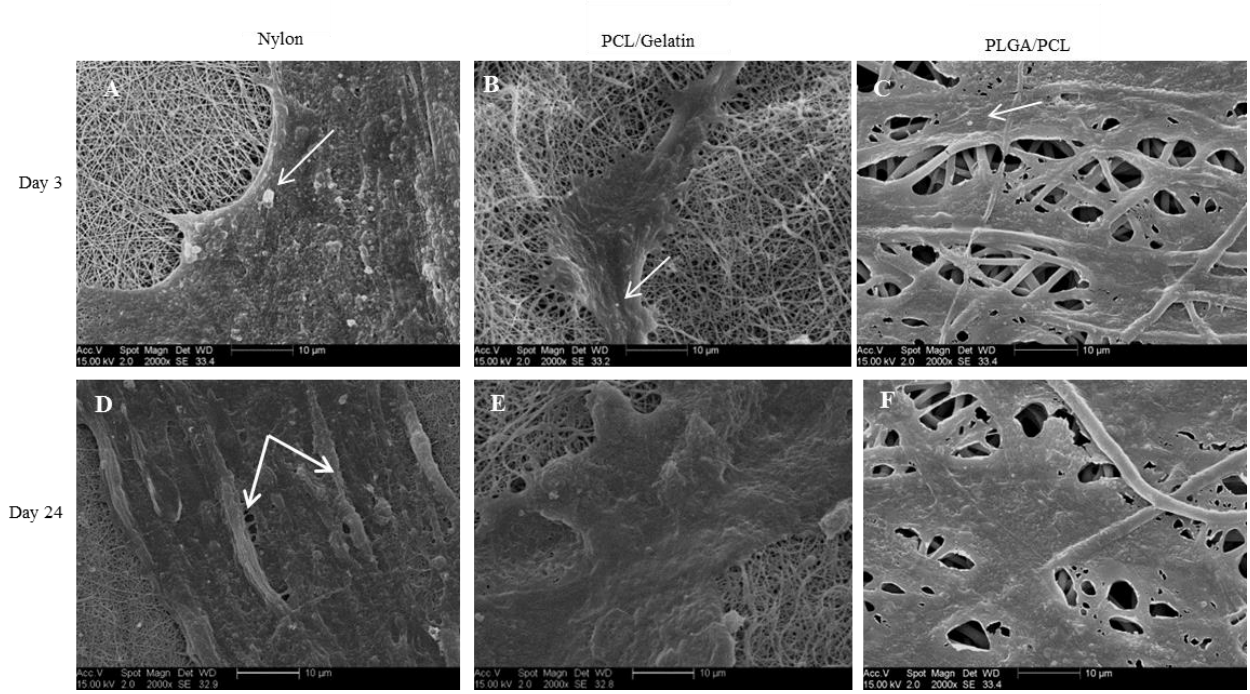

Figure II.5. Representative SEM pictures demonstrating adhesion of healthy vaginal fibroblasts cultured on electrospun matrices after 3 (A-C) and 24 days (D-F). Note the micro-vesicles (thin arrows) and the ECM bundle-like proteins on Nylon (thick arrows). The vesicles on PCL/Gelatin look immature. Scale bar is 10 µm.

4. Discussion

The use of knitted polypropylene meshes for the surgical treatment of Pelvic Organ Prolapse (POP) has led to safety warnings from the Food and Drugs Administration (FDA)[22] due to serious complications. Electrospun nanofibrous matrices could be a new solution because of their unique microstructure resembling the natural extracellular matrix (ECM). Our aim was to evaluate the potential of three different biomaterials for their mechanical and biological properties. We found

that both POP and non-POP human vaginal fibroblasts are able to attach, proliferate and produce ECM on the electrospun matrices of which Nylon performed somewhat better than the others.

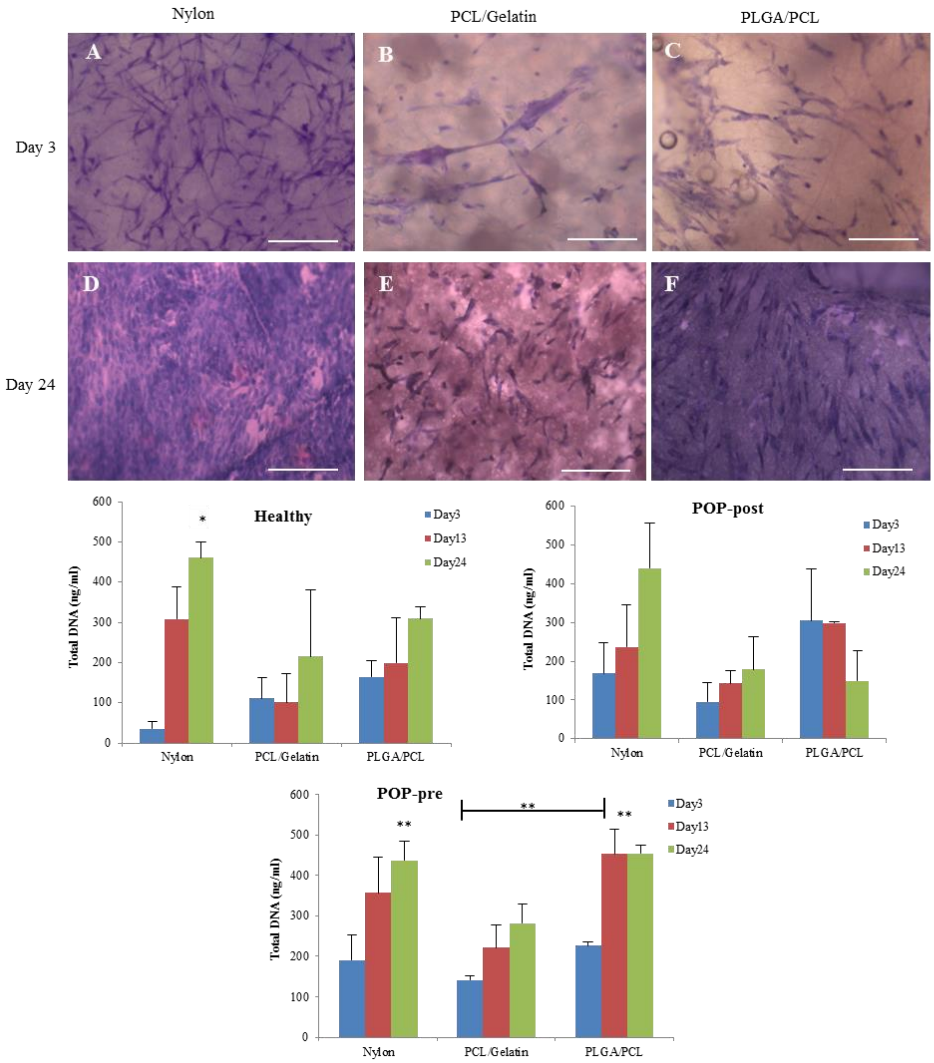

Figure II.6. Proliferation of healthy vaginal fibroblasts on electrospun matrices, after 3 (A-C) and 24 (D-F) days determined by H&E staining. Black arrows point out the cells aggregation. Scale bar is 200 µm. Chart graphs show the total number of different cells on electrospun matrices, assessed with Total DNA assay (&**P<0.05, analyzed with one-way ANOVA, comparisons were made between three cell groups, (n=2). Abbreviations are healthy vaginal fibroblasts (from non-POP site), POP-post and POP-pre fibroblasts from post-menopausal and pre-menopausal POP-patients, respectively.*

The electrospun matrices in this study had a homogenous microstructure with >65% porosity, resulting in low-weight implants and high permeability for nutrients and waste products. This is commensurate with the recommendation to use medium-to-light-weight (< 30-45 g/m^2) meshes

for pelvic floor repair[44]. Although the pore size of electrospun matrices is smaller than that suggested by the Amid classification for knitted meshes [30]; electrospun matrices have entirely different (fibrous) microstructure. Highly porous and interconnected, we think that the surface texture and the microstructure of the electrospun matrices provide a distinct pattern for cellular interactions and thus are more relevant factors for this new class of implants. Yet, studies have shown that cells can infiltrate the electrospun matrix and produce new matrix [70,74]. *In-vivo* experiments are required to determine what recommendations apply to electrospun matrices.

To prevent stress-shielding and shear stress at the implant-tissue interface, the implant should not be stiffer than the surrounding soft tissue[25,32,34,87,88]. Healthy anterior vaginal wall tissue has stiffness 5.51±0.36 MPa[89]; which is close to what we observed in the Nylon nanofibrous matrices. By contrast, all the commercially available transvaginal synthetic meshes are stiffer[19,32,49]. Electrospun nanofibrous matrices showed mechanical properties close to the soft pelvic tissues, which might contribute to reduce stress shielding [89,90]. Evaluation of mechanical properties under highly continuous dynamic conditions like coughing will be the subject of future studies.

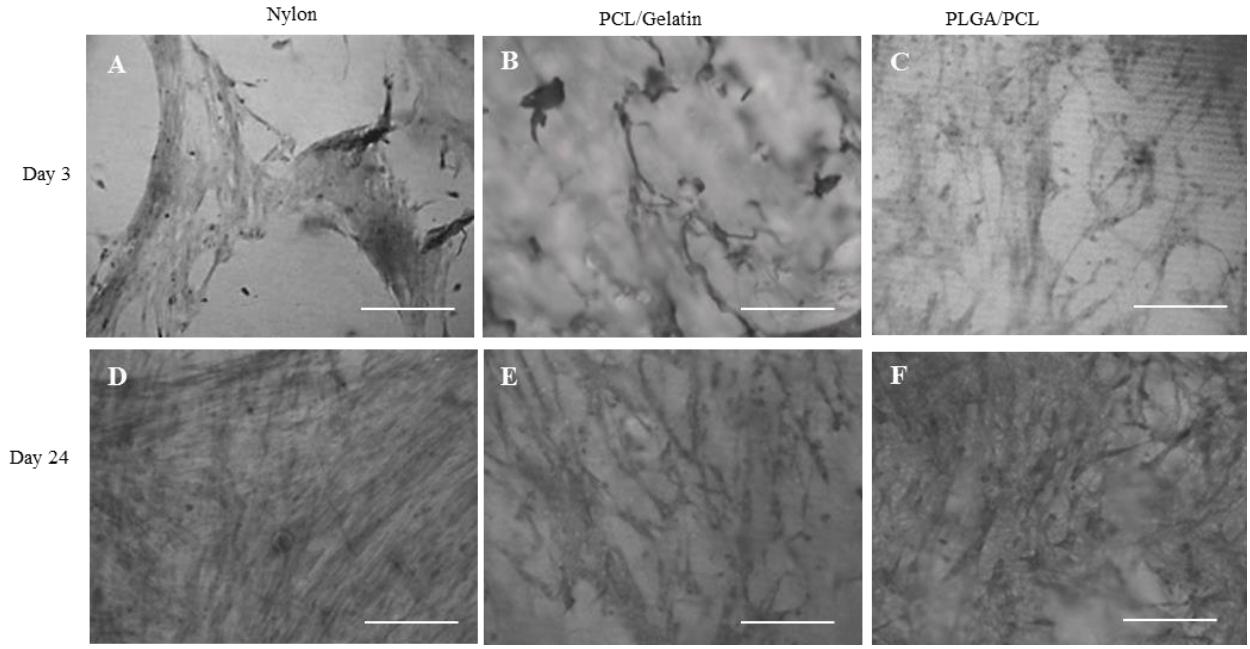

Figure II.7. Gray scale pictures of total collagen staining (picrosirius red) of healthy vaginal fibroblasts cultured on electrospun matrices, after 3 (A-C) and 24 days (D-F). It is observed that healthy fibroblasts (from non-POP site) deposited abundant amount of collagen on all the matrices detected by the stained area. Scale bar is 200 µm.

Implant stiffness is also a determinant of cellular behavior at the surface[91,92,] in dry and wet conditions[93,94]. The compressive micro-stiffness of our electrospun matrices dropped after one hour of wetting in DMEM, showing that the properties of an implant change in the aqueous surroundings of the body because water acts as plasticizer in polymer networks. The compressive micro-stiffness of all matrices was remarkably lower than their tensile stiffness. Nylon had the highest micro-stiffness, while PLGA/PCL had the softest micro-stiffness but with high tensile stiffness. Such results are important for optimizing the mechano-biological performance of an implant.

A biomaterial is generally accepted as biocompatible if cells remain viable, adhere, proliferate, and produce matrix[95,96]. Excellent cell spreading is also a sign of favorable cell-material interaction [95,96]. In this study, both POP and non-POP cells adhered well to all matrices and increasingly

proliferated and produced new matrix over time. Moreover, micro-vesicles were identified on different electrospun matrices in SEM micrographs. These micro-vesicles have an important role in transporting proteins between cells[97], thereby substantiating the biocompatibility of the matrices.

Hydrophilicity (the affinity with water) is essential for the adhesion of host tissue cells and macrophages. Other studies showed that cell adhesion improves with reduced fiber size of an electrospun material[98,99], presumably because it provides more surface area for cell adhesion. In our study, Nylon had the smallest fiber size and also was the most hydrophilic among the three matrices, resulting in higher proliferation and more matrix production.

It is remarkable that both POP and non-POP vaginal fibroblasts remained functional on the matrices identified by adhesion, proliferation and matrix deposition. This supports our initial intention to show that POP cells are able to function on our matrices for 24 days *in-vitro*. From a clinical perspective, this is a great asset of this study because it shows the potential of implanting the matrices in a diseased environment. However, the immunological responses to these matrices are not studied here, which given the small pore sizes of the matrices, should strongly be taken into account for *in-vivo* use. In our future experiments we will evaluate these electrospun matrices in animal models for biocompatibility and induced foreign body reaction.

5. Conclusions

Electrospun nanofibrous matrices show feasible mechanical strength and great biocompatibility for POP and non-POP fibroblasts *in-vitro* and thus may be candidates for a new generation of implants for pelvic floor repair. As experimental conditions did not include mechanical or immunological conditions that would be presented *in-vivo*, this study aimed only to evaluate the

function of POP versus non-POP cells on three different materials *in-vitro*, and the design parameters for an optimal implant are yet to be considered in next steps. Future animal experiments are also required to assess the clinical feasibility.

Acknowledgments

We thank Mr. Koen Van der Laan who kindly helped us with performing the micro-indentation tests.

Supplementary data:

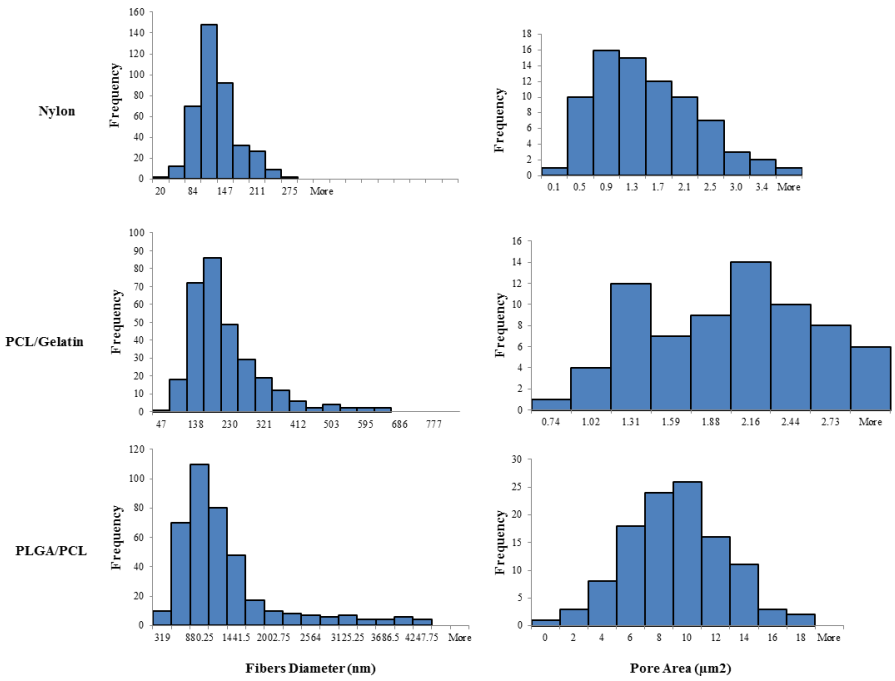

Suppl. Figure II.1. Distribution histograms of fibers diameter and pores size in different electrospun matrices.

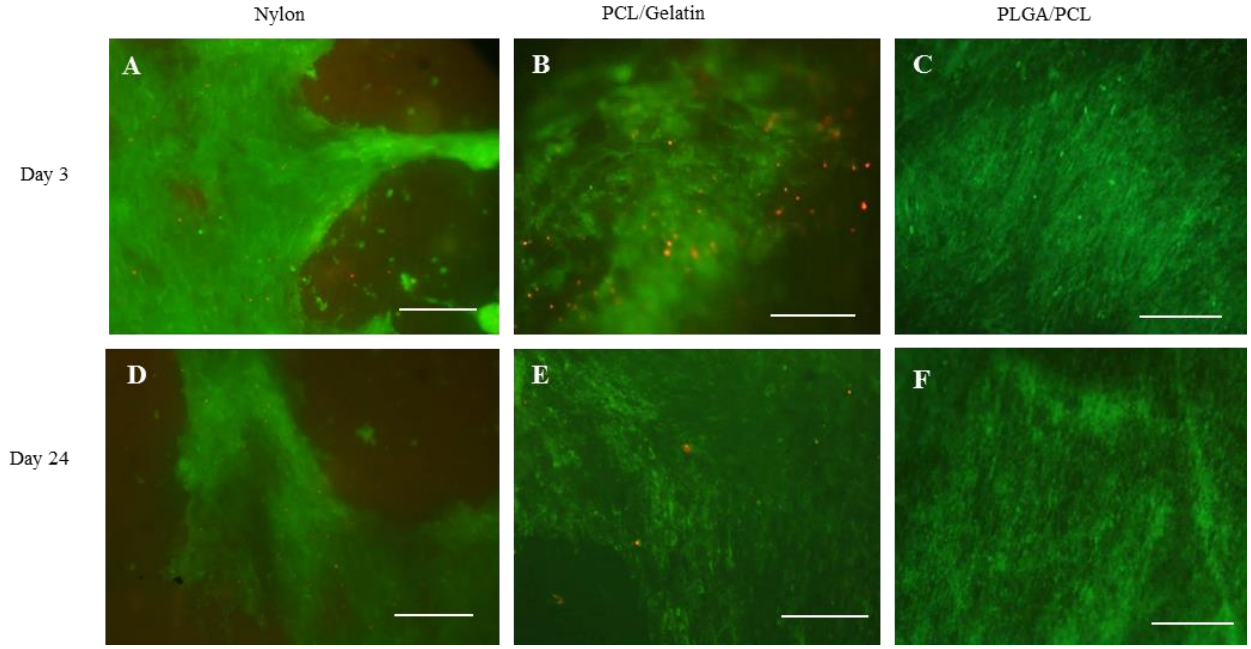

Suppl. Figure II.2. Live/Dead staining of fibroblasts derived from post-menopausal severe patients (POP-post) on different electrospun matrices after 3 (A-C) and 24 (D-F) days. Alive cells are green and red cells are dead. Scale bar

is 200 µm. Both POP-cells (POP-pre and POP-post) showed similar results so POP-post cells are shown as representative.

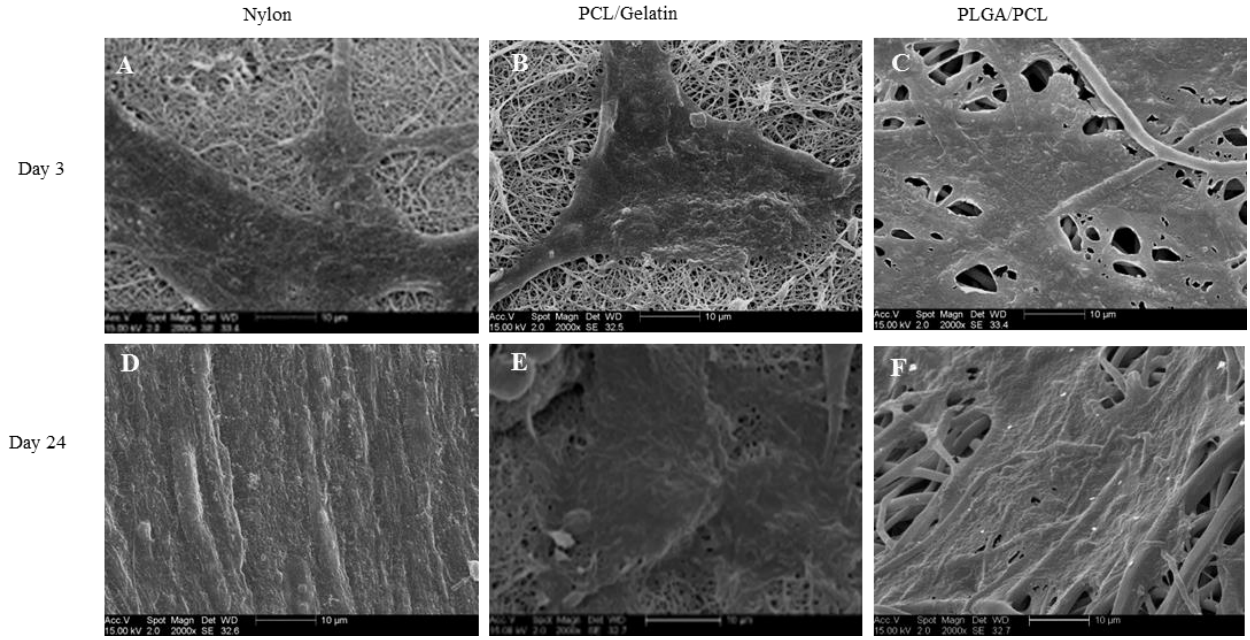

Suppl. Figure II.3. Representative SEM pictures demonstrating adhesion of fibroblasts derived from post-menopausal severe patients (POP-post) cultured on electrospun matrices after 3 (A-C) and 24 (D-F) days. Both POP cells showed similar results so only POP-post cells are shown as representative.

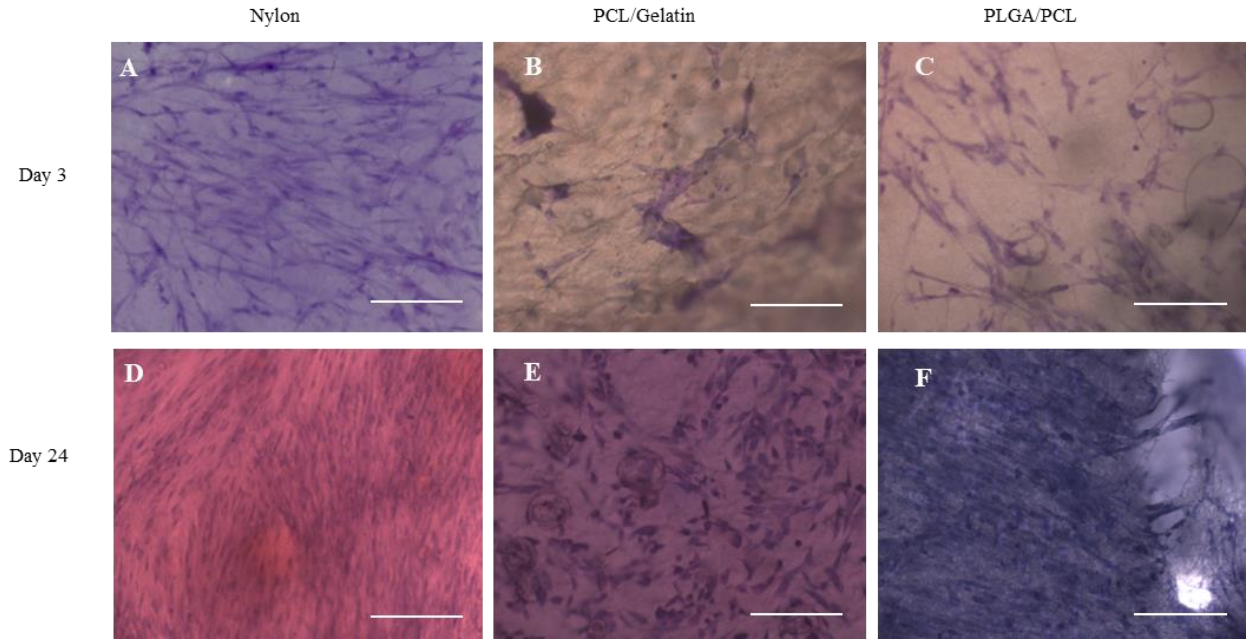

Suppl. Figure II.4. H&E staining of fibroblasts derived from post-menopausal severe patients (POP-post) cultured on electrospun matrices, after 3 (A-C) and 24 (D-F) days. Both POP cells (POP-pre and POP-post) showed similar results so only POP-post cells are shown as representative. Scale bar is 200 µm.

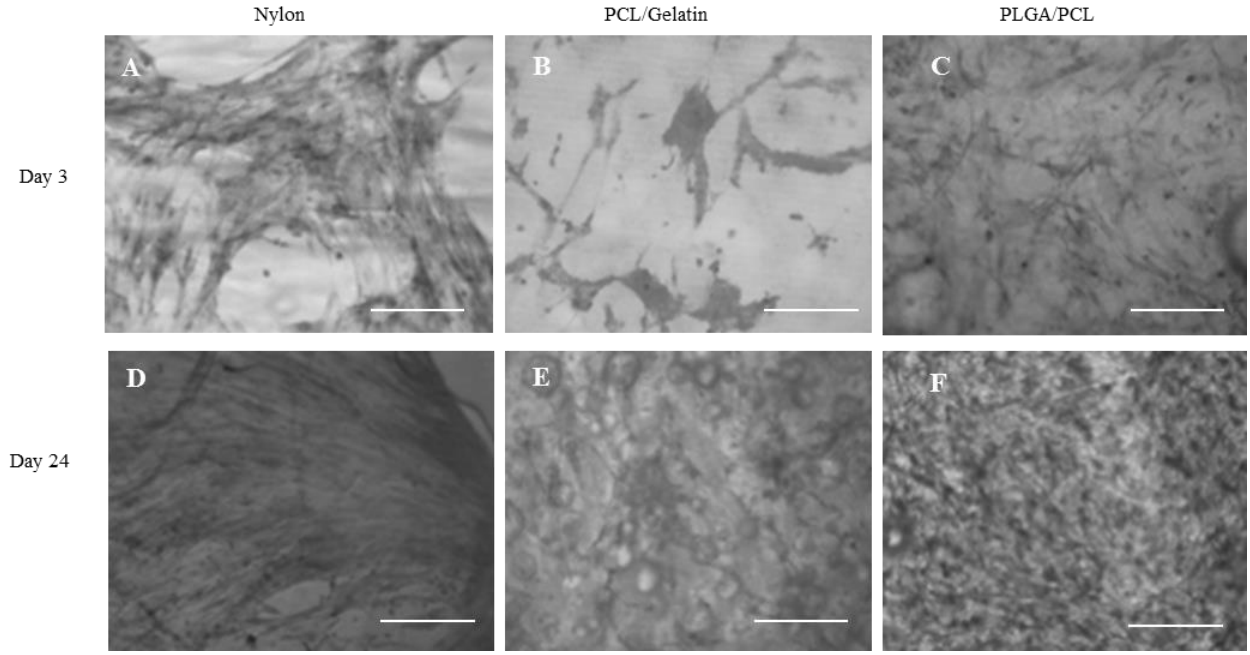

Suppl. Figure II.5. Gray scale pictures of total collagen staining (picrosirius red) of fibroblasts derived from post-menopausal severe patients (POP-post) cultured on electrospun matrices, after 3 (A-C) and 24 (D-F) days. Both groups of POP-cells (POP-post and POP-pre) showed similar results, so only POP-post cells are shown as representative. POP-cells deposited abundant amount of collagen on all matrices detected by stained area. Scale bar is 200 µm.

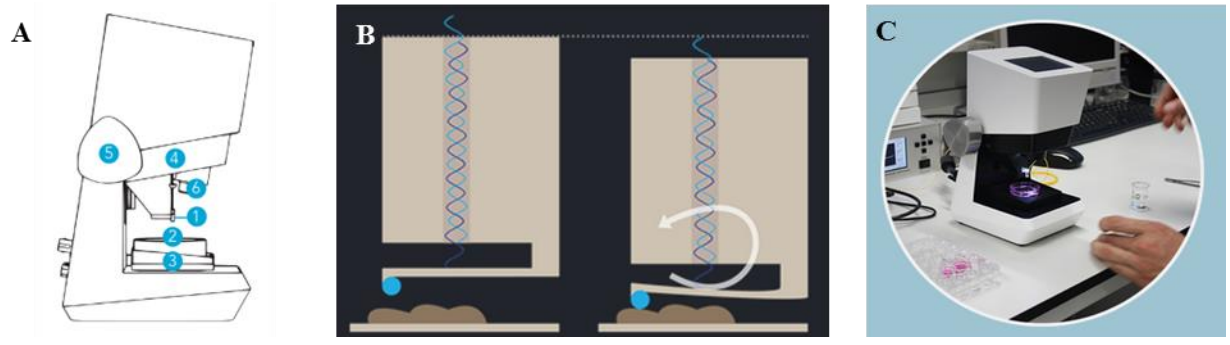

Suppl. Figure II.6. A) schematic cross-sectional view of micro-stiffness indentation device, B) schematic illustration of principles of the indentation device, C) Piuma set-up used in this study showing how the samples were tested. For the detailed principal of how the device works please see the reference No.19 in reference list 19.

Chapter III

Electrospun Matrices for Pelvic Floor Repair: Effect of Fiber Diameter on Mechanical Properties and Cell Behavior

Mahshid Vashaghian, Behrouz Zandieh-Doulabi, Jan Paul Roovers, Theo H. Smit

Tissue engineering Part A 2016; 22(23-24):1305-1316.

Abstract

Electrospun matrices are proposed as an alternative for polypropylene meshes in reconstructive pelvic surgery. Here, we investigated the effect of fiber diameter on i) the mechanical properties of electrospun poly (glycolide-*co*-lactide acid)-blended-poly(caprolactone) (PLGA/PCL) matrices; ii) cellular infiltration; and iii) the newly-formed extracellular matrix (ECM) *in-vitro*. We compared electrospun matrices with 1- and 8μm fiber diameter and used non-porous PLGA/PCL films as controls. The 8-μm matrices were almost twice as stiff as the 1-μm matrices with 1.38 MPa and 0.66 MPa, respectively. Matrices had the same ultimate tensile strength, but with 80% the 1-μm matrices were much more ductile than the 8-μm ones (18%). Cells infiltrated deeper into the matrices with larger pores, but cellular activity was comparable on both substrates. New ECM was deposited faster on the electrospun samples, but after two and four weeks the amount of collagen was comparable with that on non-porous films. The ECM deposited on the 1-μm matrices and the non-porous film was about three times stiffer than the ECM found on the 8-μm matrices. Cell behavior in terms of myofibroblastic differentiation and remodeling was similar on the 1-μm matrices and non-porous films, in comparison to that on the 8-μm matrices. We conclude that electrospinning enhances the integration of host cells as compared to a non-porous film of the same material. The 1-μm matrices result in better mechanical behavior and qualitatively better matrix production than the 8-μm matrices, but with limited cellular infiltration. These data are useful for designing electrospun matrices for pelvic floor.

1.Introduction

Due to weakening of supportive soft tissues in pelvic floor, the pelvic organs such as vagina, uterus or bladder prolapse through the vaginal canal. Such disorders are often accompanied by chronic pain and reduced quality of life in many patients above the age of 50 [2,15]. Reconstructive pelvic surgery attempts to restore the mechanical anatomy of prolapsed organs. If the primary surgery with the native tissue repair recurs, then in most of the cases a knitted polypropylene mesh is used [72]. However, these meshes have not been optimized in their characteristics and occasionally result in severe post-surgical complications [25,71], including exposure , erosion and pain related to scar tissue formation [47]. This may occur because of the mismatch of mechanical properties between the implant and the surrounding soft tissue [32], but it also appears that the microstructure of the mesh is not compatible with cells.

Electrospun matrices have been recently proposed for regeneration of soft tissues in the pelvic floor as an alternative for knitted meshes [74,100–102]. Electrospinning is a method of fabricating polymeric nano-to-micro fibers using an electric potential. With their ultrathin fibers, electrospun matrices mimic the extracellular matrix (ECM), thus providing a better support for cells and their functions such as adhesion, proliferation and matrix production. To understand the potential of electrospun matrices for regenerative medicine, it is important to study the effect of their morphological properties on cellular function. There is evidence that apart from the material, microstructural and topographical properties like fiber morphology (diameter and orientation) influence cellular behavior [98,99,103–105]. However, the relationship between microstructure and the mechanical properties of the electrospun matrices on the one hand, and on the other hand the interaction of electrospun matrices with adherent mammalian cells, have been less investigated. Therefore, when producing electrospun matrices for the purpose of tissue regeneration, it is important to identify the specific microstructural parameters and assess their effect on cell behavior.

To address some of these issues, we conducted a series of experiments with the following aims: first, we assessed how fiber diameter affects the mechanical properties of poly (lactic-*co*-glycolic acid)-blended-poly(caprolactone) (PLGA/PCL) electrospun matrices. Second, we wanted to know the effect of fiber size on cell behavior in terms of migration, activity, matrix deposition and enzymatic activity. Third, we characterized the newly-made matrix as a function of fiber size.

We selected PLGA/PCL because both polymers, PLGA and PCL, are FDA-approved for biomedical and tissue engineering applications. Degradable materials for treatment of pelvic disorders have been suggested because they may overcome the complications of permanent meshes [106–108]. PLGA/PCL is also attractive because it can be electrospun in a wide range of fiber diameters. We chose human vaginal fibroblasts for this series of characterizations because they are responsible for remodeling and maintenance of the matrix in vaginal soft tissue. We used healthy cells in this study to rule out the effects that the disease can have on the behavior of cells in case of a pelvic floor disorder [76].

We spun PLGA/PCL matrices with average fiber diameters of 1 and 8μm. We characterized them for microstructure (morphology and porosity) and uniaxial tensile properties. Non-porous PLGA/PCL films were used as controls. We also characterized the newly-deposited ECM in terms of myofibroblastic differentiation, collagen I production, level of secretion of active matrix metalloproteinase-2 (MMP-2) and micro-stiffness. The results are useful to append the trend of ECM development as a function of fiber size of the PLGA/PCL electrospun matrices.

2. Materials and Methods

2.1. Preparation of 1-μm and 8-μm electrospun matrices and non-porous films

PLGA/PCL (Purac, Netherlands) polymer solutions with ratio of 75:25 and final concentrations of 15% (w/v) and 25% (w/v) in CHCl3/MeOH and CHCl3 were prepared for 1-μ and 8-μ matrices, respectively. Matrices with 1-μm and 8-μm fibers were spun at room temperature (IME Technologies, Netherlands) on a grounded static collector and using a syringe pump (Harvard apparatus, PHD 2000, USA). The samples, circular with 5cm in diameter, were separated from the collector and vacuumed over night to remove residual solvent. The 15% solution PLGA/PCL was used to solvent cast non-porous films. Films were also vacuumed overnight to ensure all the solvent is evaporated. All samples were disinfected with two changes of 70% ethanol, and overnight incubation in 1% antimicrobial culture medium at 37°C.

2.2. Matrices characterizations

2.2.1 Microstructure

Matrices were sputter-coated with gold and their morphological microstructure was evaluated with a Scanning Electron Microcopy (SEM; Philips, XL20, Fei, Netherlands) under a high vacuum and 15 kV. Fiber diameter, pore size and their distribution were calculated using pictures of five random spots per sample. About 50 measurements were made per picture using Image J 1.44p software (NIH, USA).

2.2.2 Mechanical properties

The mechanical properties of the samples were tested with uniaxial tensile (ASTM-F2150) and micro-indentation tests. Electrospun matrices and non-porous films were cut to bone-shape (60x20 mm size) and tightly clamped between two vertical sand-paper-glued clips to create maximum friction, leaving a free length of 40 mm between the clamps. A universal material testing device (Instron 8872, Netherlands) was used to stretch the matrices (n=4). Samples were first preloaded at a rate of 0.1 mm/min to ensure that all of them start from the same reference point and then stretched at a rate of 1 mm/min until rupture. Stress-strain curves were generated from force-displacement curves and with knowing the thickness of the samples, ultimate tensile strength (MPa), ultimate strain (%) and stiffness (MPa) were determined.

An indentation device (Piuma, Optics11, Netherlands, suppl.fig.III.2) was used to obtain the micro-stiffness of the samples after 14 and 28 days of soaking in basic culture medium (wet condition). With a spherical probe of 93.5μm radius, a total of 64 indentations were applied per sample with an average distance of 500 μm between the indentation points (for indentation mapping see suppl.fig.III.2.C). Indentation speed and depth were set at 8μm/s and 20 μm, respectively. Young's modulus (micro-stiffness) for each indentation test was automatically calculated in the Piuma Nanoindentation software [83,85]. Micro-stiffness mean values were reported in MPa ±SD.

2.3. Assessment of cellular responses

2.3.1 Cell isolation & seeding on matrices

Approval for tissue collection and patient informed consent was obtained from the medical ethical committees of VU University Medical Centre (Amsterdam) and Kennemer Gasthuis Hospital (Haarlem). A woman operated for benign gynecological reasons was selected as a healthy donor.

A full-thickness 1 cm^2 biopsy was taken from the anterior pre-cervical region. Within 24h, healthy vaginal fibroblasts were isolated and cultured until passage 4 or 5 in an incubator at 37°C, 95% humidity and 5% CO_2, with culture medium (Dulbecco's modified Eagle's medium-DMEM) supplemented with 10% fetal bovine serum (FBS), 100µg/ml streptomycin, 100U/ml penicillin, and 250µg/ml amphotericin-B. Healthy fibroblasts were counted and their viability was determined using a Count and Viability assay and a Muse Cell Analyzer (Merck Millipore, Darmstadt, Germany). Cells were cultured with 10%-culture medium supplemented with 50 µg/ml vitamin C (for collagen maturation) on the electrospun matrices and films at a density of 150,000 cells/cm^2 in 48-well plates and refreshed every 3-4 days.

2.3.2 Assessment of cellular infiltration through matrices

After 14 or 28 days, samples (n=2 for each sample group and time point) were fixed with 4% formalin. The nuclei were stained with 4,6-diamidino-2phenylindole (DAPI) at a 1:100 dilutions in phosphate-buffered saline (PBS). Cell-seeded matrices were soaked in PBS placed in small petri-dishes and covered with glass slides. Cells were visualized with a florescent microscope (Axio Zoom.V16, Zeiss, Germany). Using the microscope extension (ApoTome.2, Zeiss, Germany) optical sections of 5µm were made through the entire thickness of the matrices, taking the initial fully-focused layer as starting layer. The black-and-white (B&W) images were uploaded in ImageJ 1.44p software (NIH). Inspired by [109], we measured cellular infiltration in each of the matrices as following: we first stained cells for DAPI, and looked at them through each of the four thickness layers we had considered (0-25%, 25-50%, 50-75%, 75-100%). In each layer, we took random pictures from different areas and counted the number of stained-cells in each single picture. By adding the numbers of different areas, we obtained the total number of cells penetrated in each layer (NP) as well as the total number of cells found in each sample (NT) (total of cells found in the four layers). Cell infiltration was calculated as:

$$\text{Infiltrated cells (\% of total) through the matrices} = \frac{\boldsymbol{N_p}}{\boldsymbol{N_T}} \times \mathbf{100}$$

This method was repeated for different random areas of each sample and different optical images that resulted from amplified images at various layers. Images from every 25-µm-thick layers were analyzed.

2.3.3 Cellular mitochondrial metabolic activity

On days 14 or 28, 10% AlamarBlue (V/V) (Invitrogen, USA) was directly added to each sample-containing well and incubated in dark under room temperature for 4 h. Light absorbance at 570 nm was then read with a colorimetric plate reader (Synergy^{TM} HT, Biotek) to assess the metabolic activity of cells at these time points. A cell-free culture medium was read to obtain baseline values and cellular activity was normalized to the baseline. DNA assay was performed to quantify the number of cells at each ending point. The cellular activity was then normalized to the number of cells and reported.

2.3.4 Cell viability

Cells were cultured on disinfected matrices for 14 and 28 days s. Cell viability was assessed by LIVE/DEAD viability/cytotoxicity kit for mammalian cells according to the manufacturer's protocol. Briefly, cells were washed with D-PBS and incubated for 5–10min at room temperature in a mixture of the probes: calcein AM for esterase activity in living cells (green), and ethidium homodimer-1 which penetrates dead cells (red). Live and dead cells were visualized with an inverted Leica DMIL microscope (Microsystems, Germany).

2.3.5 Semi-quantification of total collagenous proteins

Sirius red/fast green collagen staining kit (Chondrex Inc., Redmond, USA) was used. Briefly, a mixture of 0.1% Sirius Red and 0.1% Fast Green solution saturated with picric acid was added to the pre-fixed samples at 14 or 28 days. After 30 min, the dye was removed and samples were rinsed with distilled water. The absorbance values of the extracted dyes were read at 540 nm (Sirius Red) and 605 nm (Fast Green) in a colorimetric plate reader (Synergy^{TM} HT, Biotek). The absorbance values read for non-cell seeded well-plate were used as baseline. The amounts of collagenous and non-collagenous proteins were calculated according to the manufacturer's protocols and normalized to the baseline.

2.3.6 Immunohistochemistry

To characterize the cells on the samples for collagen type I deposition and myofibroblastic de-differentiation, we washed cell-seeded samples with PBS and fixed with 4% formalin for 2 h, washed again with PBS and blocked with a 1% BSA solution (in PBS) for 1 h at room temperature

with the primary antibody mouse anti-human collagen I (Abcam plc., UK) and α-SMA (Dako, Denmark) with a dilution factor of 1:200 in 1% BSA solution (in PBS). We then washed samples three times with 1% BSA solution (in PBS) and incubated with the secondary antibody of goat anti-mouse Alexa Fluor 488 (Invitrogen, USA) with a dilution factor of 1:200 in 1% BSA solution (in PBS). To semi-quantify the deposition of collagenI and myofibroblastic de-differentiation, the stained samples were imaged with a fluorescent microscope (Leica DMIL Microsystems, Wetzlar, Germany). The B&W images were uploaded in ImageJ and the colored-areas per image (stained with collagen I or α-SMA) were quantified and reported as a percentage of the total area of the image. This was done for 10 different spots per sample and the average was reported.

2.3.7 Enzymatic activity of secreted MMP-2

Conditioned medium from both types of matrices was collected after 3, 14 and 28 days. Enzymatic activity of secreted MMP-2 was analyzed (suppl.fig.III.1) using Novex zymogram gels (10% zymogram gelatin gel, Life Technologies) following manufacturers' protocol. Dark bands of gelatinolytic activity were visualized using an eStain protein staining device (GeneScript, Piscataway, NJ, USA). Images were taken using BiospectrumAC (UVP) and ImageJ (NIH) was used to quantify the density of the bands. Values were calculated as follows: Total MMP-2 = inactive MMP-2 + active MMP-2; and percentage of active MMP-2 = (active MMP-2 x 100)/Total MMP-2.

2.3.8 Measuring the micro-stiffness of newly-made matrix

We characterized the stiffness of newly-made matrix on 1-μm and 8-μm matrices using a micro-indenter (Piuma, suppl.fig.III.2) after 14 or 28 days and compared it to PLGA/PCL cell-seeded non-porous films. Micro-indentation was performed to see the changes of the surface mechanical properties of the produced matrix during time. Cell-seeded matrices were first gently washed with Dulbecco's phosphate-buffered saline (DPBS), and underwent the measurements in basic culture medium. Samples without cells (wet condition) were used as control, to see the effect of ECM deposition over time, as described in section 2.2.2. With a spherical probe of 93.5μm radius, 16 indentations were applied in 5 different areas of each sample (a total of 80 per sample, suppl.fig.III.2.C, indentation map) with an average distance of 500 μm between the indentation points. Indentation speed and depth were 8μm/s and 20 μm, respectively. Young's modulus

(micro-stiffness) for each indentation test was automatically calculated in the Piuma Nanoindentation software [83,85]. Micro-stiffness mean values were reported in MPa ±SD.

2.4. Statistical analysis

Statistical analyses were performed using the software Prism version 5.02 (GraphPad Software Inc., La Jolla, CA, USA). Data were expressed as the mean ±standard deviation (SD) for individual measurements. One-way analysis of variance (ANOVA) followed by Bonferroni *post hoc* test was used to test differences between all the groups and the level of significance was set at $p < 0.05$.

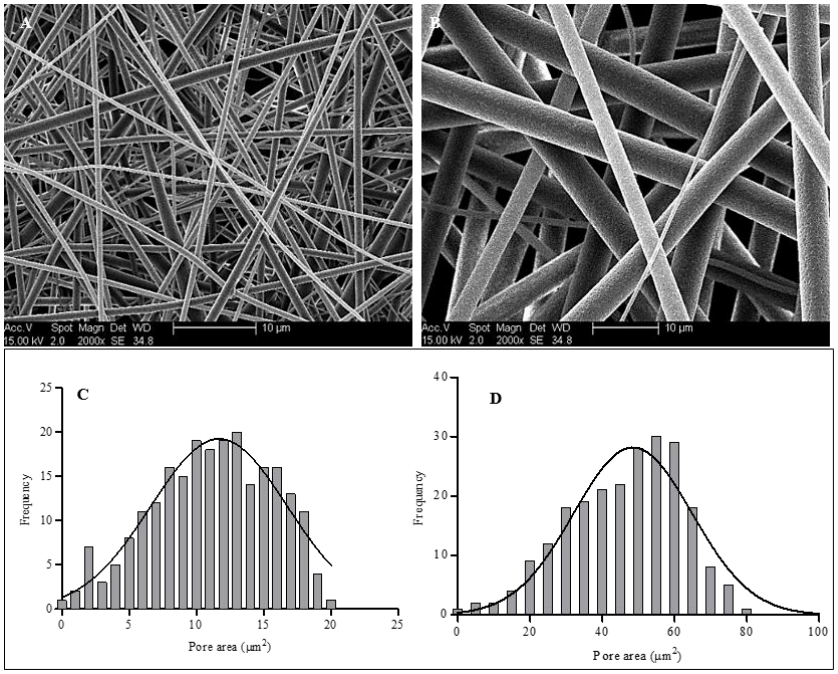

Figure III.1. Microstructure and distribution of the pore area in (A, C) 1-mm and (B, D) 8-mm electrospun PLGA/PCL matrices characterized by scanning electron microcopy. PLGA/PCL, poly (lactic-co-glycolic acid)-blended-poly(caprolactone).

3.Results

The polymers were reproducibly spun, resulting in coherent and intact matrices for both fiber diameters. Cell culture experiments went on until 28 days without noticeable abnormal changes in color during culture time, or infection symptoms.

3.1 Microstructure

Fig.III.1 shows the microstructure and the distribution histogram of pore size in the 1-μm and 8-μm matrices. The average values of pore size for 1-μm and 8-μm samples were (mean ±SD for all the results) 10.5 ±1.1 and 53 ±6.6μm^2, respectively, and the average fiber diameters were 1.0 ±0.05 and 8.0 ±0.2μm (tableIII.1). Morphology of fibers and the geometrical shape of pores were similar in both matrices, but the pore size and fiber diameter were larger in 8-μm samples. Distribution was homogenous in both types of samples accordingly (fig.III.1, histogram C&D).

3.2 Mechanical properties

Fig.III.2 shows representative stress-strain curves of two spun matrices and non-porous film under uniaxial tension. The non-porous film and 1-μm sample were much more ductile than the 8-μm sample. The ultimate tensile strength was 3.6 ±0.02 MPa for both spun samples and 6.3 ±0.06 MPa for non-porous film (normalized to the samples thickness, data not shown). Ultimate tensile strain of 1-μm, 8-μm samples and non-porous film was 80±0.5%, 18% and 144±9.6%, respectively. The stiffness of 1-μm and 8-μm samples were measured 0.66 MPa and 1.38 MPa, respectively and 0.62 ±0.03 MPa for non-porous film (summarized in tableIII.1).

3.3 Cellular infiltration through matrices

As we see in fig.III.3, cell infiltration was higher in 8-μm samples at all-time points due to larger pore size. After 14 days, most cells were still in the first upper 25% layer in the 1-μm samples and only a few reached deeper layers. On 8-μm samples, on the other hand, most cells already migrated into >50% layer after 14 days from which half were found in deeper layers. After 28 days, most cells infiltrated up to 75% of the 8-μm samples, while almost 10% went through the whole matrix. In the 1-μm samples after 28 days, most of cells penetrated less than 50%. What is observed in figureIII.3 is that more cells are visible in more surface layers of the 1-μm samples, where in the same layer in 8-μm samples fewer cells are visible, meaning that they have infiltrated to deeper layers. The large standard deviations in some bars were caused by a heterogeneous distribution of cells, sometimes on one or two edges of the samples, making the measurements over all the samples heterogeneous (fig.III.3).

3.4 Cellular metabolic activity

Mitochondrial activity of cells increased over time, with no significant difference between the samples as we see in fig.III.4. We used the AlamarBlue assay here to report a representation of cellular activity, however, cellular activity was considered with respect to the number of cells measured by DNA assay (data not shown) to rule out the over-estimation of activity that can occur in cells with multiple mitochondria.

3.5 Cell viability

After 14 days, human vaginal fibroblasts showed good survival and attachment to the surface of both 1- and 8-µm matrices while in deeper layers (>50% deep in the matrices), some cells were dead, particularly on 1-µm. After 28 days, more cells died in deep layers and particularly on 1-µm (fig.III.5).

3.6 Total collagenous proteins

The amount of total collagenous protein increased over time on 1-µm and 8-µ spun samples and non-porous films. At 28 days, the amount of collagenous-matrix was slightly higher on 1-µm samples (fig.III.6). It appears that collagen deposition occurs faster in the first two weeks on all the samples. After two weeks, the level of deposition is almost similar on all samples, although slightly less on the 8-µ matrices.

3.7 Immunohistochemistry

Deposition of collagen I and α-SMA was continuous on both spun samples and non-porous films until 28th day. Differences in the amount of collagen I was not significant between samples (fig.III.7), but α-SMA was deposited about 30% more on the 1-µm than 8-µm (fig.III.8). On 8-µm samples, deposition of collagen I occurred mostly in first two weeks, and didn't increase noticeably after that. In the first 3 days, cells on all samples were positive for α-SMA expression. α-SMA expression was not region-specific but more homogenous throughout the matrices.

3.8 Enzymatic activity of secreted matrix metalloproteinase-2 (MMP-2)

The level of total released MMP-2 and the active ratio of active MMP-2 increased over time for all samples. The ratio of active/total level of MMP-2 was higher on 1-µm samples than on 8-µm samples at all ending points. The differences were more significant after 14 days. The ratio of

active/total MMP-2 was noticeably highest on non-porous films at 14 days, which decreased to almost half after 28 days (suppl.fig.III.1).

3.9 Micro-stiffness of newly-made matrix

Micro-stiffness of spun matrices decreased over time, from non-seeded condition (wet condition where samples were dipped in culture medium) to cultured-with cells which can be due to deposition of the new ECM and reduction was more obvious (fig.III.9) on the 8-µm samples. Also the stiffness in wet condition decreased slightly over time. However, from day 14 to day 28, stiffness reduced on 8-µm samples but slightly increased on 1-µm. The stiffness of matrix was significantly higher on non-porous films than 8-µm matrices at all-time points.

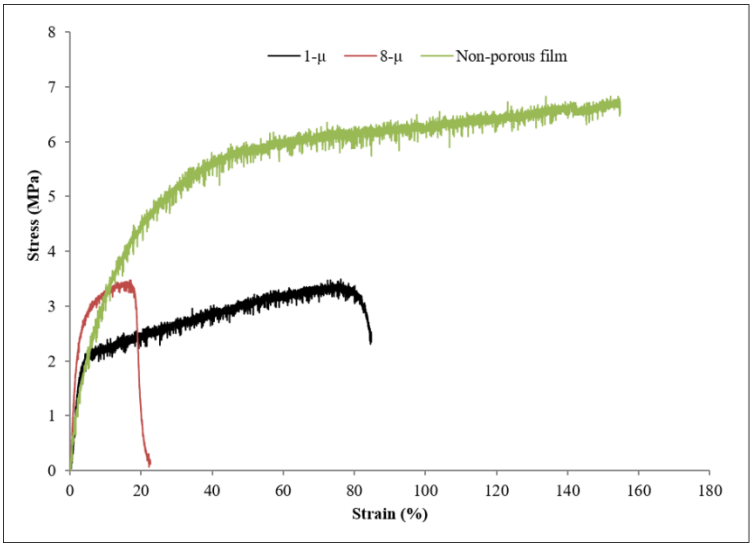

Figure III.2. Representative stress–strain curve of the 1-mm (black) and 8-mm (red) electrospun PLGA/PCL matrices and nonporous film (green) under uniaxial tensile test (n = 3).

Table III.1. Properties of 1-µm and 8-µm electrospun PLGAPCL matrices and non-porous films.

** at P < 0.05 (n=4).*

Sample type	Fiber diameter (μm)	Pore area (μm^2)	Ultimate tensile strength (MPa)	Ultimate tensile strain (%)	Tensile stiffness (MPa)
1-μm	1 ±0.05	10.5 ±1.1	3.6 ±0.00	80 ±0.5	0.66 ±0.00
8-μm	8 ±0.2	53 ±6.6	3.6 ±0.02	18 ±0.00 *	1.38 ±0.00
Non-porous film	NA	NA	6.3 ±0.06	144 ±9.6	0.62 ±0.03

4. Discussion

The microstructural behavior of the electrospun matrices and their interaction with cells should be studied in more detail to optimize their function. Here, we studied the change of mechanical properties with decreasing the fiber diameter, as previous studies have shown that mechanical properties are generally better with thinner fibers [110]. We chose 1μm and 8μm fiber size based on the previous studies which used a range of 1-10μm [110–112]. The data presented in this study show that fiber diameter not only affects cell behavior, but also has tremendous impact on the mechanical properties of the matrices.

Fiber size had no effect on the ultimate tensile strength of the spun matrices, but the 8-μm samples were almost twice as stiff as the 1-μm samples and were significantly less ductile (more brittle). In the 1-μm matrices, the fiber packing density and thus the number of fiber cross-points per unit of area is higher than the 8-μm matrices. As a result, displacements are carried along these cross-point areas and not easily propagated between individual fibers, making the 1-μm samples more ductile [113]. Non-porous films, on the other hand, were significantly more ductile than both spun samples, and twice stronger. The differences in mechanical behavior of samples derive from their microstructural properties that emerge during the process of electrospinning (1-μm and 8-μm samples) or casting (non-porous films). For example, the porosities in the structure of the spun matrices have decreased their mechanical properties compared to the non-porous films. Also, the stretching of the fibers toward the collector during spinning, alters the molecular structure of the polymer (such as crystallinity)[114], by re-orienting the molecular network. As a result, the fibers in

1-µm samples (they are more stretched than 8-µm samples) are much more ductile than 8-µm because of the re-orientation upon spinning. Besides, the 8-µm samples were prepared in 25% chloroform solution, while the fibers of 1-µm were prepared in 15% solution blend of chloroform and methanol. Methanol changes the solution properties and increases the flow of spinning. Thus, the physic-chemical properties of the polymeric fibers may also alter, as previously reported [115,116]. These parameters together determine the mechanical behavior of each of the matrices, through which an electrospun implant can be designed.

The tensile stiffness of the 8-µm samples (in macro- level) was two times higher than of the 1-µm samples, while the micro-stiffness of the 1-µm samples was almost 7-10% higher in wet non-seeded condition under indentation test. Micro-stiffness of the matrices in wet condition also decreased over time. We assume that it is because the water acts like a plasticizer and softens the polymeric network during time. The implication of this is also reflected in the findings of the ECM stiffness, since the ECM produced by cells on different fiber sizes had different rigidities. Differences in the mechanical properties at the macro- and micro-level show that the properties of an implant might be slightly scalar, meaning that they might vary in micro- and macro- scale due to differences in the geometry. It implies that an electrospun matrix could be as strong as necessary in macro-level but soft and thus gentle to cells in micro-level. Most of the knitted polypropylene pelvic meshes are strong enough, but they are too stiff to cells thus irritating the soft tissue in long term under mechanical loadings. An electrospun matrix might cause less of such mechano-biological issues owing to its gentle surface.

The pore size proportionally increases with increasing the fiber size. A homogenous distribution of pores and fibers was found in both our 1-µm and 8-µm matrices. As expected, increasing the pore size enhanced the infiltration of fibroblasts into the matrices, in a more homogenous manner Enhanced cellular infiltration has important implications in terms of implant integration *in-vivo* [109], including the macrophages penetration for clearing the bacteria in case of infection[117]. Pore size is also important with respect to cell viability. As seen in fig.III.5, cells are viable on the surface of both matrices. But if they can't penetrate inside the scaffolds because of small pore size, they remain on the surface for long time and grow on top of each other instead of three-dimensional growth. This way, a thick cell layer could form on the surface and some of the cells may die (like on 1-µm after 28 days) due to lack of oxygen or nutrition. The same happens to the cells which

migrated into deeper layers of the scaffolds. This happened more significantly in 1-µm matrices as pores are too small and the thick cellular layer formed on the surface may even more limit diffusion of oxygen and nutrients. This may also occur because the waste by-products of cellular activities (mostly acidic) which are toxic to cells are not removed efficiently which can cause local cell death. A dynamic culture system with a proper stirring might enhance the diffusion of nutrients and make them more available to the cells in deep layers.

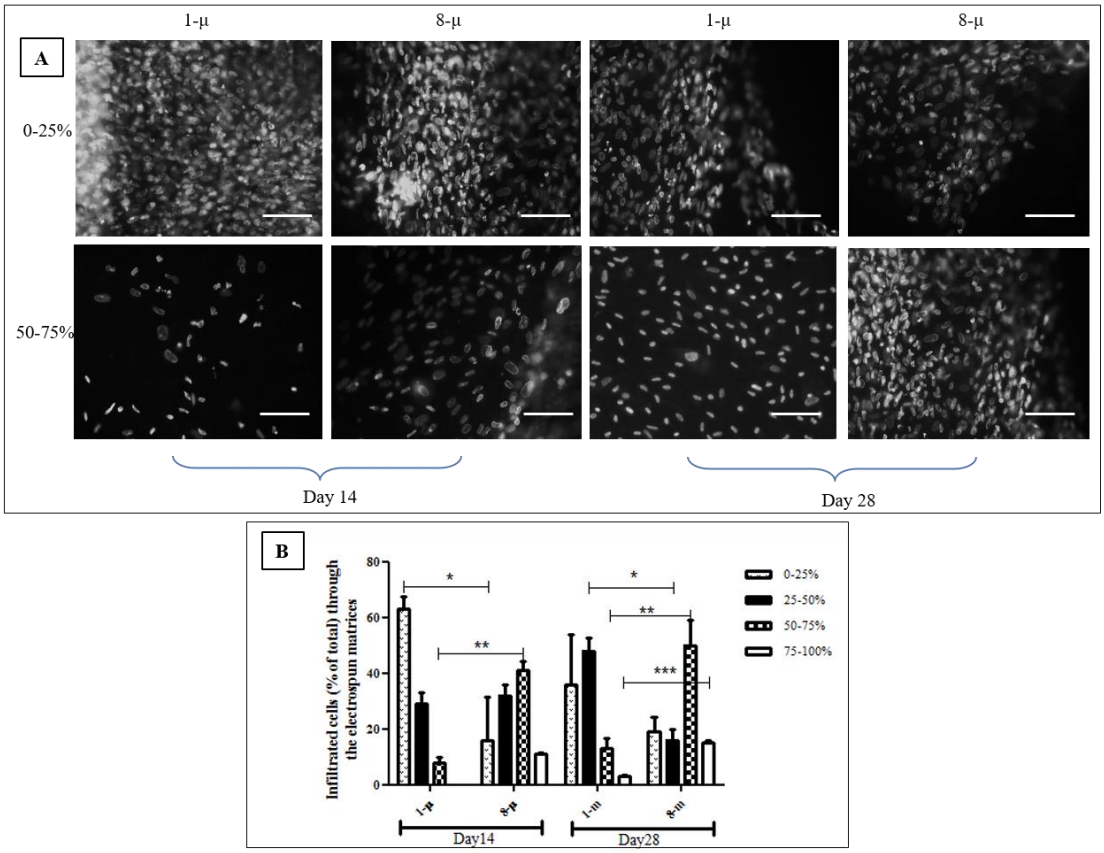

*Figure III.3. Cellular infiltration through 1-µm and 8-µm electrospun PLGAPCL matrices over 14 and 28 days. A) visualization of DAPI-stained cells in black&white (two representative layers of 0-25% and 50-75% thickness are shown only), B) quantification of cellular infiltration: the number of DAPI-stained cells were counted. Four equal layers of thickness (%) were considered for each electrospun matrix. The number of the penetrated cells in each of the layers was counted and reported as a percentage of total number of cells. scale bar is 50 µm. *, ** & *** at P < 0.05 (n=4).*

Fiber size is known to affect cell behavior in terms of adhesion, proliferation and differentiation [98,99,103,104,118,119]. For instance, adhesion and proliferation of cells enhance as the fiber diameter decreases[98,120] which can consequently affect the quality of the matrix they produce. Here, we observed that although cell proliferation was not significantly different on the two matrices, cells

produced more collagenous matrix, slightly more collagen I and expressed more α-smooth muscle actin (α-SMA) on the 1-µm matrices. It seems that cells are experiencing a different geometrical environment (3D) on the 8-µm samples, therefore their behavior and the new matrix they produce is different. These results suggest two explanations.

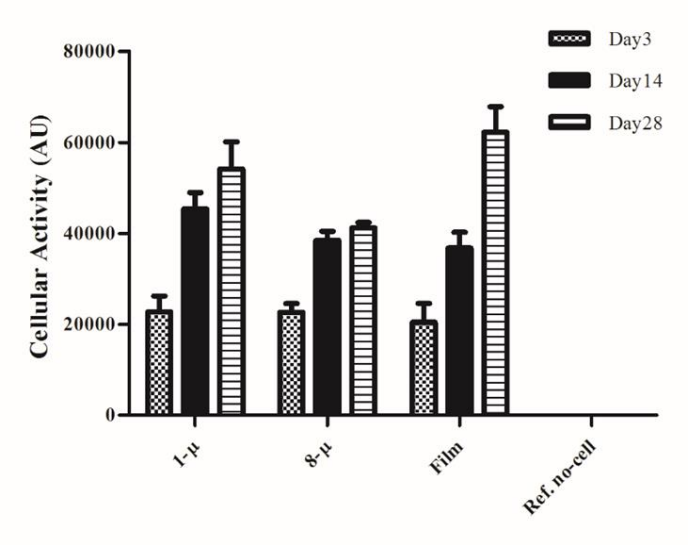

Figure III.4. The metabolic activity and proliferation of human vaginal fibroblasts on the 1-µm and 8-µm electrospun PLGAPCL matrices and non-porous film over 28 days, as assessed by absorbance of AlamarBlue stain at 570 nm. No significant statistical difference was found.

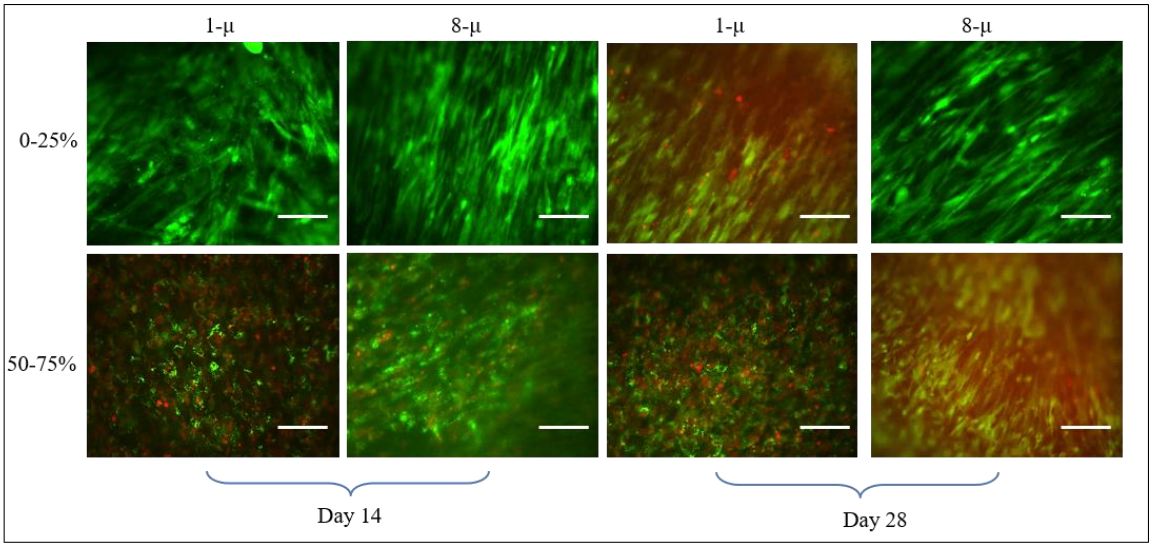

Figure III.5. Viability of human vaginal fibroblasts throughout the 0-25% and 50-75% thickness of the 1-µm and 8-µm electrospun PLGAPCL matrices over 28 days, assessed by Live/Dead staining. Green cells are alive and red ones are dead. Scale bar is 50 µm.

First, it may be that on 1-µm matrices with thinner fibers, cells generally deposit more ECM and α-SMA fibers because they are exposed to more surface area (amount of material per unit of area). If the substrate is stiffer than soft tissue, cells are triggered for myofibroblastic differentiation,

which occurs more on 1-µm samples and non-porous films compared to 8-µm matrices. From here on, cells may enter positive-feedback loop as suggested by Blaauboer et al[121], meaning that the more myofibroblastic they become the more matrix they produce, and vice versa. On 1-µm samples, cells react to the rigidity of the substrate surface by overexpressing α-SMA fibers and then differentiate into myofibroblasts[122]. For the same reason, cells produce more collagenous-matrix and more collagen type I as compared to those cultured on 8-µm matrices. This way ECM accumulates, which ultimately results in increased matrix rigidity as we measured by indentation test; the matrix synthesized by cells on 1-µm samples was stiffer.

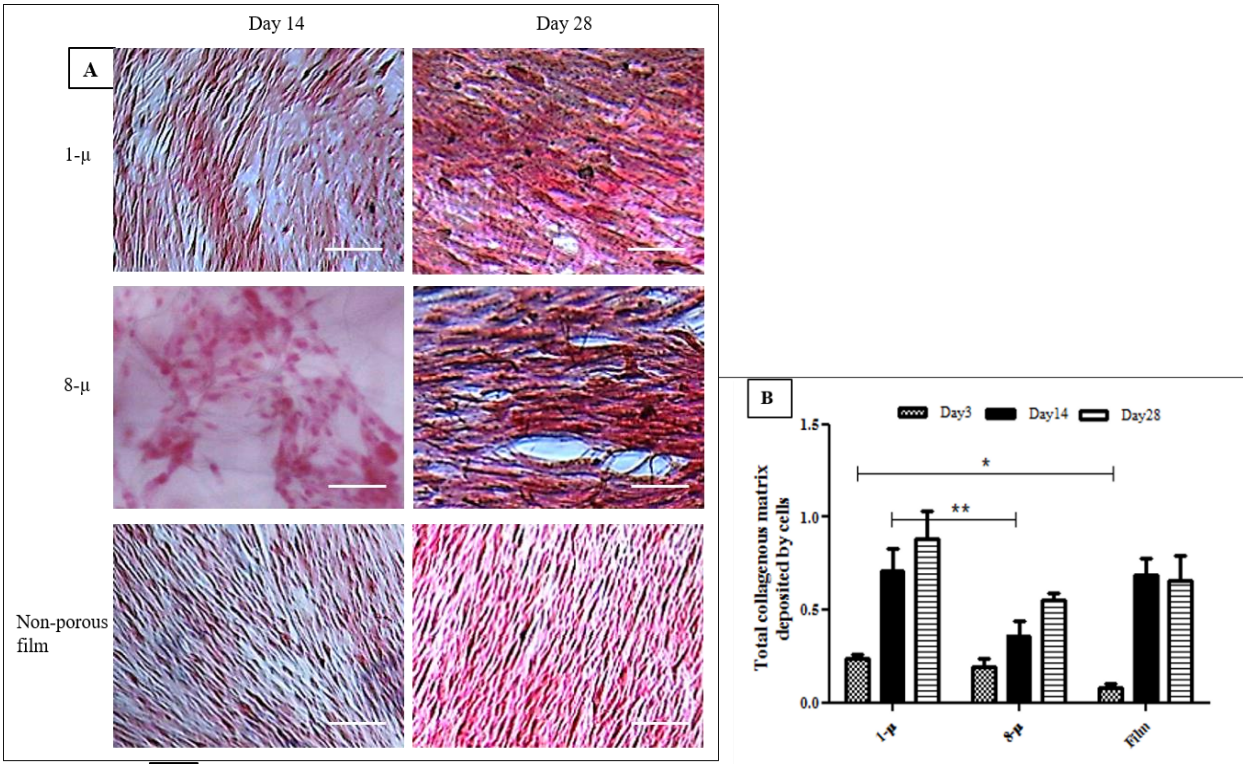

*Figure III.6. Total collagenous matrix produced by 1-µm and 8-µm electrospun PLGAPCL matrices and non-porouf film after 14 and 28 days. A) stained with picrosirius red, B) semi-quantification by picrosirus red/fast green kit. * & ** at P < 0.05 (n=4). Scale bar is 20 µm.*

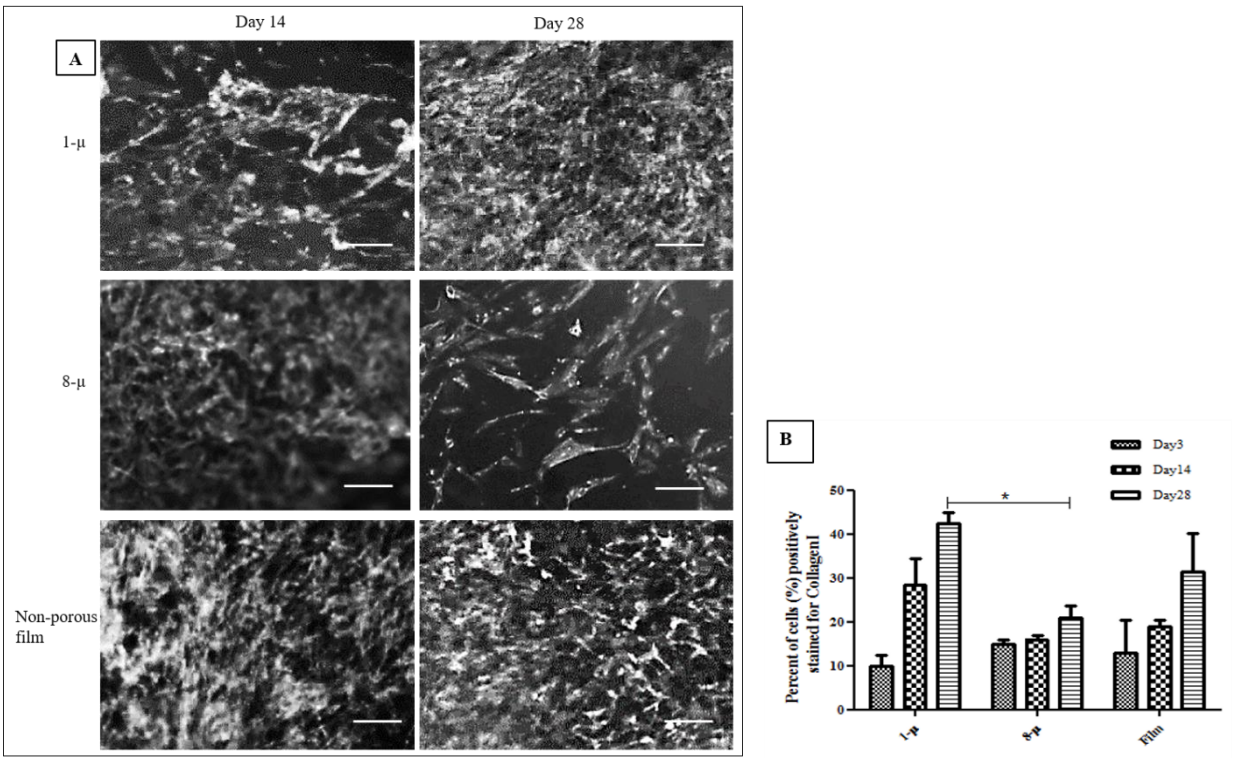

*Figure III.7. Immunohistochemistry assay for collagen type I produced by cells at the surface of 1-µm and 8-µm electrospun PLGAPCL matrices and non-porous film in 14 and 28 days. A) black&white pictures of cells positive for collagen I anti-body, B) semi-quantification of the amount of collagen type I produced by cells. * at $P < 0.05$ (n=4). Scale bar is 20 µm.*

Considering the higher amount of myofibroblastic differentiation and more amount of collagen produced on 1-µm, it was no surprise that the matrix deposited on these matrices was stiffer. This higher stiffness may then stimulate fibroblasts for even more collagen production and more cells become myofibroblastic over time. Interestingly, we did not observe noticeable shrinkage of the samples (data not shown), which could have been a reflection of upregulated α-SMA on 1-µm and non-porous films. This could be because of the ECM-accumulation and increased stiffness that result in less deformation and thus less cell contractility [123,124]. Cells expressed more α-SMA fibers on thinner fibers and non-porous films, which is in commensurate with the stiffer matrix they produced on these samples.

The second explanation for more deposition of ECM-related proteins on 1-µm samples, is that cells penetrated deeper into the 8-µ samples (three-dimensional migration) so the new collagenous matrix they produced or the α-SMA fibers they expressed, was not visible in our surface-staining and therefore was not counted in the semi-quantification of the new matrix.

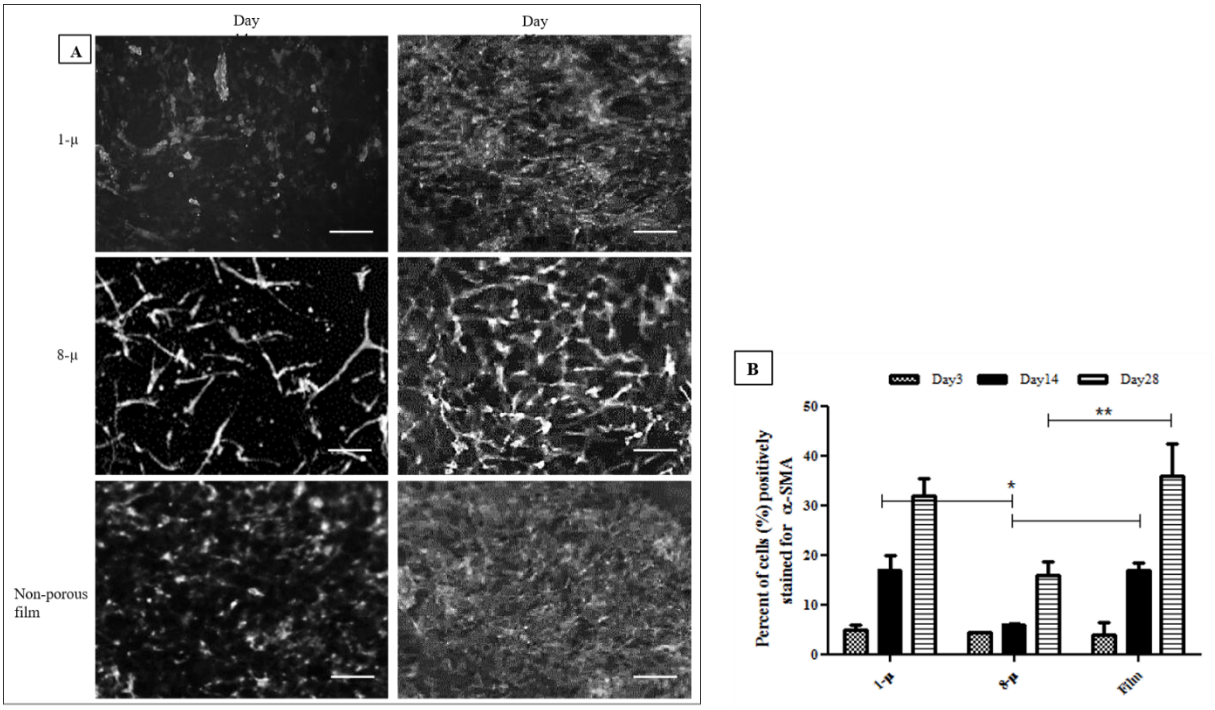

*Figure III.8. Immunohistochemistry assay for alpha-smooth muscle actin (α-SMA) activation of cells on the surface of 1-µm and 8-µm electrospun PLGAPCL matrices and non-porous film after 14 and 28 days. A) black&white pictures of cells positive for α-SMA, B) semi-quantification of the amount of α-SMA expression. * & ** at P < 0.05 (n=4). Scale bar is 20 µm.*

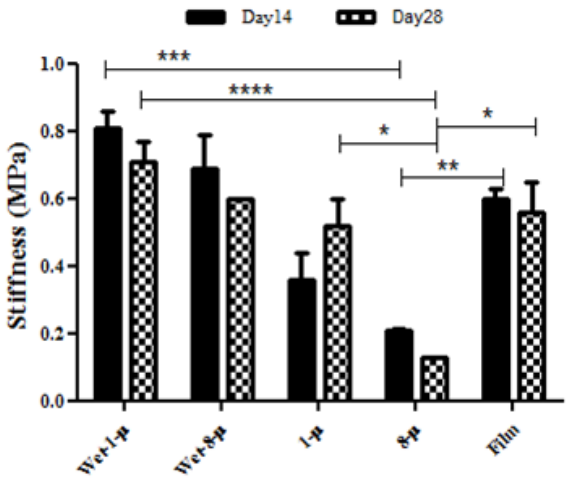

*Figure III.9. Micro-stiffness of the non-seeded matrices (wet) maintained and of the newly-deposited matrix as measured by indentation testing. Differences especially with 8-µm, likely due to deposition of ECM inside the samples rather than on the samples. Numbers are reported as the mean values ±standard deviation of normally distributed values. *, **, *** & **** at P < 0.05 (n=4).*

Matrix metalloproteinases, MMPs, (like MMP-2) enzyme are responsible for the break down and therefore remodeling of the collagen protein in the natural tissues. We chose MMP-2 as a representative remodeling enzyme as it was shown before in our group that POP-cells regulate their remodeling by secretion of MMP-2 [86]. The amount of active MMP-2 decreased after 14 days on all samples and particularly on non-porous films. Our results suggest that remodeling was going on for 28 days, but the results were not significantly different and thus not conclusive enough. Further investigations are needed to understand the underlying mechanisms of the enzyme-regulated remodeling occurring on nanofibrous structures. The current study was limited by the fact that the findings only apply to the *in-vitro* situation, while implants are exposed to a much more complicated environment in body, including diseased cells [75], mechanical straining, inflammation, and other foreign body reactions. Exploring whether the matrices of different fiber size behave differently *in-vivo* needs further studies in animal models to address common implant-related issues such as fibrosis, immunological responses and erosion under dynamic conditions.

5.Conclusion

The aim of this study was to explore the role of fiber diameter in mechanical behavior of electrospun PLGA/PCL matrices and the characteristics of the ECM produced by human fibroblasts on each fiber size. The data suggest that matrices with 1-µm fibers result in better mechanical behavior (more ductility and less stiffness) and qualitatively better ECM production than the 8-µm matrices. Cells experience a different environment on 8-µm matrices because they penetrate into them and grow three-dimensionally compared to the 1-µm matrices and non-porous

films where they remain mostly on the surface. Thus, cells produce a different type of matrix on the matrices which results in different cellular behavior (such as α-SMS expression and different micro-stiffness qualities) in return. However, the integration capacity is jeopardized in 1-µm matrices because the pores are smaller and cellular infiltration becomes limited. Overall, an optimal fiber size has yet to be found for an electrospun matrix to meet all the requirements of pelvic floor. Rational design of an implant requires functionalization studies through animal models which will be addressed in future experiments.

Acknowledgment

We thank Dr. Manon Kerkhof for tissue collection, Dr. Alejandra Ruiz-Zapata for cell isolation and Mr. B. Nelemans and Mr. M. Schmitz for helping us with the Zeiss microscope. We also thank department of Oral Cell Biology, Academisch Centrum Tandheelkunde Amsterdam (ACTA)-Vrij University Amsterdam for facilitating our experimental works. M.V and T.S. acknowledge financial support from ZonMW-VICI grant 918.11.635 (The Netherlands).

Author Disclosure Statement

Authors report no disclosure for this study.

Supplementary data:

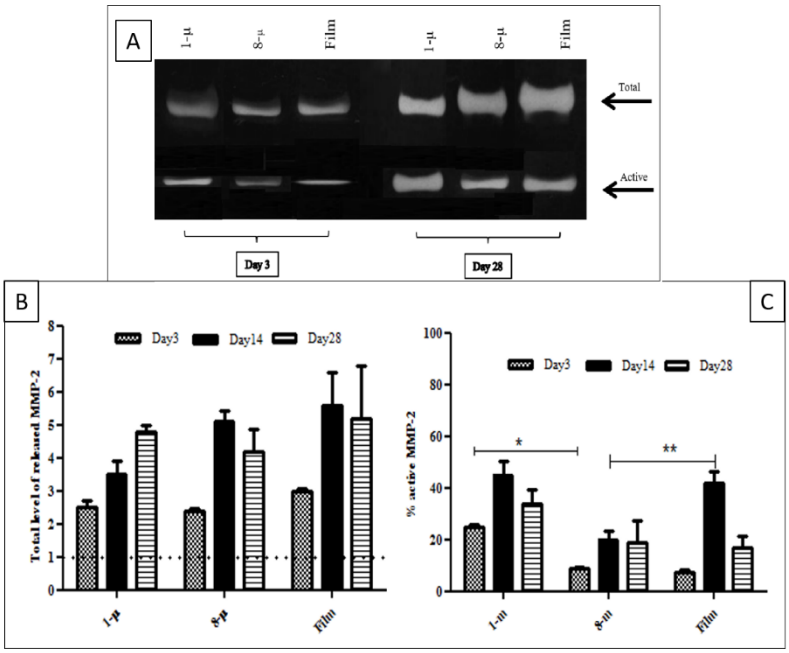

*Suppl. Figure III.1. A) Zymogram gel image of MMP-2 released by cells on 1-µm and 8-µm electrospun PLGA/PCL matrices and non-porous film, and semi-quantification of the B) total amount of MMP-2 and C) active MMP-2 released by cells. Ongoing remodeling over 28 days is visible in total MMP-2 level. Active MMP-2 reduced after 14 days. * & ** at P < 0.05 (n=4).*

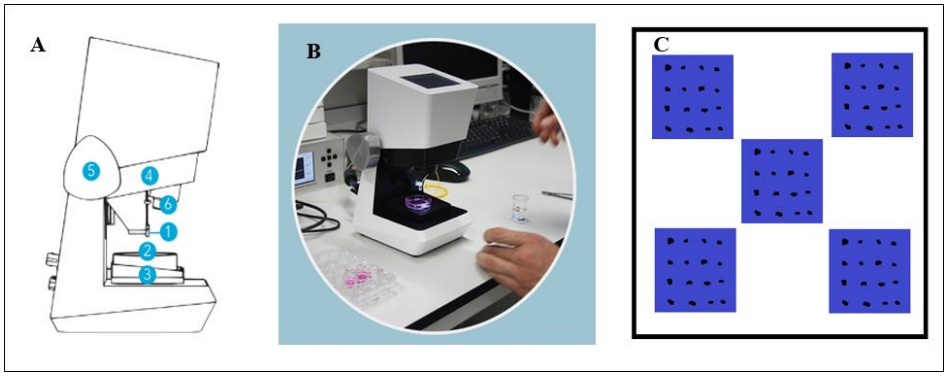

Suppl. Figure III.2. A) Schematic cross-section and B) a photopgraph of the Piuma micro-indentation device. C) the schematic of indentation map of our experiment. 16 indentations were made in 5 different areas of each sample; at the corners and in the center of each sample for a total of 80 indentations. An average distance of 500µ was considered between the indentation points.

Chapter IV

Gentle Cyclic Straining of Human Fibroblasts on Electrospun Scaffolds Enhances Their Regenerative Potential in a New Model of Pelvic Floor Loading

Mahshid Vashaghian, Chantal M. Diedrich, Behrouz Zandieh-Doulabi, Arie Werner, Theo H. Smit, Jan Paul Roovers

Submitted, Feb. 2017.

Abstract

The extracellular matrix (ECM) of fascia-like tissues is composed of a resilient network of collagenous fibers that withstand the naturally-occurring forces in pelvic cavity. When overstretched, this extracellular matrix may tear with serious clinical consequences, like pelvic organ prolapse (POP). Synthetic implants are used to provide additional support and to evoke a host response that induces new matrix production, thereby reinforcing the fascia. However, there is considerable risk of scar formation and tissue contraction leading to severe complications. Matrix producing fibroblasts are both mechanosensitive and contractile, and their behavior depends on the surface texture of the implant as well as mechanical straining. Here we investigate the effect of both in a newly-designed experimental setting. Electrospun Nylon and PLGA/PCL scaffolds and a non-porous PLGA/PCL film were clamped like a drumhead and seeded with fibroblasts derived from POP patients. Upon confluency, scaffolds were strained in cyclic, hammock-like manner for 24 or 72h at a frequency of 0.2 Hz and a stretch amplitude of 10%, thereby mimicking gentle breathing. We used non-loaded condition as control. Strained fibroblasts on electrospun scaffolds loosened their actin-fibers, thereby preventing myofibroblastic differentiation. Mechanical loading upregulated genes involved in matrix synthesis (significant effect on collagen I, III, V and elastin), matrix remodeling (α-SMA, TGF-β1, MMP-2) and inflammation (COX-2, TNF-α, IL8, IL1-β). Also, collagen genes were expressed earlier under mechanical loading and the ratio of I/III collagen increased. Matrix synthesis and remodeling genes were more upregulated on the electrospun scaffolds, while inflammation markers were more prominent on the non-porous film. Our findings suggest that mechanical straining enhances the regenerative potential of fibroblasts for regeneration of fascia-type tissues and limit the risk of scar

tissue formation; the effects increase by an electrospun texture. However, our design parameters are not generic, and should be adjusted to the implant specific function in future.

Key words: fascia, electrospinning, fibroblasts, dynamic loading, myofibroblast, pelvic organ prolapse

1. Introduction

Soft tissue injuries in the abdomino-pelvic disorders such as pelvic organ prolapse (POP) are frequently associated with symptoms of pelvic floor dysfunction that reduce the quality of life. There is much evidence that mechanical loading plays a significant role in pathophysiology of such disorders, like obesity or an excessive straining experience during child delivery [9]. Injuries like these rupture fascia; a resilient collagenous network that mechanically support and protect the skin, muscles and organs. During the last two decades, physicians have attempted to improve the outcome of POP surgery by using synthetic knitted meshes that provide mechanical support for the organs in the pelvic cavity, while the damaged tissues regenerate and regain their strength. However, these meshes bear a considerable risk for serious, sometimes irreversible, adverse events; like dyspareunia, pelvic pain, and exposure in the vagina [3,15].

Electrospun scaffolds have recently been suggested as alternative implants for fascia regeneration in general and reconstructive pelvic surgery in particular [1251,2]. The reason is that the surface texture of the electrospun scaffolds provides a structural resemblance to natural extracellular matrix (ECM) to which cells better attach, proliferate and function. Furthermore, electrospun scaffolds provide good strength and biocompatibility. Our group has recently shown that human vaginal fibroblasts from both prolapsed and non-prolapsed vaginal tissue are able to proliferate and deposit new collagenous matrix on electrospun scaffolds under static *in-vitro* conditions [1]. There is also

an important role for mechanical stimuli, which may critically affect tissue remodeling during the wound healing process [3,4]. On the other hand, lack of mechanical straining, *e.g.* as a result of implanting a stiff mesh, disturbs the remodeling processes at the tissue-implant interface. Soft tissue erosion is an example of a complication that may arise due to the rigidities in the interfacial region [32,34,126]. It is suggested that mechanical stimulation improves cell behavior when seeded on an electrospun scaffold [127,128]. Fibroblasts maintain ECM-remodeling of soft tissues in response to naturally-occurring forces in the pelvic floor like breathing[5,6]. Cells do this by producing ECM proteins such as collagen and elastin and by releasing matrix-degrading enzymes like matrix metalloproteinases (MMPs). However, the capacity of fibroblasts for modulating this process through their metabolic activities alters in pelvic floor disorders [7], and also in the presence of an implant [128]. Thus, both mechanical loading and surface structure of the implant influences the responses of host tissue cells once cells encounter the implant, under shear stresses of the body.

The objective of this study was to evaluate the effect of breath-mimicking strain on the behavior of POP-fibroblasts. Furthermore, we hypothesize that an electrospun biomimetic may enhance the mechano-biological response of fibroblasts because cells better adhere to such a surface. To investigate this, we designed a novel *in-vitro* cell culture system to stimulate POP-fibroblasts by a hammock-like straining simulating abdominal pressure. Cells are seeded on electrospun scaffolds of Nylon (non-degradable) and PLGA/PCL (degradable), or on non-porous casted films of PLGA/PCL. We subjected the cell-seeded scaffolds to cyclic loading, for 24 and 72 hours (fig.IV.1), and characterized cells for their morphology and regenerative capacity by analyzing genes involved in i) cell proliferation, ii) ECM-synthesis, iii) ECM-remodeling, and iv) catabolic activity.

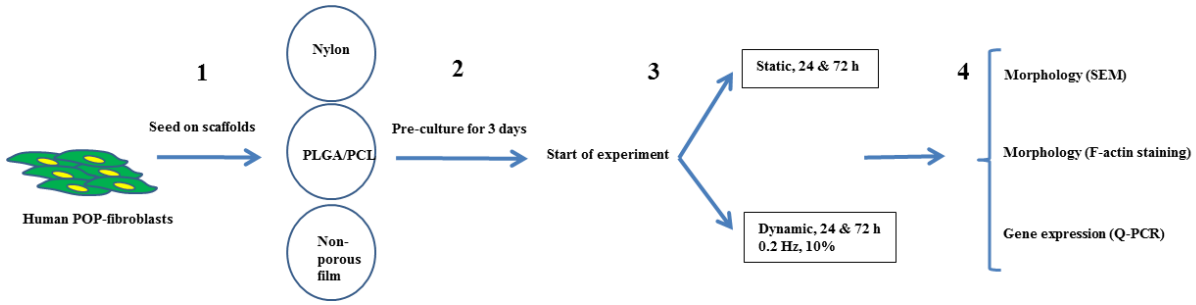

Figure IV.1. Experiment design: fibroblasts from POP-patients were pre-cultured on scaffolds, and then subjected to mechanical loading for 24 or 72h.

2. Materials and Methods

2.1. Preparation of the scaffolds

Polymer solutions of PLGA/PCL (75:25, 15%w/v, Purac, Netherlands) and Nylon (20%, Sigma, Netherlands) were prepared in chloroform and formic acid, respectively. Scaffolds were electrospun (IME Technologies, The Netherlands) at room temperature using a grounded static collector and a syringe pump (Harvard apparatus, PHD 2000, USA). Non-porous films were casted from the PLGA/PCL solution overnight. Circular samples with 2.5 cm in diameter were vacuumed overnight to remove the residual solvents. At this point, all of the scaffolds were clamped in between two sample clamps rings using pre-designed screws (fig.IV.2, C-E schematically shows how the samples were clamped like a drumhead using the screw system). The sample clamps were made of PEEK and designed with screws to increase the tightening of the scaffolds (fig.IV.2, C-E). After being clamped, scaffolds were disinfected by complete immersion in two rinsing steps of 70% ethanol, and overnight incubation in 1% antimicrobial culture medium at 37°C.

2.2. Cell isolation and pre-culturing on scaffolds

Tissue collection was approved by the medical ethical committees of VU University Medical Centre (Amsterdam) and Kennemer Gasthuis Hospital (Haarlem). Full-thickness (1 cm^2) biopsies of the anterior vaginal wall were taken from a patient undergoing reconstructive surgery of the anterior vaginal compartment. The patient was in her menopause and had a cystocele stage 2 (POP_Q classification). Within 24 h, cells were isolated and cultured as described previously [86]. Prior to the experiments, cells were grown until passage 3 in an incubator at 37 ºC, 95% humidity and 5% CO2, with culture medium: DMEM supplemented with 10% FBS, 100mg/ml streptomycin, 100 U/ml penicillin, and 250mg/ml amphotericin-B. Cells were counted and their viability was determined using a Count and Viability assay and a Muse Cell Analyzer (Merck Millipore, Darmstadt, Germany). Cells were cultured with 10%-culture medium on all clamped scaffolds at a density of 150,000 cells/cm^2 for 3 days until confluency.

2.3. Dynamic multiaxial mechanical loading

The mechanical loading experiment was performed with a custom-made instrument (fig.IV.2, A) capable of generating sinusoidal displacements with a resolution of 0.01 mm at rates between 0.01-30 Hz as described previously[9]. The instrument consists of six culture chambers and six spherical stainless-steel indenters with a diameter of 6 mm. Culture chambers and indenters were autoclaved prior to the experiment. The cell-seeded scaffolds were clamped like a drumhead (fig.IV.2, C-E), put inside the chambers and filled with culture medium. The indenters were brought into contact with the scaffold's surface (fig.IV.2, B) and fixed. Indenter displacement was controlled by a custom-made software (implemented in LabVIEW 8.2, National Instruments, Austin TX). After three days of pre-culture with POP-cells, two samples from each scaffold group were served as control (t=0, static, n=2) and two samples were subjected to a cyclic strain (t=0, dynamic, n=2) of

10% at a frequency of 0.2 Hz. Samples were harvested after 24h or 72h for evaluations of i) the immediate effects of dynamic strain (after 24 h) or ii) the effect of continuous straining (after 72 h). FigureIV.1 shows a scheme of our study design. A strain magnitude of 10% and a frequency of 0.2 Hz were chosen to mimic continuous respiration as reported previously [10]. The experiments were performed three times resulting in n=6 for each condition.

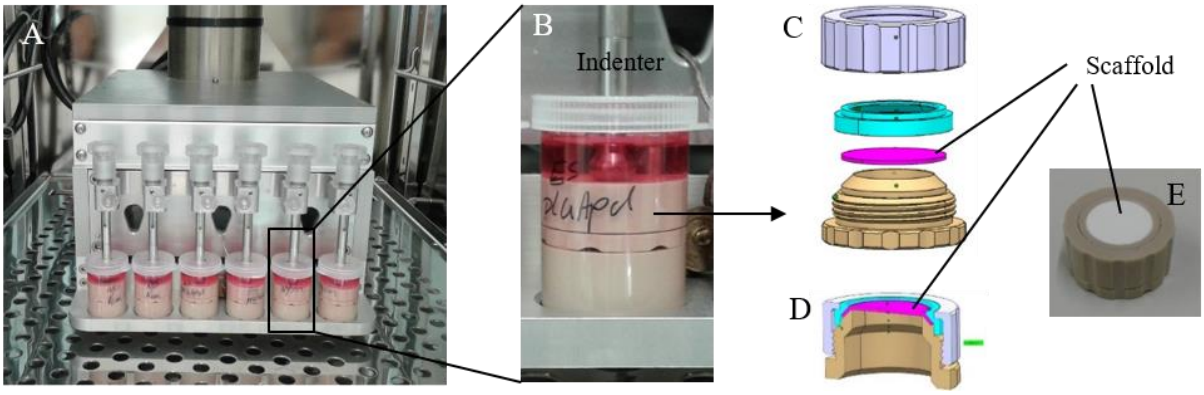

Figure IV.2. A) In-house made experimental device [129] used in this study with 6 culture chambers that can be simultaneously loaded by 6 indenter arms, B) a single culture chamber consisting of sample holder seeded with cells filled with the culture medium, C) schematic of sample clamping system designed for the scaffolds (screws help better tightening of the sample within the blue ring), D) a schematic cross-section of sample clamped between screws and rings, E) a representative clamped scaffold used in this study from top view.

2.4. Cell morphology

Cell morphology and adhesion were qualitatively evaluated by scanning electron microscopy (SEM) after 72h. Cell-seeded samples were fixed in 4% formaldehyde (pH 7.2) and underwent serial dehydration with ethanol and then sputter-coated with gold. Several magnification pictures were obtained from random spots on each sample.

2.5. F-actin staining

Cell alignment and attachment was qualitatively evaluated by F-actin staining after 72h. Cells were fixed with 4%formaldehyde and stained with Alexa Fluor 488 phalloidin (Molecular Probes, Leiden, The Netherlands). We used an inverted Leica DMIL microscope (Leica Microsystems, Germany) for evaluation.

2.6. Gene expression analysis

For gene expression analysis, cell-seeded samples were washed with PBS, and the total RNA was extracted using TRIzol (Gibco) according to the manufacturer's protocol to a final concentration of 250 ng/ml. Extracted RNA was reverse transcribed to complementary DNA (cDNA) using Fermentas synthesis kit (Life Technologies, USA), following the manufacturer's protocol. Gene expression of KI-67, COL1A1, Col3A, COL5A1, elastin, α-SMA, TGF-β1, COX2, IL1-β, IL-8, TNF-α and MMP-2 were normalized to the housekeeping genes tyrosine 3-monooxygenase/tryptophan 5-monooxygenase activation protein, zeta popypeptide (Ywhaz) and hypoxanthine-guanine phosphoribosyltransferase (HPRT). Genes were evaluated using the primers listed in Table IV.1 (Invitrogen, Thermos Fisher), with the SYBR Green Reaction Kit following suppliers' specifications (Invitrogen, Thermo Fisher) and measured by reverse transcriptase polymerase chain reaction (RT–PCR) in a Light Cycler 480 device (Roche, Germany). Gene expression levels were normalized using a factor derived from the equation $\sqrt{(Ywhaz \times HPRT)}$. Crossing points were assessed using the Light Cycler software (version 4) and plotted versus serial dilutions of cDNA derived from a human universal reference total RNA (Clontech Laboratories Palo Alto, CA, USA).

2.7. Statistical analysis

Three independent experiments were performed in duplicate, and data are expressed as mean ± standard error of the mean (SEM) or shown in graphs as mean ±standard deviation (SD). Statistical analysis was performed using Graphpad (Prism version 5.02, GraphPad Software Inc., La Jolla, CA, USA). Unpaired *t-test* was used to identify the differences between static versus dynamic values, and between 24h versus 72h values with a level of significance at $p < 0.05$. One-way analysis of variance (ANOVA) followed by Tukey–Kramer's *post hoc* test was used to identify statistical differences between three scaffolds, with a level of significance at $p < 0.001$.

Table IV.1. Primer sequences used for reverse transcriptase polymerase chain reaction (RT-PCR)

Target gene		Oligonucleotide sequence	Annealing temperature (°C)	Product size (bp)	Gene role
KI67	Forward Reverse	5'CCCTCAGCAAGCCTGAGAA 3' 5'AGAGGCGTATTAGGAGGCAAG 3'	57	202	Cell proliferation
COL1A1	Forward Reverse	5' TCCGGCTCCTGCTCCTCTTA 3' 5' GGCCAGTGTCTCCCTTG 3'	57	336	Matrix synthesis
COL3A	Forward Reverse	5' GATCCGTTCTCTGCGATGAC 3' 5' AGTTCTGAGGACCAGTAGGG 3'	56	279	Matrix synthesis
COL5A1	Forward Reverse	5' CAGGCCGATCCTGTGGATG 3' 5' GTGGCCTTCTGGAAAGAGT 3'	56	174	Matrix synthesis
Elastin	Forward Reverse	5' TTCCTGGAATTGGAGGCATCG 3' 5' AGCTCCTGGGACACCAACTA 3'	56	152	Matrix synthesis
α-SMA	Forward Reverse	5' TGGACCAACATAGTGGTGTTCT 3' 5' GAGAGGCTTTAATGTACCAGTT 3'	56	234	Matrix remodeling
MMP-2	Forward Reverse	5' GGCAGTGCAATACCTGAACA 3' 5' AGGTGTGTAGCCAATGATCCT 3'	56	232	Matrix remodeling
TGF-β1	Forward Reverse	5' CTACTACGCCAAGGAGGTCA 3' 5' CACGTGCTGCTCCACTTT 3'	56	199	Matrix remodeling
COX-2	Forward Reverse	5' GCATTCTTTGCCCAGCACTT 3' 5' AGACCAGGCACCAGACCAAAGA 3'	57	299	Inflammation mediator
IL1-β	Forward Reverse	5' TGGAGCAACAAGTGGTGTTCT 3' 5' GAGAGGTGCTGATGTACCAGTT 3'	56	270	Inflammation mediator
IL-8	Forward Reverse	5' TCTGCAGCTCTGTGTGAAG 3' 5' TGTGTTGGCGCAGTGTGG 3'	56	147	Inflammation mediator
TNF-α	Forward Reverse	5' AGAGGGCCTGTACCTCATCT 3' 5' AGGGCAATGATCCCAAAGTAG 3'	56	315	Inflammation mediator
Ywhaz	Forward Reverse	5'GATGAAGCCATTGCTGAACTTG 3' 5'CTATTTGTGGGACAGCATGGA 3'	56	229	House-keeping
HPRT	Forward Reverse	5' GCTGACCTGCTGGATTACAT 3' 5' CTTGCGACCTTGACCATCT 3'	56	260	House-keeping

Table IV.2. Characteristics of different scaffolds used in this study.

Scaffold type	Thickness (µm)	Fiber size (µm)	Pore size (μm^2)	Tensile strength (MPa)	Stiffness (MPa)
Nylon	50 ±4.5	117 ±7.81*	1.3 ±0.1*	15.4 ±3.3	13.74 ±0.8
PLGA/PCL	136 ±27	994 ±115	8.8 ±0.6	13.8 ±0.9	13.8 ±2
Non-porous film	55 ±12	NP	NP	6.3 ±0.06	0.62 ±0.03*

*Data are presented as mean ±standard deviation (*P<0.05, analysed with t-test for Nylon and PLGA/PCL, and one-way ANOVA for all three scaffolds, n=3)*

3. Results

3.1. Characteristics of scaffolds

The scaffolds were previously characterized for structural (fiber size and porosity) and mechanical properties including [59,100]; thickness, fiber size, pore size and uniaxial tensile stiffness and strength. Table IV.2 provides an overview of these properties. Nylon had thinner fibers (0.1µm) and smaller pores (1.3 μm^2) than those of PLGA/PCL (with values of about 1 µ and 8.8 μm^2, respectively). Both electrospun scaffolds were about 2.5 times stronger and 20 times stiffer than the non-porous film (tableIV.2).

3.2. Cell morphology

Under gentle cyclic loading the cells remained intact and well attached to the scaffolds (fig.IV.3). However, cyclic loading disturbed the actin-mediated cell alignment. Therefore, protein bundles and myofibroblastic-like (elongated instead of spindle-shaped) cells were observed on Nylon and film under static conditions, but not under dynamic loading (fig.IV.3).

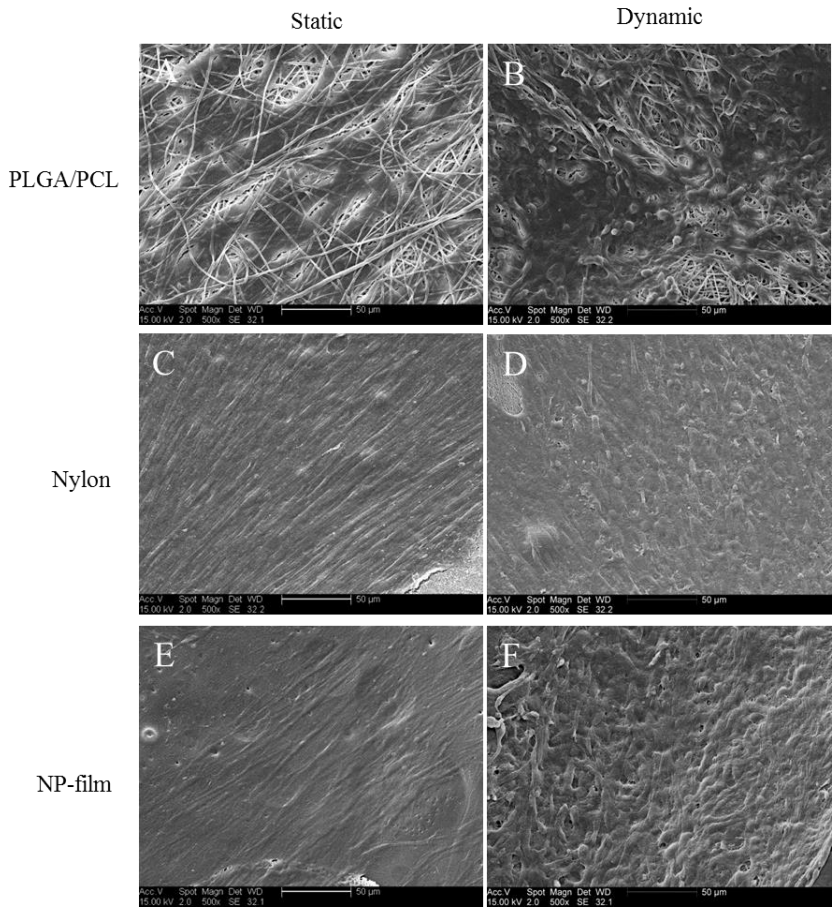

Figure IV.3. Adhesion of human vaginal fibroblasts to A, B) electrospun PLGA/PCL; C, D) electrospun Nylon; E, F) non-porous PLGA/PCL film; under static and dynamic condition, imaged by SEM after 72h. Scale bar is 50µm. Cells are elongated in static condition, but mechanical loading dis-oriented their alignment, interfering with their possible myofibroblastic differentiation.

3.3. F-actin staining

F-actin staining (fig.IV.4) confirms the outcome results of the SEM experiment. Actin fibers are more vividly active and similarly aligned under static condition, while cyclic loading disturbed the configuration of fibers in all samples. Actin fibers are irregular and unaligned under dynamic conditions.

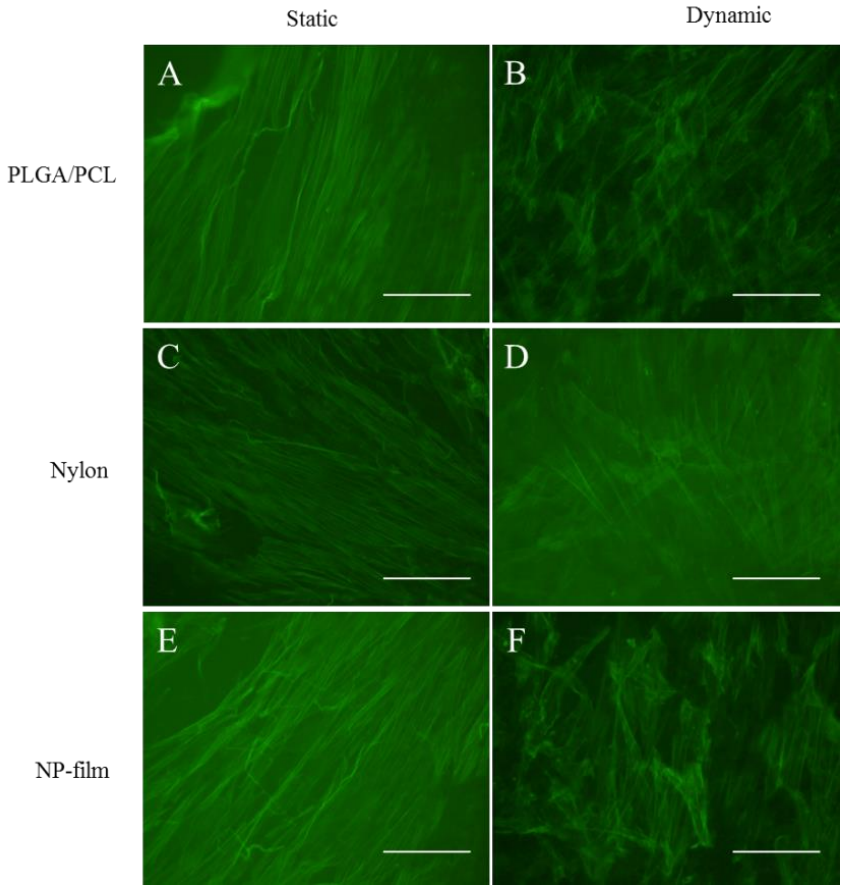

Figure IV.4. Alexa Fluor 488 phalloidin staining of human vaginal fibroblasts (F-actin fibers) on A, B) electrospun PLGA/PCL; C, D) electrospun Nylon; E, F) non-porous film; under static and dynamic condition, imaged by fluorescent microscope, after 72h. Scale bar is 50µm. Cells adhesion to the biomaterial is mediated by actin-fibers alignment in static, but mechanical loading disturbed the stretching of the fibers and cells orientation, thus myofibroblastic differentiation.

3.4. Gene expression analysis

The expression of mRNA was affected by mechanical loading (fig.IV.5) in most of the genes monitored and the effect was more significant in the first 24h. On Nylon, the cells were slightly more mechano-biologically responsive than on PLGA/PCL and the non-porous film. Expression of inflammatory mediator genes had a decreasing trend on electrospun PLGA/PCL from 24h to 72h, while it increased on non-porous film.

KI-67, a gene associated with cell proliferation, increased over time in all samples, with no significant difference between the static or dynamic condition. Matrix synthesis genes (Col I, III and V, elastin) generally upregulated over time, and faster in the first 24h. Collagen I/III ratio increased under mechanical loading conditions, particularly at 24h on the electrospun scaffolds. Elastin showed a low gene expression on all conditions. Mechanical loading also increased the relative expression of genes associated with matrix remodeling (MMP-2, TGF-β1 and α-SMA), particularly after the first 24h. Furthermore, mechanical loading generally increased the expression level of inflammatory mediator genes (TNF-α, IL1- β, IL-8 and COX-2) over time. The expression increased on the non-porous film and electrospun Nylon, but the expression was comparatively lower on electrospun PLGA/PCL. Supplementary data provides statistical differences between the scaffolds in suppl.fig.IV.1-2 and the expression values in suppl.tablesIV.1-3.

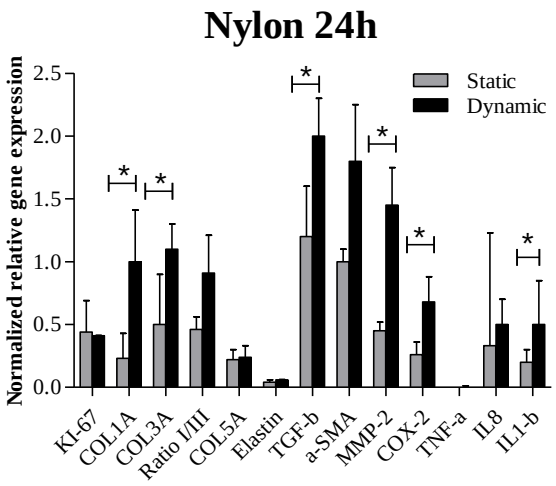
Nylon 24h
Normalized relative gene expression
Static
Dynamic
KI-67
COL1A
COL3A
Ratio I/III
COL5A
Elastin
TGF-b
a-SMA
MMP-2
COX-2
TNF-a
IL8
IL1-b

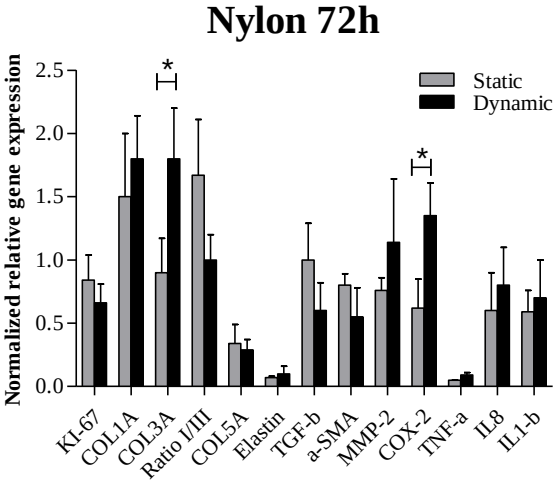
Nylon 72h
Normalized relative gene expression
Static
Dynamic
KI-67
COL1A
COL3A
Ratio I/III
COL5A
Elastin
TGF-b
a-SMA
MMP-2
COX-2
TNF-a
IL8
IL1-b

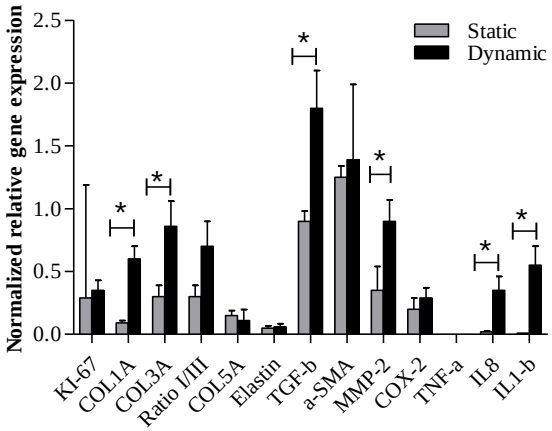
PLGA/PCL 24h
Normalized relative gene expression
Static
Dynamic
KI-67
COL1A
COL3A
Ratio I/III
COL5A
Elastin
TGF-b
a-SMA
MMP-2
COX-2
TNF-a
IL8
IL1-b

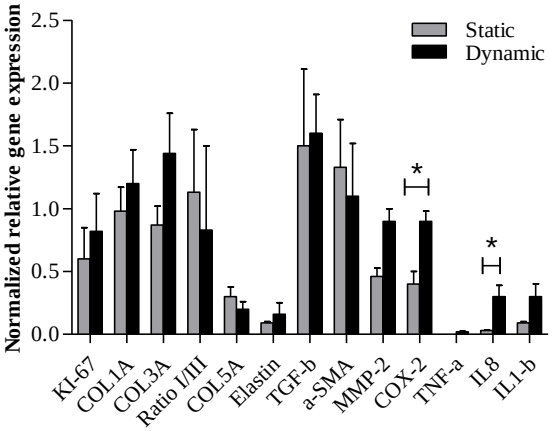
PLGA/PCL 72h
Normalized relative gene expression
Static
Dynamic
KI-67
COL1A
COL3A
Ratio I/III
COL5A
Elastin
TGF-b
a-SMA
MMP-2
COX-2
TNF-a
IL8
IL1-b

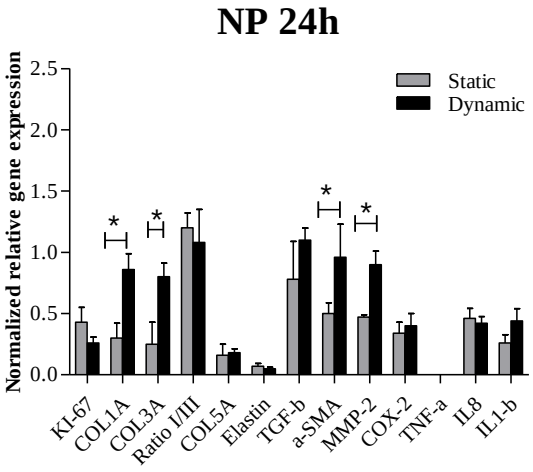
NP 24h
Normalized relative gene expression
Static
Dynamic
KI-67
COL1A
COL3A
Ratio I/III
COL5A
Elastin
TGF-b
a-SMA
MMP-2
COX-2
TNF-a
IL8
IL1-b

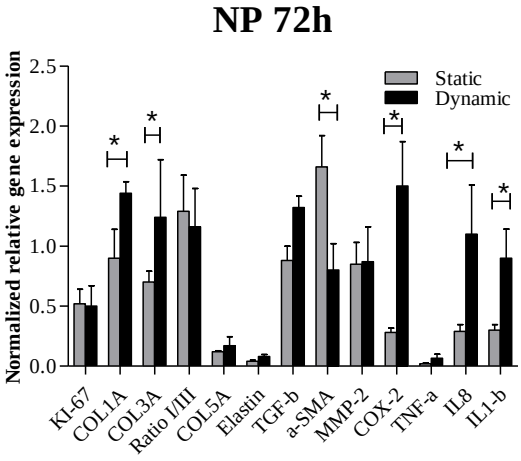
NP 72h
Normalized relative gene expression
Static
Dynamic
KI-67
COL1A
COL3A
Ratio I/III
COL5A
Elastin
TGF-b
a-SMA
MMP-2
COX-2
TNF-a
IL8
IL1-b

Figure IV.5. Relative expression of genes involved in proliferation, matrix synthesis and remodelling, and catabolic activity of cells seeded on electrospun Nylon, electrospun PLGA/PCL and non-porous (NP) films, under static and dynamic conditions after 24h and 72h. Mechanical loading noticeably enhanced the expression of matrix synthesis, remodelling and inflammatory mediator genes, and the effect was higher in the first 24h. Each bar represents the average of the means of replicates within each subject ±SD. Unpaired t-test was used for statistical analysis of differences between static and dynamic values (P < 0.05). [In supplementary data; unpaired t-test was used for statistical analysis of differences between 24h versus 72h values (* P < 0.05) , represented in suppl.fig.IV.1. ANOVA followed by Tukey–Kramer's post hoc test was used for analysis of statistical differences between the three scaffolds (*P <0.001), represented in suppl.fig.IV.2]*

4. Discussion

Mechano-biological events that occur at the tissue-implant interface affect tissue integration and long-term clinical outcomes of an implant in reconstructive surgery [15,130,131]. The implant surface should be gentle to cells and have elastic moduli similar to the adjacent soft tissues, to avoid high interfacial shear stresses and the formation of fibrous tissue and thus prevention of proper integration [34,74,132]. Electrospun scaffolds allow adhesion of host cells and their ECM synthesis; therefore, they can be potential alternatives for vaginal polypropylene meshes [100,125]. In the current study, we designed an *in-vitro* model to evaluate the effect of gentle cyclic straining on the behavior of human vaginal fibroblasts on electrospun scaffolds. Gentle loading reduces the myofibroblastic differentiation (the cells responsible for scar tissue formation and contraction) and at the same time enhances the expression level of matrix synthesis and remodeling genes. We further observe that an electrospun surface texture may contribute to a beneficial mechano-responsive behavior.

POP-cells exhibited an elongated shape (myofibroblastic morphology) on both electrospun scaffolds and non-porous film under static conditions. Mechanical loading disturbed actin-mediated stretching, which indicates that mechanical loading interferes with myofibroblastic differentiation. This result is in agreement with the observations by Blaauboer *et al.*[121] who showed

that dynamic mechanical loading prevents myofibroblastic differentiation of lung fibroblasts. Actin fibers are cellular mechanical tools to respond to mechanical tensions [133–135] , and we qualitatively show here that they are disturbed under mechanical loading. One reason might be a lack of collagen; mature collagen (which has proper alignment), can dictate cellular alignments [136], while in the dynamic condition of this study, collagen is not yet present on the scaffolds (or is very immature). It may also be that fibroblasts attachment is frustrated under cyclic loading: cells adhere to their surface prior to loading in the pre-culture period but they become disoriented after loading. As the actin cytoskeleton requires cellular tension, cells cannot find the proper counterpart to create tension and thus desorient. Prolonged experiments are required to address actin-mediate adhesion of cells under such loading conditions.

The mechano-responsive genes are mainly categorized into three types: ECM-synthesis, ECM-remodeling and inflammation [137]. Our results showed that mechanical loading upregulates all of these genes with some major findings. First, consistent with previous studies, our results showed that the enhancing effect of loading is more in the first 24h and the effect reduces after 72h [138]. When cells presumably enter matrix remodeling pathways, they release enzymes like matrix metalloproteinases that can lower their collagen production rate [139]; thus the expression is higher in the first 24h. Second, matrix synthesis genes (particularly collagen I and III) are significantly upregulated under dynamic loading, while cell proliferation was not affected as much. This implies that mechanical loading enhances the capacity of cells for regulation of their collagen genes, and the results are not a mere cause of increase in cell number. Elastin expressed low without significant increase over time. The reason may be that elastin development starts at later stages of remodeling and it also depends on strain magnitude, frequency and duration [140,141], so our study was too short-time for a proper response. The collagen I/III ratio increased by mechanical

stimulation. This ratio is important for the load-bearing characteristics of tissues, as it is shown to decrease in e.g. hernia patients [142]. Together, the results suggest that the mechanical loading enhances the ability of cells in regulating their matrix synthesis genes.

Our third finding highlights the simultaneous upregulation of the genes during experiment, and depicts an ongoing remodeling, as well as the mutual effects of genes on one another. For instance, three genes upregulated at the first 24h of loading which influence each other subsequently; α-SMA, collagen and TGF-β1. α-SMA is a precursor for collagen synthesis and cells produce collagen when differentiating to myofibroblasts (characterized by α-SMA) [57]. On the other hand, TGF-β1 is a growth factor required for both myofibroblast differentiation and collagen production [121,143]. Under mechanical loading, fibroblasts secrete TGF-β1 directly into the matrix which induces collagen synthesis and maturation [144,145]. Together, this may explain that all these genes upregulate at first 24h to induce/initiate matrix deposition, and their expression slows down after 72h. After 72h, the matrix enters a new pathway to sustain its turn-over and preventing from accumulation and scar formation; cells activate their genes for matrix-degrading enzymes (like MMPs) and release them into the matrix, while downregulating their α-SMA gene [146,147]. This sustaining pathway is particularly important in wound healing, because an excessive production of collagen can lead to accumulation and stiffening of the matrix [143], which creates problems such as implant contraction and pain. Thus, a gentle straining is required for the cells on a scaffold, that induces cells to regulate their new matrix, but at the same time prevents the abovementioned adverse events. We showed here that gentle cyclic mechanical loading of cells on the electrospun scaffolds, is beneficial because it reduces myofibroblastic differentiation, while it enhances the matrix-regulating of cells.

Our fourth finding regards the expression of inflammatory markers. Inflammation is a key aspect in wound healing after implantation of a biomaterial [148], because cells produce catabolic markers and inflammatory mediators to identify a foreign material [149]. In our study, catabolic genes generally upregulated under loading, except for TNF-α gene which was expressed very low and thus was not conclusive. Simultaneous upregulation of IL1-β and MMP-2 under cyclic loading are commensurate with previous findings that these two genes have mutual effects on one another, because inflammatory cytokines such as IL1-β upregulate MMPs in the presence of mechanical loading [150–152]. The simultaneous upregulation of COX-2 also suggests that the release of IL1-β under mechanical stimulation may be a synergetic trigger on matrix remodeling/destruction via COX-2 expression [150].

Finally, we observed that cells expressed relatively higher levels of mechano-responsive genes on electrospun scaffolds than on non-porous film, except for the inflammatory markers which expressed more strongly on the non-porous film. Cellular mechano-responsiveness is based on the ability of their focal adhesion proteins to maintain attachment to a surface [122]. An electrospun texture improves cell adhesion [153] (because it modulates the focal adhesions) and thereby enhances cells mechano-responsive behavior. Differences in surface characteristics of the scaffolds also plays a role in activating different genes. For instance, the electrospun PLGA/PCL fibers are larger than Nylon fibers, thus the surface appears rougher to the cells than on the Nylon and non-porous film (entirely smooth). In addition, electrospun Nylon has stiffer surface than PLGA/PCL [100]. Hence, surface texture may induce different levels of inflammatory pathways. On the non-porous film, cells don't grow three-dimensionally, while a porous structure provides a different pattern thus a different level of functionality for cells. Our observations suggest an interesting effect of

surface topography, which should be studied in longer-term experiments where cell infiltration occurs, and becomes a factor.

The results of this study show that POP-cells respond to cyclic mechanical loading and that the behavior depends on the scaffold's surface texture as well as on the particular loading condition, as shown by others before [59,75,76,86,100,154–156]. To the best of our knowledge, this is the first study to use electrospun scaffolds in combination with mechanical loading in a hammock-like, bi-directional stretch model instead of uniaxial tension; our model thereby better mimics the normal breathing strains occurring in the pelvic floor [86,121]. The set-up can also be used to study cell-implant interactions in other load-bearing tissues, like pulse-like abdominal pressure peaks mimicking coughing or laughing. Such experiments give a more quantitative understanding of the effect of mechanical loading on cell-matrix behavior and can also be performed to pre-clinically evaluate new implants. We need to find an optimum regime of mechanical loading that is essential for cells function without creating fibrotic tissue.

	Effect of loading at 24h			**Effect of loading at 72h**		
	Nylon	**PLGA/PCL**	**Film**	**Nylon**	**PLGA/PCL**	**Film**
Cell proliferation (KI-67)	……	……	……	↑	↑	↑
Matrix synthesis (COLI,III,V,elastin)	⇈	⇈	⇈	↑	↑	↑
Matrix remodelling (TGF-β1, α-SMA, MMP-2)	⇈	⇈	⇈	↓	↑ (α-SMA increased)	↓ (α-SMA decreased)
Inflammation mediators (COX-2, TNF-α, IL8, IL1-β)	⇈	⇈	↑	⇈	↑	⇈

Figure IV.6. Overview of up/down regulation (up/down-pointing arrows) of different genes under mechanical loading over time for three scaffolds. Cell proliferation was mainly affected after 72h. Genes involved in matrix synthesis, remodelling and inflammatory significantly upregulated under dynamic condition (double-arrows) after24h, on all three scaffolds. The effect reduced after 72h, causing the downregulation of matrix remodeling genes on Nylon and film. Upregulation of inflammatory mediator genes continued after 72h on Nylon and non-porous film.

Conclusion:

Cells change their morphological characteristics such as actin-fibers expression in response to mechanical stimuli. Measured at gene level, matrix synthesis and remodeling (in particular collagen) started earlier and significantly enhanced by mechanical loading. Inflammatory mediator markers upregulated by loading, and expressed at higher level on non-porous films. Our findings suggest that dynamic condition significantly enhances the behavior of the POP-cells on scaffolds in terms of adhesion, morphology and expression of their measured mechano-responsive genes. depending on the surface texture, and both parameters should be considered in mesh-based prolapse surgery. Electrospun scaffolds thereby appear to provide attachment for the cells and thus higher mechano-sensitivity.

Acknowledgment:

We thank Mr. Koops from the Department of Physics and Medical Technology at VU University medical center for designing the mechanical loading device.

Supplementary data:

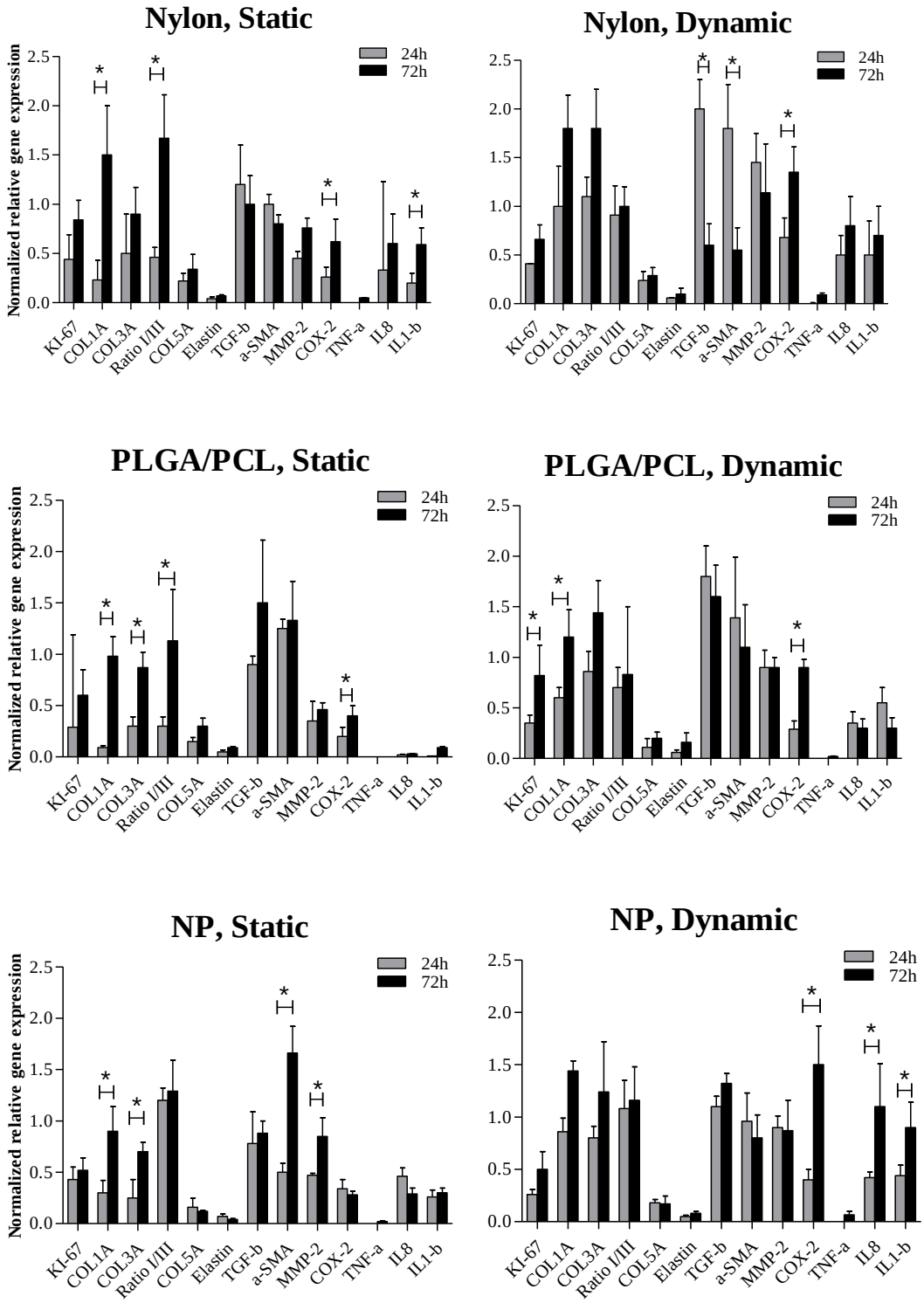

Suppl. Figure IV.1. Relative expression of genes involved in proliferation, matrix synthesis and remodeling, and catabolic activity of cells seeded on electrospun Nylon, electrospun PLGA/PCL and non-porous (NP) films, under static and dynamic conditions after 24h and 72h. Each bar represents the average of the means of replicates within each subject ±SD. Unpaired t-test was used for statistical analysis of differences between 24h versus 72h values (p < 0.05).*

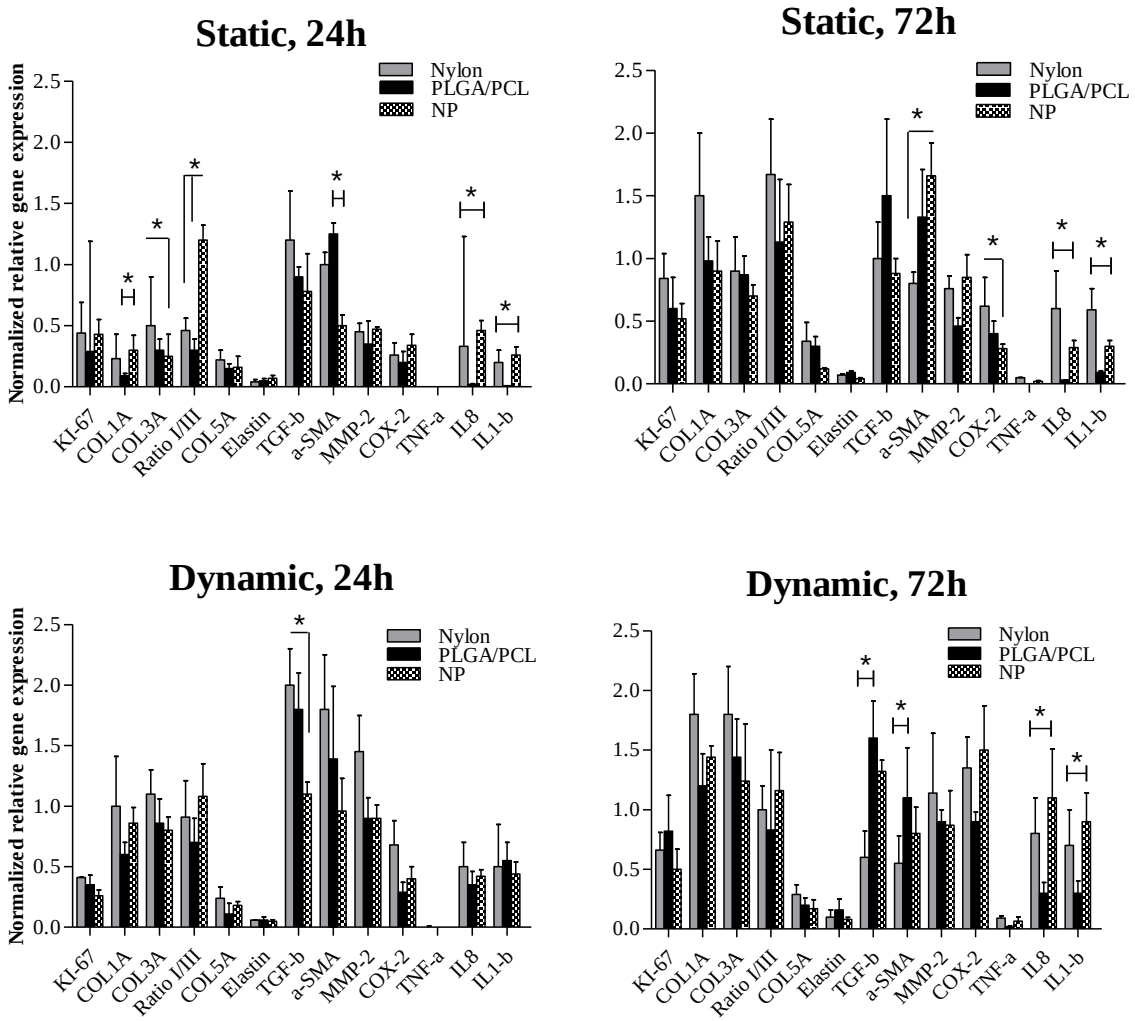

Suppl. Figure IV.2. Relative expression of genes involved in proliferation, matrix synthesis and remodeling, and catabolic activity of cells seeded on electrospun Nylon, electrospun PLGA/PCL and non-porous (NP) films, under static and dynamic conditions after 24h and 72h. Each bar represents the average of the means of replicates within each subject ±SD. ANOVA followed by Tukey–Kramer's post hoc test was used for analysis of statistical differences between the three scaffolds (p <0.001).*

Supp. Table IV.1. Relative expression values of genes involved in proliferation, matrix synthesis and remodeling, and catabolic activity of cells seeded on electrospun Nylon, under static and dynamic conditions after 24h and 72h. Each value represents the average of the means of replicates within each subject ±SD.

Nylon, 24h **Gene**	**Static**	**Dynamic**	**Nylon, 72h** **Gene**	**Static**	**Dynamic**
KI-67	0.440 ±0.25	0.410 ±0.002	**KI-67**	0.840 ±0.200	0.660 ±0.150
COL1A	0.230 ±0.20	1.000 ±0.410	**COL1A**	1.500 ±0.500	1.800 ±0.340
COL3A	0.500 ±0.40	1.100 ±0.200	**COL3A**	0.900 ±0.270	1.800 ±0.400
Ratio I/III	0.460 ±0.10	0.910 ±0.300	**Ratio I/III**	1.670 ±0.440	1.000 ±0.200
COL5A	0.220 ±0.08	0.240 ±0.090	**COL5A**	0.340 ±0.150	0.290 ±0.080
Elastin	0.040 ±0.02	0.060 ±0.001	**Elastin**	0.070 ±0.010	0.100 ±0.060
TGF-β	1.200 ±0.40	2.000 ±0.300	**TGF-β**	1.000 ±0.290	0.600 ±0.220
α-SMA	1.000 ±0.10	1.800 ±0.450	**α-SMA**	0.800 ±0.090	0.550 ±0.230
MMP-2	0.450 ±0.07	1.450 ±0.300	**MMP-2**	0.760 ±0.100	1.140 ±0.500
COX-2	0.260 ±0.10	0.680 ±0.200	**COX-2**	0.620 ±0.230	1.350 ±0.260
TNF-α	0.001 ±0.00	0.001 ±0.010	**TNF-α**	0.050 ±0.001	0.090 ±0.020
IL8	0.330 ±0.90	0.500 ±0.200	**IL8**	0.600 ±0.300	0.800 ±0.300
IL1-β	0.200 ±0.10	0.500 ±0.350	**IL1-β**	0.590 ±0.170	0.700 ±0.300

Supp. Table IV.2. Relative expression values of genes involved in proliferation, matrix synthesis and remodeling, and catabolic activity of cells seeded on electrospun PLGA/PCL, under static and dynamic conditions after 24h and 72h. Each value represents the average of the means of replicates within each subject ±SD.

PLGA/PCL, 24h **Gene**	**Static**	**Dynamic**	**PLGA/PCL,72h** **Gene**	**Static**	**Dynamic**
KI-67	0.290 ±0.900	0.350 ±0.080	**KI-67**	0.600 ±0.250	0.820 ±0.300
COL1A	0.090 ±0.020	0.600 ±0.100	**COL1A**	0.980 ±0.190	1.200 ±0.270
COL3A	0.300 ±0.090	0.860 ±0.200	**COL3A**	0.870 ±0.150	1.440 ±0.320
Ratio I/III	0.300 ±0.090	0.700 ±0.200	**Ratio I/III**	1.130 ±0.500	0.830 ±0.670
COL5A	0.150 ±0.038	0.110 ±0.088	**COL5A**	0.300 ±0.076	0.200 ±0.061
Elastin	0.050 ±0.018	0.060 ±0.025	**Elastin**	0.090 ±0.012	0.160 ±0.092
TGF-β	0.900 ±0.080	1.800 ±0.300	**TGF-β**	1.500 ±0.610	1.600 ±0.310
α-SMA	1.250 ±0.090	1.390 ±0.600	**α-SMA**	1.330 ±0.380	1.100 ±0.420
MMP-2	0.350 ±0.190	0.900 ±0.170	**MMP-2**	0.460 ±0.067	0.900 ±0.100
COX-2	0.200 ±0.090	0.290 ±0.081	**COX-2**	0.400 ±0.100	0.900 ±0.080
TNF-α	0.001 ±0.000	0.001 ±0.000	**TNF-α**	0.000 ±0.000	0.020 ±0.005
IL8	0.020 ±0.007	0.350 ±0.111	**IL8**	0.030 ±0.003	0.300 ±0.090
IL1-β	0.009 ±0.000	0.550 ±0.150	**IL1-β**	0.090 ±0.012	0.300 ±0.102

Supp. Table IV.3. Relative expression values of genes involved in proliferation, matrix synthesis and remodeling, and catabolic activity of cells seeded on non-porous PLGA/PCL film, under static and dynamic conditions after 24h and 72h. Each value represents the average of the means of replicates within each subject ±SD.

Film, 24h **Gene**	**Static**	**Dynamic**	**Film, 72h** **Gene**	**Static**	**Dynamic**
KI-67	0.430 ±0.120	0.260 ±0.049	**KI-67**	0.520 ±0.120	0.500 ±0.170
COL1A	0.300 ±0.120	0.860 ±0.128	**COL1A**	0.900 ±0.240	1.440 ±0.096
COL3A	0.250 ±0.180	0.800 ±0.111	**COL3A**	0.700 ±0.090	1.240 ±0.480
Ratio I/III	1.200 ±0.120	1.080 ±0.270	**Ratio I/III**	1.290 ±0.300	1.160 ±0.320
COL5A	0.160 ±0.090	0.180 ±0.031	**COL5A**	0.120 ±0.009	0.170 ±0.076
Elastin	0.070 ±0.022	0.050 ±0.011	**Elastin**	0.040 ±0.009	0.080 ±0.018
TGF-β	0.780 ±0.310	1.100 ±0.098	**TGF-β**	0.880 ±0.120	1.320 ±0.095
α-SMA	0.500 ±0.087	0.960 ±0.270	**α-SMA**	1.660 ±0.260	0.800 ±0.220
MMP-2	0.470 ±0.020	0.900 ±0.110	**MMP-2**	0.850 ±0.180	0.870 ±0.290
COX-2	0.340 ±0.090	0.400 ±0.100	**COX-2**	0.280 ±0.037	1.500 ±0.370
TNF-α	0.001 ±0.000	0.001 ±0.000	**TNF-α**	0.020 ±0.006	0.066 ±0.033
IL8	0.460 ±0.081	0.420 ±0.056	**IL8**	0.290 ±0.055	1.100 ±0.410
IL1-β	0.260 ±0.066	0.440 ±0.100	**IL1-β**	0.300 ±0.045	0.900 ±0.241

Chapter V

Biomimetic Implants for Urogynaecology

Mahshid Vashaghian, Sebastian A.J. Zaat, Theo H. Smit, Jan Paul Roovers

Neurourology and Urodynamics 2016; under revision.

Abstract

Aims: polypropylene implants are used for the reconstructive surgery of urogynaecological disorders, but severe complications associated with their use have been reported. There is evidence that the difference of biomechanical properties between the implant and the surrounding tissues contribute to these adverse events. Electrospinning is an innovative engineering alternative that provides a biomimetic microstructure of implants, resulting in a different mechano-biological performance. The main objective of this review is to stage the potential of electrospun matrices as an alternative modality for the treatment of pelvic floor disorders, based on the current *in-vitro* and *in-vivo* studies for soft tissue engineering.

Methods: publications with the following studies of electrospun matrices were reviewed; i) the technique, ii) *in-vitro* use for soft tissue engineering, iii) *in-vivo* use for reconstruction of soft tissues in animals and iv) clinical use in humans.

Results: based on the current literature, electrospun matrices provide a synthetic mimic of natural extracellular matrix (ECM) and (thus) favor cellular attachment, proliferation and matrix deposition, through which a proper tissue-implant interaction can be established. Electrospun sheets can also be created with sufficient mechanical strength and stiffness, which makes them suitable for load-bearing implants.

Conclusion: electrospun matrices mimic the structural topography of the extracellular matrix and can be functionalized for better biological performance. As such, they have great potential for the next generation of urogynecological implants. However, their long term safety and efficacy must still be evaluated *in-vivo*.

Key words: biomimetic, electrospun, nanofibers, reconstructive surgery, ECM.

Outline of the review:

1. Clinical limitations of polypropylene as biomaterial for pelvic floor surgery

2. The role of poor microstructure on clinical complications

I. Porosity

II. Mesh weight

III. Filament type

IV. Elasticity and strength

V. Degree of (an)isotropic

3. Electrospun biomimetic matrices: alternative biomaterials for pelvic floor repair

3.1.Technique

3.2.Characteristics of electrospun biomaterials

I. Effect of material

II. Effect of (micro)structure

4. What issues are clinically relevant *in-vivo*

I. Host response, new matrix deposition and tissue regeneration

II. Integration and vascularization

III. Biomechanics

5. Biomaterials functionalized with electrospun nanofibers

6. Challenges and future prospects

7. Conclusion

1. Clinical limitations of polypropylene as biomaterial for pelvic floor surgery

Soft connective tissues provide mechanical support to the organs in the abdominal cavity and contribute to the Intra-Abdominal Pressure (IAP). Their mechanical properties are vital for their functioning, meaning that overstretching can result in tissue damage and the development of conditions such as pelvic organ prolapse (POP) and stress urinary incontinence (SUI).[1] These conditions affect more than 50% of the people worldwide [3]. Additional mechanical support then is required for functional repair. One of the current treatments is the application of an implant through reconstructive surgery [12]. Implants are either derived from native tissues like SIS or are synthetic knitted polypropylene, commonly known as "mesh" [12], with different knitting textures and styles [13, 14]. The native tissue implants normally lack the sufficient mechanical strength for load-bearing areas like pelvic floor and lose their integrity after sometime [10,11]. Synthetic meshes, on the other hand, are stronger for longer-term use without significant loss of their mechanical properties. The meshes proved satisfactory in many patients, but also have caused severe complications in a significant part of the operated women. Chronic inflammation and pain, vaginal erosion [16] (15.6-24%), dyspareunia [17] (9%) (difficult or painful sexual intercourse) and bleeding are some frequent problems associated with use of transvaginal knitted meshes in up to 70% of the patients within 10-years [18,19]. Due to the repeatedly reported complications, the US Food and Drug Administration (FDA) released a safety warning recall associated with the use of meshes several times [20–23]. Such high numbers of patients and complications with the current surgical meshes, draws our attention to a serious unmet demand for development of new solutions.

2. The role of poor microstructure on clinical complications

An ideal biomaterial for repair of the weakened tissues of the pelvic floor should be like a hammock: mechanically strong, relatively stiff under tension, and flexible under bending. As an implant, it also should be biocompatible, able to induce host response (bioactive rather than bio-inert) and provide a proper environment for cell interactions. Bioactive here refers to the mechano-biological function of the implant: how mechanical stiffness and forces activate, regulate, control, and influence cell behavior like adhesion, proliferation and new matrix production. Current implants are biomechanically strong enough to support the protrusion of organs, but their bioactivity may not be optimal. Characteristics of an ideal implant, are determined by its microstructure as well as its chemical composition (material type). These characteristics should be

essentially orchestrated together in order to bring good clinical outcomes. The first one, microstructure, is predominantly dictated by the fabrication method. Among the available techniques for fabricating the pelvic floor meshes, knitting is the most common one.

Polypropylene knitted mesh is non-degradable, inert, nontoxic, antigenic and macro-porous, according to Amid's classifications [30]. To date, there are different knitted polypropylene meshes with different microstructures available [31]. The importance of the microstructure becomes more relevant once we realize that it plays a significant role in the pathology of the mesh-related complications [32–34]; because based on the previous findings, it appears to be not optimal for the vaginal repair surgery. The most determinant (and also problem making) parameters of the microstructure in these meshes are: size and shape of the porosities, weight (gr of material/m^2) and filaments type.

Porosity of the mesh refers to geometry and size of the mesh, and the overall void space (known as "porosity") of the pores. In general, porosity is a factor of the knitting style of the mesh [35]. The pore size, for example, should be large enough (>75µm) to allow cellular infiltration[35,157]. Mesh flexibility also enhances with smaller pores [26]. Small pore size limits cellular infiltration, and therefore proper integration of the mesh with the host tissue. Lack of proper integration can further develop to encapsulation and erosion of the mesh [36]. Multifilament meshes generally have smaller pores (around 10µm or less), and thus inhibit ingrowth of collagenous ECM [158]. In addition to size, geometry of pores is also important. For instance, pores with rectangular sections were found to lead to formation of larger amounts of tissue compared to square section pores; and between elliptic and circular pores in porous scaffolds [38]. Similarly, force transmission through the mesh structure under mechanical loading, differs between various pore shapes [31,39,40]. In addition, porosity may decrease significantly under high (uniaxial) mechanical loading [39,40] that can limit tissue integration *in-vivo* [40,159]. Thus, mesh should be porous enough with proper pore shape and geometry to allow cellular infiltration and optimal integration.

Mesh weight is another structural feature that to some extent depends on porosity; meshes with higher porosity are relatively lighter [41]. Relatively heavy meshes cause more complications such as fibrosis at the tissue-implant interface than the lighter ones [42,43]. In heavy meshes, there is more amount of surface of the foreign material being exposed to the host tissue, which induces more

foreign body reaction [44–46]. In general, less foreign material may lead to better clinical outcomes in longer-term. Therefore, a thinner lighter mesh could have potential benefits.

Filament type, is another factor of the knitting fabrication. Knitted meshes are mono- or multi-filaments based. Multifilament meshes, are generally suggested to cause more complications (fibrosis and inflammatory response) compared to monofilaments [47,48]. The reason here is also the more amount of materials being available to the host tissue in multifilament meshes which induces more foreign body reactions [44]. Also, in multifilament meshes the gap between individual filaments are small which inhibits penetration of the immune cells to clear bacteria in case of an infection [36]. Thus, there is more rate of infection with multifilament meshes [160]. Furthermore, bacterial adherence is greater in multifilament braided meshes than monofilaments, because bacteria more easily propagate in the tissue between the multifilaments [161,162]. Monofilament meshes, or in other words thin and light meshes with more homogenous pore geometry would be advantageous. Thus, the implant microstructural characteristics have impact on the clinical outcome not only through direct biomechanical and mechano-biological characteristics, but also by indirect effects such as increasing susceptibility to infection.

Elasticity and strength of the mesh determine its biomechanical behavior *in-vivo*. Prolapse meshes are generally stiffer than the soft tissue, which is because of their knitting microstructure, as well as their material [31,49,50]. When the stiff mesh slides along the soft tissue under shear stresses, it creates frictions at the tissue-implant interface, particularly at the bulge-like areas where the filaments are knitted into each other. Due to these interfacial frictions (known as "stress-shielding"), the remodeling capacity of underlying tissue cells in response to mechanical stimuli declines, which can eventually result in vaginal erosion [52,53]. In addition, these interfacial mechano-biological events can cause excessive matrix production. This newly-made matrix, accumulates and develops into a stiff, fibrotic and thus non-functional tissue [19,32,34,72,121]. This is why soft tissue stiffens in the months after mesh implantation [163]. Mesh contractions and fibrotic encapsulation can also result from the scar tissue formation around the mesh [54–57]. Therefore, an ideal implant should be strong and to some extent stiff, but should be gentle at the same time to provide proper host response under loading.

Degree of (an)isotropic architecture of the vaginal mesh is another important factor, given the anisotropic characteristics of the pelvic organs [90,164,165], and the multidimensional nature of the

forces in pelvic floor [165,166] which the mesh is exposed to. An isotropic mesh has the same structural and mechanical properties along all loading directions, while in anisotropic one, those of the properties are directionally dependent or contingent on the loading direction. Some studies suggest that surgeons should consider the anisotropic behavior of the mesh prior to implantation [49]. For instance, the mesh had better be implanted from its stiffer direction, aligned with the transverse direction of the abdominal muscle tissues to put up with the forces more effectively [44]. One way is to design meshes that can mimic the anisotropic behavior of the host tissues [168–171], although the challenge is to keep the consistency because the (bio)mechanical properties of the meshes change after long-term implantations[170,172]. On the other hand, many studies have suggested to use isotropic implants; that can tolerate forces in multiple axis. Whether an isotropic or anisotropic implant is preferred for the complicated anatomy of pelvic floor or not, is not yet well-documented. More studies are first required to address the biomechanics of pelvic floor, for designing an appropriate implant.

Given the fact that the knitted meshes were initially designed for the hernia repair (where they also created complications [26,27]), their characteristics were never tailored for vaginal prolapse surgery [28,29]. Unsuccessful trials with different materials and textures suggests that implant structure might be an important problem-making paradigm; macro-scale structure may be invasive for cells as the protein adsorption mechanisms, cell-cell and cell-biomaterial interactions may not be optimal. A knitted implant, comes with certain characteristics that can harm cells and disturb their natural remodeling and wound healing process. One way to improve the existing mesh-based treatments, is to introduce and investigate a different level of microstructure with cell-scale fibers that cells can adhere and respond to. Such microstructure, which may be a beneficial alternative to regulate cell-biomaterial interactions, can be created by electrospinning technique. Electrospinning is an opportunity to produce a different class of implants with nano-to-micro fibers and versatile variety of parameters.

Matrices produced by electrospinning (fig.V.1), consist of nano-to-micro fibers that provide an architecture similar to the architecture of the native extracellular matrix (ECM), like the collagen fibrils which are around 300-375 nm. An electrospun matrix deforms without shearing the fibers and thus is gentler to the cells. This geometrical resemblance in microstructure, plus the high surface area-to-volume ratio of the nanofibers supports cell-cell and cell-substrate bindings

(fig.V.2). Such a micro-environment facilitates cell adhesion to their surface and therefore their matrix producing capacities [66,68] as well as their mechano-biological function improves.

We continue this review with a general presentation of the electrospinning technology and then discuss the potential of this techniques for soft tissue engineering in general, and urogynaecological applications in particular.

3. Electrospun biomimetic matrices: alternative biomaterials for pelvic floor repair

3.1. Technique

Electrospinning uses electrostatic forces to create polymeric nanofibers from polymer solutions or melts. The set-up (fig.V.1) consists of a voltage supplier, a syringe pump for extrusion of polymer solution/melt, syringe container, the needle and a conductive collector. The polymer solution is ejected through the syringe needle in the form of a jet. An electric potential is created between the negatively-charged needle and the collector, which draws the polymer jet towards the collector. This process results in ultrathin fibers, continuously deposited on the collector resulting in fabrication of a non-woven matrix. Fibers typically have a diameter ranging from 10 nm to 10 μm, leading to matrices with high surface-area-to-volume ratio (fig.V.2).

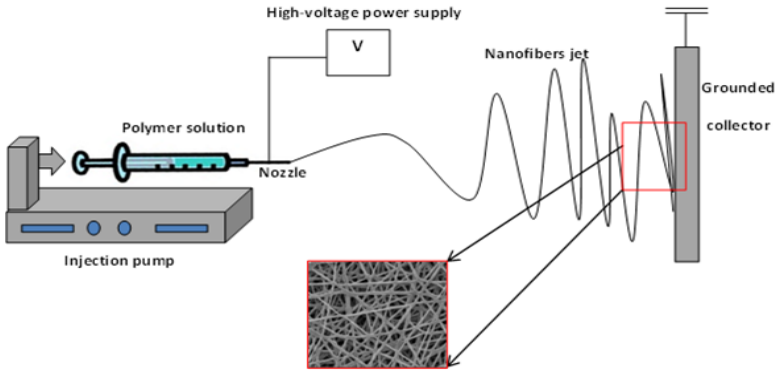

Figure V.1. Schematic illustration of the electrospinning setup. The nozzle of the syringe becomes electrically charge when a high voltage is applied. This creates an electrical charge difference between the nozzle and the grounded-collector. By simultaneously ejecting a polymer solution through the nozzle, a polymeric (nano)fiber jet is formed toward the collector that results in random deposition of nano-to-micro fibers on the collector.

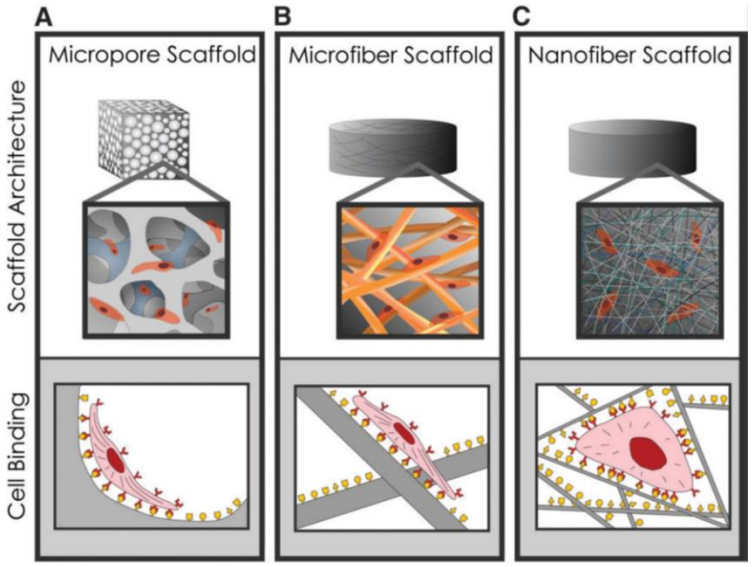

Figure V.2. Scaffold architecture affects cell binding and spreading. (A and B) Cells binding to scaffolds with microscale architectures flatten and spread as if cultured on flat surfaces. (C) Scaffolds with nanoscale architectures have larger surface areas to adsorb proteins, presenting many more binding sites to cell membrane receptors. The adsorbed proteins may also change conformation, exposing additional cryptic binding sites [66].

The geometrical and mechanical properties of electrospun matrices are fine-tuned through alteration of the process parameters [173–181]. Polymer concentration, rate of spinning, voltage, type of solvent and ambient conditions such as temperature are the most important conditions to achieve a particular result. While this wide range of variables can serve to control the material characteristics, it also creates a challenge to replicate the outcome of the spinning process. Thus, these variables should be controlled as much and precisely as possible. For excellent reviews on the effect of specific processing conditions, we refer to previous publications [177–181]. Here we discuss the potential of electrospinning with respect to the requirements for regeneration of soft tissues in the pelvic floor.

3.2. Characteristics of electrospun biomaterials

Mechanical and structural characteristics of an implant are determined by its material chemistry and its microstructure. In this review, we mainly discuss these characteristics in an electrospun matrix with respect to how they affect cellular responses or the implant behavior based on the cell culture and animal studies, respectively.

i) effect of material

Electrospun fibers can be made of a wide range of biological or synthetic polymers and the choice depends on the specific application and patient condition [182,183]. Age, obesity, parity, genetics, soft tissue disorders and medical history are important to consider. For example, in post-menopausal or older patients whose remodeling capacity might have changed, a permanent implant might be needed that can last for decades. In pre-menopausal or younger patients, a degradable material can be used which simulates body heal itself and degrades while the new tissue matures.

First of all, a biomaterial is required that cells can attach to, because most of the mammalian cells are anchorage-dependent; meaning that they only function if they can adhere well to their substrate. Hydrophilic materials have more affinity to absorb water, so absorb adhesion proteins existing on the cell membrane [184]. If a material is hydrophobic, it can be blended with a more hydrophilic component [185], or post-modification methods such as plasma, laser or grafting [186,187] are used to increase the hydrophilicity. Nevertheless, electrospun matrices in general, absorb more adhesion protein molecules compared to a non-fibrous surface because of their higher surface area-to-volume ratio [188], therefore promote cell adhesion.

Biological polymers such as collagen, silk or fibrin are generally more adhesive for cells than synthetic ones, because their chemical composition is comparable to the natural tissues with protein ligands on their surface. These protein binding sites, for instance present on electrospun collagen, fibrinogen or silk [189–192] , promote cell adhesion and thus regulating cell functions such as proliferation, matrix deposition and remodeling [193]. For instance, silk-fibroin electrospun matrices that were used for reconstruction of the urethra, supported the growth of urothelial cells at implantation site and regeneration of the urethra after 6 months [191]. However, these matrices are often discouraged for load-bearing applications, in particular because of their long-term mechanical properties: due to their inherent biodegradability they lose their integrity and strength leading to premature resorption or failure of the biomaterial and the tissues in regeneration.

Synthetic polymers provide better mechanical properties than natural polymers and are more commonly used for electrospinning, although some of them are not conventionally spin-able. For instance, polypropylene cannot be dissolved in organic solvents, and therefore it is very challenging to electrospin. Synthetic polymers are either degradable or non-degradable. Degradable polymers are commonly FDA-approved polyesters which are biocompatible and well-suited for biomedical applications. Examples of these polymers are polycaprolactone [82,194] (PCL),

polylactic acid [74](PLA), polylactic-co-glycolic-acid (PLGA), polyurethanes [102](PU), and mixtures of these. Non-degradable biomaterials include polymers such as polyamides [147,195], polyethylene terephthalate (PET) [196], polystyrene [195] and Nylon. Non-degradable materials are not degraded through metabolic activities of the body, and therefore are generally associated with more risks involved with their long-term use.

Since there are no cellular adhesion sites on synthetic materials, sufficient cell adhesion should be provided through either a proper chemistry (hydrophilic materials) or geometrical topography. For instance, human mesenchymal stem cells (hMSCs) secreted more of the focal adhesion protein paxillin (an adaptor protein involved in cells adhesion) when cultured on eletrospun PLGA matrices than on non-porous PLGA films [197]. Different types of cells have demonstrated great biocompatibility with electrospun matrices, including fibroblasts, hMSCs, vein endothelial cells, smooth muscle cells [22, 36,199]. Cells can anchor between the nanofibers and elongate their actin proteins better than on non-fibrous membranes [82,194]. Through such interactions with the surface, cells can proliferate and deposit new layers of ECM. Electrospun PLA matrices have shown to allow adhesion of fibroblasts and rat embryonic stem cells. Cells produce abundant amounts of matrix proteins like collagen and elastin on fibrous PLA, more than they do on non-fibrous surface [74]. Fibroblasts and breast epithelial cells also produce a 3D network of ECM fibers like fibronectin on electrospun polyamide matrices [147,195]; indeed, these exhibit the morphology and characteristics of their *in-vivo* counterparts better on fibrous matrices than on non-porous membranes. Our group recently showed that human vaginal fibroblasts derived from healthy tissues and from pelvic organ prolapse patients remained functional on Nylon, PLGA/PCL and PCL/Gelatin electrospun matrices for 24 days, proliferating and producing abundant amount of new collagen on all of these matrices [100]. These findings suggest that cells are adherent and thus functional on electrospun nanofibers.

Sometimes, a blend of polymers is used to improve particular properties of the electrospun matrices. Semi-synthetic matrices are composed of synthetic and biological components or tissue extract component [200] (the latter is often referred to as “hybrids”). In this case, the biological component provides adhesion ligands for cellular reaction, as well as growth factors which promote tissue remodeling [201], while the synthetic component provides mechanical strength [22, 36,199]. Cells show great biocompatibility, adhesion and matrix deposition on semi-synthetic

electrospun matrices [81,175,202,203]. Incorporation of biological components in a hybrid may compromise the mechanical properties, because increasing the ratio of biologic part led to decreased tensile strength and ultimate strain of the implants [199,200]. However, the biological component promotes cell adhesion through which they produce a new layer of matrix and sustain the mechanical integrity of the biomaterial when the polymer degrades [199,204]. Yet, the mechanical properties of hybrids are not as good as those of synthetic ones.

The biomaterial can also be a blend of two synthetic polymers. For example, PLGA/PCL blend has mechanical properties comparable to those recommended for reconstructive pelvic surgery [80,205]. The PCL component is used to improve the tensile strength [205] while PLGA adds to the hydrophilicity of the mixture, since PCL alone is very hydrophobic [81]. Electrospun PLGA alone also has shown considerable shrinkage when seeded with cells, while adding PCL limits the shrinkage in the blend composition [206]. In addition to the material properties, fibroblasts showed to contribute to enhancing the biomechanical properties of the electrospun PLGA/PCL matrices by producing new layers of matrix around them *in-vitro* [204]. The mechanical strength of the non-seeded electrospun PLGA/PCL kept in the medium decreased over time due to partial degradation of the polymers, while when they were seeded with fibroblasts, the strength and elongation increased because cells compensated for the mechanical loss with deposition of new matrix. This revealed that electrospun PLGA/PCL have the potential for regeneration of the chronic wounds on the long-term [204].

The minimum necessary considerations to take when selecting a material for spinning are: spin-ability, hydrophilicity, mechanical properties and the degradability. Although there are not so many materials that can meet all the above criteria, but if a material has some advantages that makes it suitable for a specific application, there are often ways to improve its properties by methods which were briefly mentioned earlier.

ii) effect of (micro)structure

A) porosity

Biomaterial should be porous enough to allow cellular infiltration [187,207], for integration and vascularization of the implant. The newly-formed tissue is more functional if it grows 3-dimensionally and there are vessels in it to feed the cells. Electrospun matrices have a reputation

to limit the cellular infiltration because of their small pore size. In biological-based or semi-synthetic (hybrid) electrospun matrices, such as PCL/Gelatin, cells have more potential to infiltrate the matrices by partially degrading (enzymatic) the biological part [189,190]. Bladder smooth muscle cells infiltrated electrospun fibrinogen and remodeled it by increasingly replacing the fibrinogen with collagen [208]. Or in semi-synthetic matrices, increasing the concentration of biological component, enhanced cellular infiltration and matrix deposition [203]. Increasing the porosity in an electrospun hybrid of PLGA with bladder acellular matrix, improved the ingrowth of bladder smooth muscle cells, while new tissue was formed around the implants [209]. In another study, increasing the porosity in a bilayer electrospun PLA matrix, allowed substantially more cell penetration and better vascularization of the implant [109]. Subcutaneous implantation of the same matrices in rabbits showed that cells infiltrated through the entire thickness of the implants within 7 days and produced new collagen and new blood vessels were formed [70].

The above may occur to a lesser extent in synthetic biomaterials that degrade slower. Therefore, different techniques have been proposed to increase the pore size in synthetic electrospun matrices; changing the process conditions, using sacrificial polymers or space holders, cryo-spinning, custom-designed electrospinning platforms, ultrasonication, and laser cutting. Due to these techniques, cellular infiltration and maturation of the tissue within electrospun matrices enhanced *in-vitro* and *in-vivo* [111,113,173,175,209–215].

Although cellular penetration has yet remained a challenge, electrospun matrices are a new class of pelvic floor implants with different characteristics than conventional knitted meshes, thus different classifications and criteria may apply to them, because the highly porous and interconnected geometry of the electrospun matrices can compensate for their small pore size. However, new classifications should be thoroughly addressed.

B) fiber diameter

Fiber diameter define many properties in an electrospun matrix [103,104,110,216,217]. It can directly affect the mechanical properties for instance. Increasing the diameter of fibers, made of the same material, significantly increased the biomaterial ductility [59]. Increasing the fiber diameter also increases the permeability of the biomaterial against proteins [218,219]. The reason for the latter is mainly that the porosities become larger in thicker fibers. Fiber diameter also as influence on

adhesion, proliferation, and differentiation of cells [98,99,103,104,118,119]. For example, adhesion and proliferation of cells enhance as the fiber diameter decreases[98,120] which can consequently affect the quality of the matrix they produce. We recently showed in our group that decreasing the fiber size, enhances the myofibroblastic differentiation of human vaginal fibroblasts [59].

Fiber orientation also determines some of the aspects of the implant. For instance, highly aligned fibers (like those in fig.V.3) also have higher tensile strength in the direction of fibers orientation, which is advantageous for regeneration of some anisotropic soft tissues like bladder and vagina [187,169, 164, 90].

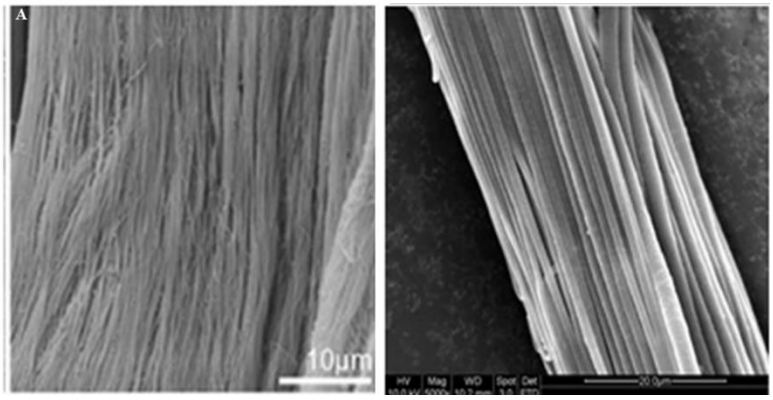

Figure V.3. A) decellularized tendon ECM, B) electrospun elastin fibers [220].

In conclusion, material and microstructure, both define the end properties of an electrospun implant (e.g. mechanical) [80,101,176,221]. Selecting the appropriate material, spinning it into a well-studied texture, and post-implantation evaluations, are steps toward a proper design of the implant. TableV.1 is a summary of varuous electrospun biomaterials used *in-vitro*.

4.What issues are clinically relevant *in-vivo*

A biomaterial should be evaluated for biocompatibility and functionality in an animal model which represents the anatomical situation of human as close as possible [222]. Animal models that are used for pelvic floor are generally subcutaneous or urogenital-organ models (tableV.2). Subcutaneous models are often used for preliminary evaluation of the implant for biocompatibility when accessibility to the organ-specific model is difficult and expensive. Organ-specific models are used to address issues that are specific to the implantation site. Host response, new tissue formation,

integration with the host tissue, biomechanical behavior, post-implantation symptoms such as surgical adhesion or herniation and neovascularization of the implant are normally addressed with *in-vivo* models. To the best of our knowledge, most of the electrospun matrices that have studied *in-vivo* for pelvic floor, are hybrids. The reason is perhaps due to their advantages discussed earlier.

i) host response, new matrix deposition and tissue regeneration

Studies in different animals show that synthetic or semi-synthetic electrospun matrices can provoke a host reaction that induces cells to deposit new ECM through which a new tissue can be formed [102,223]. Electrospun PLA and PLA/Gelatin biomaterials have shown great biocompatibility in subcutaneous rat model with no sign of toxicity or inflammation after 8 weeks of implantation [224]. Electrospun PLA matrices were pre-cultured *in-vitro* with mesenchymal stem cells, and then implanted subcutaneously in a rabbit model. Implants evoked an acute response followed by deposition of new collagen inside the matrices after 7 days [70]. An electrospun blend of PCL/PHB/PHV was implanted through cystotomy in another (rat) model for regeneration of urinary bladder. The implants evoked an inflammatory reaction in the beginning, but it disappeared within one month due to bladder augmentation and the remodeling of the implants (identified by a significant amount of new collagen) [106]. Electrospun PCL and PLLA/PCL matrices were studied in a canine bladder model for biocompatibility and tissue formation. New tissue was identified by new collagen synthesis around and within the implants after 14 days [225]. We found only one study where a semi-synthetic electrospun PET/chitosan implant induced severe host response as well as migration of foreign body reaction (FBR) cells into the implantation site higher than in commercial braided mesh (control) in a rat abdominal wall model [94]. Authors concluded that the severe response occurred due to the high surface contact of the electrospun materials.

Hybrids electrospun matrices have also shown good tendency to provoke cells producing new matrix. For example, an electrospun implant made of a mixture of the ECM-extracts (from porcine dermal tissue) and synthetic polyurethane, showed great biocompatibility and bioactivity in inducing new tissue formation in a rat model [221]. Increasing the concentration of the biological component enhanced the production of new matrix around the implants within 8 weeks after implantation. The same hybrids were used in another rat model where they promoted in-depth tissue formation identified by increased thickness of the tissue after implantation [200]. An electrospun hybrid made of PLGA/PCL incorporated with a fibrin-based extract, was pre-cultured

with dermal fibroblasts and implanted subcutanously in rabbit. Significant amount of collagen and elastin was deposited within the hybrid implants [204]. In another study, an electrospun implant was made from urinary bladder matrix and poly(ester-urethane)urea (PEUU) and imaplnted subcutenously in a rat model. Cell adhesion was higher in the hybrid implants than that on the non-hybrids [199].

In general, studies show that a electrospun matrices have the potential to induce a positive host response resulting in formation of new tissue; however, implant integration with the host tissue, is not yet ideal in electrospun matrices.

ii) integration and vascularization

As mentioned before, in functional tissue engineering, implant is required to integrate with the host tissue and become vascularized. Formation of blood vessels inside the implant, is critical for nutrition and oxygenation of the local cells and removing their by-products. Here again, the extent of this integration depends on the material and the microstructure.

From different studies, it is evidenced that that electrospun matrices can potetially be integrated with the surrounding tissue *in-vivo*, and new capillaries can grow into the electrospun matrices [102,109,113,226,227], if the material shows good biocompatibility. Electrospun PLA biomaterials were entirely integrated and deposited with new collagen within 7 days post-implantation in rabbits [70]. Electrospun PLLA/PCL biomaterials implanted in a canine model, also found to be fully integrated with the surrounding bladder tissue after three months [225]. Still, semi-synthetic or hybrid materials apparently have more integrating capacity. For instance, an electrospun hybrid biomaterial made of PLGA/PCL incorporated with a fibrin-based extract, was pre-cultured with dermal fibroblasts and then implanted. Significant cell migration as well as in-depth collagen production was observed within the hybrid implants [204]. Also, cell infiltration was higher in the electrospun hybrid implants made of urinary bladder matrix and poly(ester-urethane)urea (PEUU) than non-hybrids, which were subcutenously implanted in a rat model [199]. Increasing the concentration of the biological component in hybrid implants also results in more cellular infiltration and therefore increased integration [200].

Unfortunately, the average pore size is not mentioned in many of these studies and thus it is hard to estimate how the porosity have helped or limited integration. From our electrospinning

experience, and based on the technical knowledge available in literature, most of these implants must have pore sizes larger than at least 1 μm^2. Reaching this pore size is completely possible and relevantly standard with electrospinning, and therefore promising for the field, although methods of increasing the pore size discussed earlier, can enhance the integration and vascularization capacity further.

iii) biomechanics

post-implantation, the biomechanical properties of the implant change; thus it is critical to monitor how these changes occur within the body over time. Unfortunately, there is a lack of sufficient studies on explanted electrospun matrices; so we don't have enough knowledge about how the enzymatic environment of body can affect the mechanical properties of these biomaterials. The mechanical strength of the electrospun matrix may be partially compensated over time due to the production of new layers of matrix by host tissue cells around it *in-vivo* [204]. Mechanical assessment of PEUU electrospun matrices explanted from an abdominal wall rat model after 8 weeks (fig.V.4), also demonstrated that the biomaterials were remodeled and integrated with the newly-formed tissue, and due to such, their mechanical properties improved and became closer to the natural tissue [102]. Here again, synthetic electrospun matrices have shown superior mechanical properties over biological or hybrid ones [221], and thus are usually preferred for reconstruction of load-bearing tissues [199,200].

Although mechanical strength of electrospun matrices are yet in doubt for some researchers, there is opportunity for further improvements. Post-modification methods such as thermal annealing [64,186,228], can be used to tailor the mechanical behavior of the implants, and consequently improve their behavior in body.

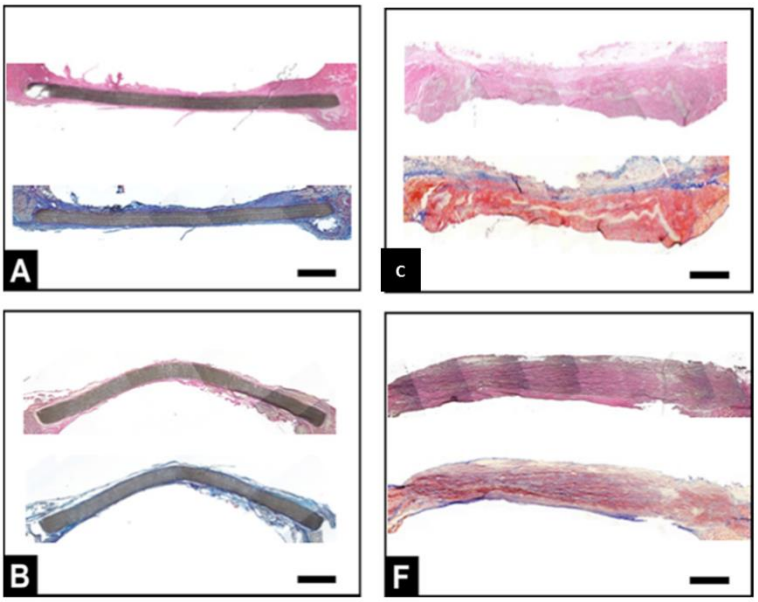

Figure V.4. Cross-section images of implanted grafts in abdominal wall rat model, PTFE patches (A and B), and electrospun polyurethane (C and D). The upper row is from 4 week explants (A, and C) and the lower row from 8 week explants (B and D). Within each box, staining for the upper image is with H&E, and for the lower image with Masson's trichrome. Scale bar: 1 mm [102].

5. Biomaterials functionalized with electrospun nanofibers

As we discussed earlier in this paper, it is true that the implant should be strong, but it should also have good mechano-biology to be gentle to cells; a surface with modulated microstructure for cell-biomaterial interactions. We propose a biphasic urogynecological implant, constitutive of one surface fibrous layer produced by electrospinning and one core membrane. Such implant (fig.V.5) is gentle and soft at surface, preferably degradable, with nano-to-micro pores that have architectural resemblance to natural tissues. At core, it is a strong, macro-porous membrane to withstand the abdominal pressures, which allows cells penetration for integration and neovascularization. The first layer is made of nanofibers coated on a base membrane. This coated layer is bioactive because of its geometry, and induces cells adhesion and proliferation. This layer is not stiffer than surrounding native tissue to avoid stress shielding and yet more elastic than the base membrane to allow gentle deformation of cells at the interface. Having a proper topography (mimicking the ECM) as well as low stiffness, this layer can prevent myofibroblastic differentiation of host cells. Thus, an implant which is coated with a layer of nanofibers may provide better mechano-biological function than a normal non-coated one.

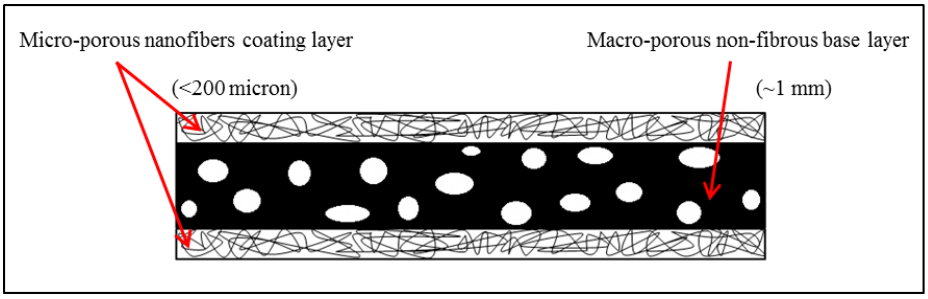

Figure V.5. Schematic cross section of a biphasic implant functionalized with nanofibers coating. The values are not to the scale in the picture.

6. Challenges and future prospects

Electrospinning creates an opportunity to tailor the characteristics of an implant according to need, however it is challenging to control all the parameters in one process. There are many safety and efficiency considerations before we introduce a new implant to the market.

First of all, we need new classifications for this type of implants. Previously classified pelvic meshes, were mainly knitted and macro-porous. These meshes have typically bulge-like areas where the macro-filaments are knitted (or waved) into each other. Electrospun matrices, are micro-porous, with highly interconnected porosities, and without bulges. Thus, the profile of force distribution through the material is different, which makes its biomechanical behavior different. High porosity and interconnectivity of the pores are unique futures of electrospun matrices. It is true that the pores are smaller than those in the knitted meshes, but on the other hand cell-cell and cell-biomaterial interactions are improved on electrospun fibers, so the final outcome should be expected different. We certainly need new classifications for these implants regarding:

- Porosity
- Fibers orientation
- Weight
- Interconnectivity degree
- Isotropic degree
- Degradation kinetics (for degradable materials)
- Mechanical properties

We need small and large animal models to test efficacy and safety of these materials. The mechanical behavior of the implants should be monitored after implantation, because changes in the body due to the enzymatic attacks and degradation of the material, extremely alter the mechanical properties over time.

7. Conclusion

Cells interact with electrospun fibers by adhesion, growth, proliferation and deposition of new matrix *in-vitro*. Through such interactions, electrospun matrices induce cells for collagen production and tissue formation *in-vivo*. Microstructure of the fibrous implants appears to be gentle and supportive for soft tissue remodeling based on the current *in-vivo* results. Electrospinning creates the opportunities for changing, designing, developing and functionalizing the fibrous implants of different characteristics for different applications. A hybrid implant is suggested here which has a core macro-porous membrane coated with a layer of nanofibers. Such hybrid may facilitate mechano-biological functions of cells at the interface and biomechanical support of the impaired tissue at the core. Despite all the efforts until now, more mechanistic translational studies in large animals are needed to address functionality of the nanofibrous matrices such as vascularization, changes in the biomechanical properties of the native tissue post-implantation and the biomaterial itself, degradation profiles, mechano-biological effects like erosion, biomaterial-related infections and fibrosis. In this review we introduced the potential of electrospinning as the next generation of reconstructive pelvic implants, and clarified which steps need to be undertaken to introduce these implants in daily clinical practice.

Table V.1. Summary of some in-vitro studies on evaluation of interaction between electrospun matrices and cells, with urogynecological implications.

Biomaterial	**Aim and type of study**	**Main outcome(s)**
Poly(lactic-acid) (PLA)	Urogynecological alternative implant *in-vitro* study [74], vascular TE[*229], stem cells for regeneration of skin[229], ascorbic-acid releasing biomaterials for pelvic floor repair [230]	Phenotypical morphology and functionality maintained, increased cell metabolic activity and proliferation, matrix deposition, increased collagen production [230]
Poly-(caprolactone) (PCL)	Skin TE [194], pre-seeded with MSCs[**] for hernia repair [101]	Cell penetration, high strain and cell viability [194], High suture and tensile strength, cell adhesion and proliferation [101]
Poly (lactic-co-glycolic) (PLGA)	Mass production of artificial ECM[***197], urethra TE [206], bladder TE hybrid with acellular bladder matrix [209]	Highly homogenous nanofiber morphology, great cell proliferation and matrix deposition by human-MSCs [197], scaffold contraction, reduced tensile strength upon sterilization but increased after cell seeding [206], good support for growth, attachment and proliferation of primary bladder smooth muscle cells [209]
Polyamides	Non-degradable implant for soft TE [195,231], TE and ECM mimic [54], blended with gelatin for biomedical applications [84], alternative implants for pelvic floor (Nylon) [100]	Biocompatibility with fibroblasts and rat kidney cells [195], spreading and cytoskeleton organization of the embryonic fibroblasts [54], increased biocompatibility due to gelatin, proliferation, adhesion of osteoblasts [84], great cell adhesion and matrix deposition [100]

Poly (polyol Sebacate) (PPS) or blends	Soft TE (e.g. skin and muscle) [232,233]	Great mechanical properties, biocompatibility to soft tissue cells, fine-tunable degradation rate [232,233]
Poly (Lactic-co-ethylene) (PELA)	Anti-adhesive in abdominal surgery	Biocompatible, anti-tissue adhesion [234]
Poly (urethane) (PU)	Soft TE and ECM mimic blended with urinary bladder matrix [199], subcutaneous implants in rat abdominal wall model [102]	Great mechanical properties, smooth muscle cell adhesion and proliferation [199], Cell attachment, high tensile strength [102]
Collagen (type I, II and III)	TE scaffold [197, 193]	Homogeneity in microstructure and cell adhesion, MSCs attachment and proliferation [197, 193]
Fibrinogen	TE scaffold seeded with rat cardiac fibroblasts [190], urinary tract regeneration [208], blended with polydioxanone for *in-situ* urologic TE [203]	Cell migration into the scaffolds and ongoing remodeling [190,208], cell migration and deposition of new collagen [203]
Silk	Urethra reconstruction [191], tubular vascular graft evaluated for thrombogenicity [235]	Cell migration, adhesion and proliferation [191], endothelial and smooth muscle cell attachment and proliferation [235]
Cellulose acetate	Urinary bladder regeneration [236]	Cell penetration through implant, proliferation, matrix deposition [236]
PCL/Gelatin	Alternative implant for pelvic floor [100], scaffolds for soft TE [81,202],	Cell adhesion, proliferation and matrix deposition by healthy and unhealthy fibroblasts [100], Cell attachment, growth and migration, matrix deposition [81,202]

PCL/Collagen	Multi-layered TE scaffolds	Cell migration through scaffolds, new matrix deposition [237]
PLGA/PCL	Skin TE [80], alternative implant for pelvic floor [100]	Comparative strength to native tissue, cell adhesion and growth, migration through the scaffold [80], functional cells in adhesion, proliferation and matrix deposition [100]
PLA/PCL	Scaffold for urologic tissue reconstruction	High cell adhesion and proliferation, great permeability [238]

: tissue engineering, **: mesenchymal stem cells, *: extracellular matrix*

Table V.2. Summary of some of the in-vivo studies for evaluation of the interaction between the electrospun matrices and body, with urogynecological implications.

Biomaterial	**Aim and type of study**	**Main outcome(s)**
Poly(lactic-acid) (PLA)	Urogyneaocological alternative implant [70], implants in subcutaneous rat model for TE applications [109]	Cells migration into the implant, implant remodeling and collagen synthesis, new tissue formation [70,109]
Poly(caprolactone) (PCL)	Skin TE* and wound healing [173,194]	Re-epithelization and formation of new dermal tissue, extensive cell migration to the scaffold and wound closure [194]
Poly (lactic-*co*-glycolic) (PLGA)	Bladder tissue engineering in rat model hybrid with bladder acellular matrix	Tissue-implant integration, micro-vessels and new tissue formation [209]

Poly (Urethane) (PU)	Vascular grafts with increased porosities [173], soft TE and ECM** mimic in subcutaneous rat model hybrid with UBM ***[199], rat abdominal wall model for hernia repair [102]	Tissue formation and implant-tissue integration, collagen formation, explants had comparable tensile strength [173], bioactivity and cellular infiltration [199], implant-integration, new tissue formation, no herniation sign [102]
Poly (ethylene terephthalate) (PET)	Non-degradable mesh in Subcutaneous model	High suture and tensile strength, foreign giant cells migration into the implant site [223]
Silk	Vascular reconstructive tubes in rat model [235], urethra reconstruction in urethral mucosal dog model [191], TE-ed mesh for pelvic floor reconstruction in abdominal wall rat model [239]	Migration of cells through the graft, formation of epithelium layer, no inflammation, new tissue formation [235], cell growth into the scaffolds, biocompatibility, no inflammation, tissue growth [191], tissue ingrowth, degradation *in-vivo* [239]
Polymer blends	PLGA/PCL-fibrin hybrid for soft TE, degradation study in subcutaneously rabbit model [204], PLLA/PCL membranes for bladder TE [225], PLGA/acellular matrix for bladder regeneration in urinary rat model [240], PCL/collagen aligned scaffold for reconstruction of diaphragmatic defects in abdominal wall rat model [241]	Prolonged mechanical strength due to ECM deposition [204], Cells infiltration, new tissue and matrix formation [225], implants remodeling with no herniation sign, bladder regeneration, micro-vascularization [240], comparable tensile strength to native tissue, cell infiltration, new tissue formation [241]

: tissue engineering, **: extracellular matrix, *: urinary bladder matrix*

Chapter VI

General Discussion

General discussion

Current implants that are used for treatment of pelvic floor disorders, most commonly pelvic organ prolapse, are not optimal, because they can create long-term severe complications. This raises a demand for the development of a new generation of implants that are safe, efficient and reliable. In this thesis, we proposed using electrospun biomaterials for the treatment of damaged tissues, in particular fascia, in pelvic organ prolapse. Our aim was to study how changing the characteristics of the electrospun biomaterials can impact the interactions of the biomaterial with human fibroblastic cells. Furthermore, we studied the effect of mechanical stimuli on cell behavior and matrix production. The studies performed in this thesis, suggest that electrospun matrices can support cellular adhesion, proliferation and ECM deposition, and this capacity is increased under cyclic mechanical loading.

1.What characteristics are relevant for an electrospun biomaterial and why?

Hydrophilicity*:cells better adhere to hydrophilic electrospun biomaterials.*

Human fibroblastic cells are anchorage dependent, meaning that they only function when they adhere properly to a substrate [242]. Therefore, we need bioactive implants for pelvic floor repair, not inert ones like e.g. polypropylene meshes. Host tissue cells should be able to interact with the implant and this initiates at the implant surface where cells attachment. Our electrospun biomaterials could support cell attachment because of their electrospun textures (thin fibers promote cell adhesion). Besides the texture, we used adhesive materials that supported cell adhesion; Nylon is hydrophilic, and PCL/Gelatine (also hydrophilic) has cell binding sites due the biological component of Gelatine. In general, our findings confirmed hydrophilicity as a relevant parameter for cell-biomaterial interactions, and it can be positively affected by being electrospun.

Degradability: *choice of material depends on the specific application.*

Depending on the specific condition of the patient, we may prefer a degradable or non-degradable biomaterial. Researchers have attempted to use degradable materials, like electrospun PLA-based scaffolds [70,74,243] or silk-fibroin [108,191] for pelvic floor reconstruction. The aim was to replace the polypropylene mesh with a more biocompatible and remodel-able implant, thereby decreasing the

mesh-related complications. Furthermore, degradable materials are preferred for younger patients as they inherently prevent long-term implant-related complications. We used PLGA/PCL and PCL/Gelatine (semi-synthetic) because both combinations were hydrophilic (measured by contact-angle test in **chapter 2**), and with high mechanical strength and elasticity. However, PCL/Gelatine has a drawback in the loss of mechanical integrity for repair of load-bearing tissues in longer-term. A non-degradable material, on the other hand (like Nylon, or polyethylene terephthalate, PET [223]), can be beneficial for patients who have lower (due to aging or menopause) or altered (prolapse or connective tissue diseases) remodelling capacity [76]; so that the mechanical function of the implant is maintained. Taken our results together, we propose degradable synthetic (or semi-synthetic) materials for young premenopausal patients, and non-degradable materials for older postmenopausal patients, given that the selected material is spin-able, hydrophilic and potentially strong.

Pore size: *larger pores enhance implant integration*.

One factor for mesh bioactivity is the capacity for integration with the host tissue [244,245]. For integration, pores in a biomaterial should be large enough (>75 based on Amid's classification[30]) so that cells can penetrate inside and deposit new matrix. Small pore size has remained a challenge for electrospinning experts, and different approaches have been tested such as using sacrificial fibers[215], ultrasonication[213] and more [246]. Balguid *et al*. [111], spun PCL scaffolds into larger fiber sizes from 3.4 to 12.1 μm, and thereby increased the pore size. We used the same strategy in this thesis (but using PLGA/PCL), and we successfully enlarged the pore size by increasing the fiber size (**chapter 3**). Our results were comparable with Balguid's work because: both groups observed improved cellular infiltration in larger pores, followed by matrix deposition. We found that human vaginal fibroblasts can infiltrate pores as small as 1 μm^2 (although more efficiently in larger pores), but in such small pores, infiltrated cells were less viable, which can be due to poor transport of nutrition or waste products. Considering other factors like fiber size and mechanical behaviour, we suggest that the pore size is not a generic factor but should be optimized considering other criteria as well.

Fiber size: *thin fibers have enhanced mechanical strength and change cellular activity profile.*

Previous studies had shown that thinner fibers enhance cell adhesion and proliferation [59,120]. Similarly, in **chapter 3**, we found that cellular metabolic activity was higher on thinner fibers. In addition, increasing the fiber size increases the pore size proportionally which changes cellular behavior; because once pores are larger, cells crawl into the scaffold and experience a 3D environment compared to those remaining on the surface, and thereby their proliferation, total collagen amount, quality of their newly-deposited matrix (becomes stiffer on 1-μm fibers than that of 8-μm fibers) and their myofibroblastic differentiation increases. In addition, increasing the fiber size (from 1 to 8 μm) enhanced the elastic modulus from 0.66 to 1.38 MPa, but decreased the ductility of the biomaterial from 80% to 18% ultimate strain. Chanl *et al*., showed otherwise: in their experiments, enhancing the diameter of PCL fibers enhanced the ductility of the scaffold and decreased its stiffness [110]. This could be due to differences in polymer and solution properties, such as concentration and solvent; they used 15% PCL solution in dimethylformamide: chloroform, while we used 15% and 25% PLGA/PCL in chloroform.

Our findings in chapters 2 and 3, mean that fiber size affects the mechanical properties of the electrospun biomaterial, as well as the subsequent cellular responses; matrices of thinner fibers are stronger, but may increase the chance of scar tissue formation (because of enhanced myofibroblastic differentiation) and encapsulation of the implant (because the small pores limit the integration). The optimal fiber size should be found in a parameter study addressing both mechanical and cellular outcomes.

Mechanical behavior: *material type and fiber size both determine mechanical behavior.*

For the regeneration of load-bearing tissues, like pelvic fascia damaged in POP, we need biomaterials that are strong but somewhat compliant under tension, commensurate with the corresponding native tissues [74,247]. We showed consistency with previous studies that an electrospun biomaterials such as PLA [74] or silk-fibroin [191] can meet these requirements because: the electrospun constructs showed strength and "toe-region" elasticity (in the force-displacement curves) which can allow gentle loading in physiological ranges, like normal breathing. We showed that the mechanical behavior of an electrospun biomaterial derives from its materials type and the fiber size of its microstructure. In **chapter 2,** different spun materials within the same range of fiber size (PLGA/PCL and PCL/Gelatine), exhibited different mechanical properties reflecting the material parameter and our results were comparable to previous findings [80,205,248–251]. In **chapter**

3, spun materials of the same material (PLGA/PCL) but with different fiber size (1 μm and 8 μm) exhibited different mechanical behaviour (as abovementioned), reflecting the microstructure parameter. Overall, in design on an implant for POP repair, we may take two parameters into consideration; use a material that is strong, and spin it into an optimized (yet to-be found) fiber size.

Another important point of discussion is the shape of the load-bearing curve for electrospun biomaterials used in this thesis. Electrospun polymers start quite stiff and then yield, while textiles (braided meshes and also biological materials) are compliant in the beginning and then stiffen. This is very essential for cell behavior as we showed in **chapter 4**. In this regard, later in **chapter 5**, we proposed using a hybrid implant which has a backbone for biomechanical behavior (strong core) and a cover of electrospun fibers (fibrous sheet) for improved cell-implant interactions and integration. Such hybrid, has the benefit of biomechanical and mechano-biological behavior due to the core and the sheet layers, respectively.

Weight (gr/m2): *electrospun biomaterials are very porous and often light-weight.*

Researchers suggest that heavy biomaterials that are used for hernia or prolapse repair, can cause severe foreign body reactions [43,88,252]. The weight of a scaffold is determined by its overall porosity and the polymer density[43]; suggesting that a less dense material processed into a porous structure is preferable for pelvic floor. Electrospun biomaterials evaluated in this thesis were light compared to the polypropylene knitted meshes (**chapter 3**), because of their highly porous structure. In general, we do not know how the issue of implant weight may apply for electrospun biomaterials as these (electrospun) are more friendly for cells and therefore they may not generally induce foreign body reactions; although we suggest using low density-materials for electrospinning.

2. Diseased fibroblasts can function on electrospun biomaterials

After characterization of the electrospun biomaterials, we studied whether diseased cells (cell derived from POP-patients and have altered regenerative capacity [76,253]) can function on such structures (**chapter 2**) to show the feasibility of using electrospun matrices for pelvic floor. We found that once supported by an appropriate surface of nano-to-micro fibers, cells regain their regenerative ability even though they come from a diseased environment. POP-fibroblasts exhibited viability, proliferation and collagen production on the different electrospun biomaterials.

While it may be true that POP-fibroblasts produce a different quality of matrix (stiff with high collagen content [253]), once they are supported by a scaffolds that mimics their ECM structure, cells regain their regenerative capacity and produce collagen as much as their healthy counterparts. POP fibroblasts thereby serve as a valuable *in-vitro* model.

3. Cyclic loading promotes the regenerative capacity of POP-fibroblasts

It is evidenced by many studies that mechanical stimulation may enhance the regenerative capacity of cells, given the strains mimic the naturally-occurring forces. Smooth muscle cells, for example, produce more ECM under cyclic straining [254], and collagen-synthesis is upregulated by gentle, breath-mimicking straining [138]. Fibroblasts, also, show enhanced proliferation and collagen production when subjected to cyclic straining [198]. In pelvic floor regenerative medicine, studies have shown that POP-fibroblasts are mechano-responsive to dynamic loading [86,154,255]; meaning that they align themselves in direction of mechanical stretching and upregulate their ECM-remodeling factors. Our results were consistent in the fact that gentle cyclic mechanical loading, this time in a hammock-like regime instead of uniaxial stretching, enhances the expression of ECM-synthesis and remodeling factors. Cells also express their collagen genes earlier than under static conditions. This suggests that mechanical stimuli speed up and promote collagen production and remodeling, which may improve clinical outcome (**chapter 4**). However, our results, unlike previous studies, showed that cells lose their actin-mediated alignment under cyclic loading and become more randomly oriented. This finding, suggests that a cyclic loading may interfere with myofibroblastic differentiation of POP-cells, by disturbing their actin-mediated adhesion. Thereby, it can prevent scar tissue formation and the adverse effects that come with it.

Inflammatory markers slightly upregulated under gentle cyclic loading, which shows that shear stress plays an important role in modulating cell-biomaterial interactions and the way cells respond to a foreign material. In this thesis, we showed that prolapsed cells (that have altered remodeling capacity[76]), can also respond to mechanical loading like the healthy ones in presence of an electrospun biomaterial; a synthetic mimic of ECM that provides beneficial remodeling stimuli also for a diseased area like in pelvic organ prolapse patient.

Mechano-biological events at the tissue-implant interface are strong determinants of cell differentiation and matrix deposition and when improperly designed, can cause abnormal wound

healing and fibrotic tissue formation [132]. Matrix deposition thus depends on the implant microstructure and the loading condition:

i) fibroblasts contribute to produce new matrix, and the quality and amount depends on the fiber size of the scaffold. Fibroblasts produce a stiffer matrix containing more Collagen-I on 1-μm fibers than on 8-μm fibers (**chapter 3**). This is clinically important because if the new layer of tissue that is formed on the implant surface is too stiff, the tissue becomes fibrotic (and thus non-functional) and painful. Hence, the fiber size of the implant should not dictate production of a matrix stiffer than the host tissue, to prevent scar tissue formation and or implant contraction.

ii) cyclic loading accelerates the onset of collagen production, and changes actin-mediated adhesion and therefore mechano-responsivity of POP-cells. We found that this enhancing effect is slightly stronger on spun fibers, in comparison to non-porous films. This means that fibrous structures may contribute to better clinical outcomes because they stimulate more regenerative responses. At the same time, cyclic loading reduces the differentiation of myofibroblasts, thereby reducing the risk on scar formation and scaffold contraction.

iii) we proposed that a hybrid biomaterial may be a good combination of variables; a strong macro-porous core, covered with a sheet of spun fibers. This hybrid benefits from a strong yet compliant and pliable mechanical support (core) as well as a proper surface for mechano-biological interactions with cells (sheet).

4. Limitations of the studies

Electrospinning is a new technique for the field of pelvic floor research. Here we provide a proof of concept to start with, acknowledging the challenges for clinical implementation ahead. The best way to move forward, is to appreciate the current achievements, while acknowledging the limitations.

i) *limitation of the device*: we used a simple conventional electrospinning device for all of our experiments. Changing the ambient conditions, like temperature and humidity, strongly affects the fibers morphology while our device worked only at room condition. We were not able to test those effects. Also, we only used a static collector, while moving ones (rotating drum for example),

allows fibers alignment. To find a spun microstructure that meets the requirements of a pelvic floor implant, we would need to try some more of the technical parameters.

ii) *limitation of methodology*: in **chapter 3**, we found that the newly-made matrix produced by fibroblasts, is stiffer on thinner fibers (1 μm) compared to 8 μm). However, specific protein assays (like collagen type, cross-linking, etc.) are required to characterize the matrix for such differences. For example, Ruiz-Zapata *et al*., characterized the newly-made matrix using protein assays (like cross-links hydroxylysylpyridinoline) and they found that POP-fibroblasts deposit a different quality of matrix [253]. We performed our experiments in short-term (<1 month), but many of the cellular functions need more time to emerge, such as matrix maturation, or elastin production. In **chapter 4**, we performed gene expression analysis which gave us some first indications, but longer-term responses should be studied at protein level to obtain more accurate and informative insights about the findings.

iii) *limitation of cell source*: we used primary human vaginal fibroblasts in all the experiments. However, in reality, the implant is exposed to more diverse cell types and the cellular interactions are more complicated. For instance, immune cells (such as macrophages) and blood cells from the host tissue environment constantly react to the implant, which may result in encapsulation or remodeling of the implant [148]. Hence, it is essential to study the electrospun implant in a more complicated set-up that represents more cell types.

5. Future perspectives

Current knitted meshes for reconstructive surgery, have shown to be effective in stimulating new collagen production [256], but the nature of cell-implant interactions is suboptimal that complications may occur in longer-term [257]. Electrospun matrices create a different level of cell-implant interactions, some of which we showed in this thesis. However, there is still space to improve our understanding about the extent and level of these interactions in different aspects.

1- *new microstructure:* previously classified pelvic meshes are mainly knitted and macro-porous [30] and typically have fibers cross-over areas. Electrospun matrices are micro-porous, with highly interconnected porosities and extremely thin fibers. Hence, the fibers cross-over areas are much smaller, and therefore gentler to cells and interconnected porosities, facilitate cellular

communications and nutrients transportations. This implies that different classification criteria should be defined for differently-structured implants: electrospun versus knitted.

2- *different loading regimes*: we applied a breath-mimicking cyclic straining regime to stimulate the fibroblasts. Our culture system has a good potential for the implication of other loading regimes and longer-term experiments. For instance, excessive loading that occurs in constipated patients, vomiting, or coughing [258], can be the subject of future studies. Non-continuous regimes when the force increases suddenly in a pulse-like situation, can also be modeled with intervals in between the cycles.

3- *neovascularization*: one part of a proper tissue-implant integration, is the blood supply of the cells within and around the implant [70]. Blood vessels and capillaries should grow inside the biomaterial to provide nutrients and oxygen, and to remove cellular waste products. As shown in **chapter 3**, cells can infiltrate inside an electrospun scaffold, but it is necessary that the blood circulates through the biomaterial to feed the cells. Studies are required to particularly address the issue of neovascularization around and within an electrospun biomaterial in pelvic floor.

4- *in-vivo studies*: The mechanical characterizations performed in this study are valuable, but changes in the body due to the enzymatic attacks and degradation of the material, and persistent loading, significantly alter the properties of implant (such as mechanical behaviour). For example, the effect of creep (time-dependent failure of material under mechanical stress), or fatigue (weakening of the material under cyclic mechanical stress) on electrospun biomaterials should be studied in large animal models [259–261].

5- *biomaterials for regenerative medicine*: the results of this thesis are mainly focused on pelvic organ prolapse repair, but are not limited to it. Our results can also be useful for the regeneration of other load bearing and/or soft tissues where a synthetic mimic of ECM (provided by electrospun fibrous structure) can create regenerative benefits, for example in abdominal wall [102] or skin[237].

6- *hybrid implants*: we proposed hybrid biomaterials in **chapter 6**; a strong mechanical backbone covered with electrospun fibers. Such a hybrid implant has proper mechanical stability due to its core (provided by another method), and good mechano-biology because of the fibers. Due to time restrains we could not invest on hybrid implants in this thesis, but given their potential benefits,

studying different aspects of these implants remains an interesting topic of research for the field in future.

6. Electrospinning; a whole world of possibilities in regenerative medicine

Our findings provide evidence that electrospinning can be potentially considered as an alternative technique to produce implants for pelvic organ prolapse. Overall, electrospinning is a technique with lots of possibilities to design structural and mechanical properties. It is a relatively inexpensive fabrication method for mass production of textile biomaterials[197], relatively simple to establish and easy to scale-up. If set up and assessed appropriately, it is a reproducible, reliable and efficient manufacturing method on industrial scale. Although it is a relatively new topic for urogynecology field, in the emerging field of regenerative nanomedicine, electrospinning holds a place for further developments not only for repair of pelvic organ prolapse, but also for tissue engineering of abdominal wall [101,102,262], skin [80,263], cartilage [264,265], nerve [266,267], cardiovascular tissues [111,268] and tendon [269,270]. Our studies were designed for particularly pelvic organ prolapse, but our results may be implemented in other medical fields given a full consideration of the anatomical and histological differences of the target tissues.

Chapter VII

Summary & Nederlandse Samenvatting

Summary

This thesis explores the potential of electrospun fibers for the regeneration of fascia-like tissues that are damaged in pelvic floor disorders like pelvic organ prolapse (POP).

Chapter 1 describes Pelvic Organ Prolapse (POP), a common disease where the abdominal organs loose mechanical support and descend through the vaginal cavity. Currently used implants (knitted meshes) create complications because they are biologically inert and become encapsulated by fibrous tissues. They are also too stiff and cause stress shielding, thereby inducing migration of the implants through the host tissues. Electrospinning may be a promising technique for the fabrication of the implants because nano-fibers mimic the natural polymers and provide better conditions for integration with the host tissue.

In **Chapter 2**, we evaluated the microstructural and mechanical properties of three different electrospun matrices: Nylon, a mixture of poly-caprolactone and poly-glycolic acid (PCL/PGLA), and a mixture of PCL and gelatin. We studied their interaction with healthy (non-POP) and unhealthy (derived from POP patients) human vaginal fibroblasts in a comparative *in-vitro* study. Five major properties of the matrices were identified that are associated with their application for tissue regeneration: fiber size, pore size, overall porosity, hydrophilicity and uniaxial tensile strength. Matrices exhibited differences in their properties like fiber thickness and hydrophilicity, depending on the nature of the material and the spinning condition. This illustrates the versatility of the electrospinning technique that one can use to specify product properties. We further found that both healthy and unhealthy cells adhere to electrospun matrices, proliferate and deposit new collagenous matrix. This study provided a proof-of-concept on the potential of electrospun matrices and led us to take the next steps.

In **Chapter 3**, we studied the effect of fiber diameter (as a microstructural parameter) on mechanical properties of the scaffold and the behavior of cells seeded on them. Scaffolds with a fibers size of 8 μm were slightly stiffer but significantly more ductile than scaffolds spun with fibers of 1 μm. Furthermore, increasing the fiber size, which substantially increased the pore size, enhanced cellular infiltration through the biomaterial with more cell viability in deeper layers. This shows that pore size (as a factor of changing the fiber size) affects the cellular infiltration and therefore integration capacity of the scaffold. Furthermore, cellular activity was higher on thinner

fibers. As a result, cells became more myofibroblastic and deposited a stiffer matrix with more collagen content. This study evidenced the important role of fiber size, and the need to find a balance between different parameters that are associated with mechanical properties and cellular behaviour.

In **Chapter 4**, we designed a dynamic culture system to apply cyclic loading to electrospun scaffolds seeded with unhealthy fibroblasts from severe POP patients. A non-porous film was used as control. We observed that mechanical loading enhanced cellular responses, both in terms of morphology and gene expression. There was a stimulating effect on the expression of matrix synthesis as well as the remodeling and inflammatory genes. This shows that, in addition to the material (chapter 2) and fiber size (chapter 3) of the electrospun scaffold, dynamic conditioning noticeably affects the nature and extent of cell-scaffold interactions.

Chapter 5 is a review on the potential of electrospun matrices for regeneration of fascia-like tissues in pelvic floor repair. Electrospun fibers have a great potential because they strongly interact with cells and support their functions *in-vitro*, such as proliferation and matrix deposition, and through such interactions, induce cells for collagen production and tissue formation *in-vivo.* Some of the disadvantages of electrospun matrices, such as small pore size, can be overcome by changing the spinning parameters. We propose using hybrid implants consisting of a strong core coated with electrospun nanofibers for enhanced mechano-biological behavior of implants for pelvic floor repair.

In **chapter 6**, we conclude that electrospinning technology defines a new class of implants for pelvic floor repair and other surgical applications. Their main asset is that they have a microstructure different from the conventional knitted meshes, which allows integration with the host tissue by induction of tissue remodelling. Mechanical stimulation of this process may be enhanced by allowing gentle straining of the tissue, enabled by the right stiffness profile of the implant under tension. While our research shows that it is feasible to use electrospun biomaterials as an alternative for braided textile for the treatment of POP, large animal models will remain necessary to assess the mechanobiological function of electrospun scaffolds in the pelvic floor.

Samenvatting

Dit proefschrift onderzoekt de mogelijkheden van electrospun vezels voor de regeneratie van fascia-achtige weefsels die zijn beschadigd in bekkenbodem aandoeningen zoals verzakking (POP).

Hoofdstuk 1 beschrijft verzakking (POP), een veel voorkomende ziekte waarbij de buikorganen losse mechanische ondersteuning en door de vaginale holte dalen. Momenteel gebruikte implantaten (gebreid netten) te creëren complicaties, omdat ze biologisch inert en worden ingekapseld door vezelig weefsel. Ze zijn ook te stijf en stress veroorzaken afscherming, waardoor de migratie van de implantaten te induceren door de gastheer weefsels. Electrospinning kan een veelbelovende techniek voor de vervaardiging van de implantaten omdat nanovezels nabootsen natuurlijke polymeren en betere voorwaarden voor integratie met het gastheerweefsel.

In **hoofdstuk 2** evalueerden we de microstructurele en mechanische eigenschappen van drie verschillende matrices electrospun: Nylon, een mengsel van poly-caprolacton en polyglycolzuur (PCL / PGLA), en een mengsel van PCL en gelatine. We bestudeerden hun interactie met gezonde (non-POP) en ongezonde (afgeleid van POP patiënten) humane vaginale fibroblasten in een vergelijkende *in-vitro* studie. Vijf belangrijke eigenschappen van de matrices geïdentificeerd die samenhangen met de toepassing ervan voor weefselregeneratie: vezelgrootte, poriegrootte, overall porositeit, hydrofiliciteit en uniaxiale treksterkte. Matrices vertoonden verschillen in eigenschappen zoals vezeldikte en hydrofiliteit, afhankelijk van de aard van het materiaal en de draaiende toestand. Dit illustreert de veelzijdigheid van het elektrospinnen techniek die men kan gebruiken om producteigenschappen te geven. We vinden verder dat zowel gezonde als ongezonde cellen hechten aan matrices electrospun, vermenigvuldigen en nieuwe collageenmatrix deponeren. Dit onderzoek leverde een “proof-of-concept” op het potentieel van electrospun matrices en leidde ons naar de volgende stappen te nemen.

In **hoofdstuk 3** hebben we het effect van vezeldiameter (als microstructurele parameter) op de mechanische eigenschappen van de steiger en het gedrag van cellen gezaaid op hen. Steigers vezels met een grootte van 8 urn waren enigszins stijver maar aanzienlijk meer dan nodulair scaffolds met gesponnen vezels van 1 urn. Voorts verhogen de vezelgrootte, die in hoofdzaak de poriegrootte, verbeterde cellulaire infiltratie verhoogd door het biomateriaal meer cellevensvatbaarheid in diepere lagen. Dit toont aan dat poriegrootte (als een factor van de vezelgrootte wijzigen) invloed op de cellulaire infiltratie en derhalve opnamecapaciteit van de

steiger. Bovendien was de celactiviteit hoger dunnere vezels. Als resultaat werd meer cellen myofibroblastische gesloten en een stijvere matrix met meer collageengehalte. Dit onderzoek blijkt de belangrijke rol van vezelgrootte, en de noodzaak om een evenwicht tussen de verschillende parameters die zijn geassocieerd met mechanische eigenschappen en cellulaire gedrag vinden.

In **hoofdstuk 4** hebben we een dynamische cultuur systeem om cyclische belasting van toepassing op electrospun steigers bezaaid met ongezonde fibroblasten van ernstige POP patiënten. Een niet-poreuze film werd gebruikt als controle. We zagen dat mechanische belasting verbeterde cellulaire responsen, zowel qua morfologie en genexpressie. Er was een stimulerend effect op de expressie van matrix synthese en de verbouwing en inflammatoire genen. Dit toont aan dat, naast de materialen (hoofdstuk 2) en vezelgrootte (hoofdstuk 3) van de electrospun schavot dynamische conditionering duidelijk de aard en omvang van mobiele steiger interacties beïnvloedt.

Hoofdstuk 5 is een review over het potentieel van electrospun matrices voor het regenereren van fascia-achtige weefsels in bekkenbodem reparatie. Electrospun vezels hebben een groot potentieel aangezien zij sterke wisselwerking met cellen ondersteunen en hun functie *in-vitro*, zoals proliferatie en matrixafzetting en door dergelijke interacties induceren cellen voor collageen en weefselvorming *in-vivo*. Enkele nadelen van electrospun matrices, zoals kleine poriegrootte, kan worden overwonnen door het veranderen van de spinparameters. Wij stellen voor het gebruik van hybride implantaten bestaande uit een sterke kern bekleed met electrospun nanovezels voor een betere mechanisch-biologische gedrag van implantaten voor de bekkenbodem reparatie.

In **hoofdstuk 6**, kunnen we concluderen dat elektrospinning technologie definieert een nieuwe klasse van implantaten voor de bekkenbodem reparatie en andere chirurgische toepassingen. Hun belangrijkste troef is dat ze een microstructuur verschilt van de conventionele gebreide mazen, die de integratie toelaat door het gastheerweefsel door inductie weefsel remodellering. Mechanische stimulatie van dit proces kan worden versterkt doordat zachte overbelasting van het weefsel mogelijk door de juiste stijfheid profiel van het implantaat onder spanning. Hoewel ons onderzoek toont aan dat het haalbaar is electrospun biomaterialen gebruiken als alternatief voor gevlochten textiel voor de behandeling van POP zullen grote diermodellen noodzakelijk blijven de mechanobiologische functie van steigers electrospun beoordelen de bekkenbodem.

Appendices

References

Acknowledgment

Abbreviations list

Publications list

Portfolio

References:

1. Kerkhof, M. H., Hendriks, L. & Brölmann, H. a M. Changes in connective tissue in patients with pelvic organ prolapse--a review of the current literature. *Int. Urogynecol. J. Pelvic Floor Dysfunct.* **20,** 461–74 (2009).

2. Kenton, K. & Mueller, E. R. The global burden of female pelvic floor disorders. *J. Compil.* **98,** 1–5 (2006).

3. S. HUNSKAAR & K. BURGIO, A.CLARK, M.C. LAPITAN, R. NELSON, U. SILLÉN, D. T. in 255–312

4. Haylen, B. T. *et al.* An International Urogynecological Association (IUGA)/International Continence Society (ICS) joint terminology and classification of the complications related to native tissue female pelvic floor surgery. *International Urogynecology Journal and Pelvic Floor Dysfunction* **23,** 515–526 (2012).

5. Sand, P. K. & Dmochowski, R. Analysis of the Standardisation of Terminology of Lower Urinary Tract Dysfunction: Report From the Standardisation Sub-Committee of the International Continence Society. *Neurourol. Urodyn.* **21,** 167–78 (2002).

6. Chong, E. C., Khan, A. A. & Anger, J. T. The financial burden of stress urinary incontinence among women in the United States. *Curr. Urol. Rep.* **12,** 358–362 (2011).

7. Hamilton Boyles, S., Weber, A. M. & Meyn, L. Procedures for pelvic organ prolapse in the United States, 1979-1997. *Am. J. Obstet. Gynecol.* **188,** 108–115 (2003).

8. Boer, T. A. De, Hove, M. C. P. S., Burger, C. W., Kluivers, K. B. & Vierhout, M. E. European Journal of Obstetrics & Gynecology and Reproductive Biology The prevalence and factors associated with previous surgery for pelvic organ prolapse and / or urinary incontinence in a cross-sectional study in The Netherlands. *Eur. J. Obstet. Gynecol.* **158,** 343–349 (2011).

9. Milsom, I. *et al.* Epidemiology of Urinary (UI) and Faecal (FI) Incontinence and Pelvic Organ Prolapse (POP). *Ics* 35–112 (2009).

10. Trabuco, E. C., Klingele, C. J. & Gebhart, J. B. Xenograft use in reconstructive pelvic surgery: A review of the literature. *Int. Urogynecol. J. Pelvic Floor Dysfunct.* **18,** 555–563 (2007).

11. Badylak, S. F. The extracellular matrix as a biologic scaffold material. *Biomaterials* **28,** 3587–3593 (2007).

12. Ward, K. & Hilton, P. Prospective multicentre randomised trial of tension-free vaginal tape and colposuspension as primary treatment for stress incontinence. *BMJ* **325,** 67 (2002).

13. Candage, R. *et al.* Use of human acellular dermal matrix for hernia repair: friend or foe? *Surgery* **144,** 703-9-11 (2008).

14. Aboushwareb, T., Mckenzie, P., Wezel, F., Southgate, J. & Badlani, G. Is Tissue

Engineering and Biomaterials the Future for Lower Urinary Tract Dysfunction (LUTD)/Pelvic Organ Prolapse (POP)? **782,** 775–782 (2011).

15. Olsen, a L., Smith, V. J., Bergstrom, J. O., Colling, J. C. & Clark, a L. Epidemiology of surgically managed pelvic organ prolapsed and urinary incontinence. *Obstet Gynecol* **89,** 501–506 (1997).

16. Achtari, C., Hiscock, R., O'Reilly, B. A., Schierlitz, L. & Dwyer, P. L. Risk factors for mesh erosion after transvaginal surgery using polypropylene (Atrium) or composite polypropylene/polyglactin 910 (Vypro II) mesh. *Int. Urogynecol. J. Pelvic Floor Dysfunct.* **16,** 389–394 (2005).

17. Whiteside, J. L., Weber, A. M., Meyn, L. A. & Walters, M. D. Risk factors for prolapse recurrence after vaginal repair. *Am. J. Obstet. Gynecol.* **191,** 1533–1538 (2004).

18. Tijdink, M. M., Vierhout, M. E., Heesakkers, J. P. & Withagen, M. I. J. Surgical management of mesh-related complications after prior pelvic floor reconstructive surgery with mesh. *Int. Urogynecol. J. Pelvic Floor Dysfunct.* **22,** 1395–1404 (2011).

19. Edwards, S. L. *et al.* Characterisation of clinical and newly fabricated meshes for pelvic organ prolapse repair. *J. Mech. Behav. Biomed. Mater.* **23,** 53–61 (2013).

20. Prolapse, O. Urogynecologic Surgical Mesh: update on safety by FDA. (2011).

21. Mucowski, S. J., Jurnalov, C. & Phelps, J. Y. Use of vaginal mesh in the face of recent FDA warnings and litigation. *Am. J. Obstet. Gynecol.* **203,** 103.e1-103.e4 (2010).

22. Ellington, D. R. & Richter, H. E. The role of vaginal mesh procedures in pelvic organ prolapse surgery in view of complication risk. *Obstet. Gynecol. Int.* **2013,** 356960 (2013).

23. Hartmann, U. H. Re: Persistent Genital Arousal Disorder in Women: Case Reports of Association with Anti-Depressant Usage and Withdrawal. *Eur. Urol.* **55,** 1233–1235 (2009).

24. Shepherd, J. P., Feola, A. J., Abramowitch, S. D. & Moalli, P. a. Uniaxial biomechanical properties of seven different vaginally implanted meshes for pelvic organ prolapse. *Int. Urogynecol. J.* **23,** 613–20 (2012).

25. Ammembal, M. K. & Radley, S. C. Complications of polypropylene mesh in prolapse surgery. *Obstet. Gynaecol. Reprod. Med.* **20,** 359–363 (2010).

26. Robinson, T. N., Clarke, J. H., Schoen, J. & Walsh, M. D. Major mesh-related complications following hernia repair: Events reported to the Food and Drug Administration. *Surgical Endoscopy and Other Interventional Techniques* **19,** 1556–1560 (2005).

27. Jamadar, D. A. *et al.* Abdominal wall hernia mesh repair: sonography of mesh and common complications. *J. Ultrasound Med.* **27,** 907–17 (2008).

28. Abramov, Y. *et al.* Biomechanical characterization of vaginal versus abdominal surgical wound healing in the rabbit. *Am. J. Obstet. Gynecol.* **194,** 1472–1477 (2006).

29. Abramov, Y. *et al.* Histologic characterization of vaginal vs. abdominal surgical wound healing in a rabbit model. *Wound Repair Regen.* **15,** 80–86 (2007).

30. Amid, P. K. Classification of biomaterials and their related complications in abdominal wall hernia surgery. *Hernia* **1,** 15–21 (1997).

31. Maurer, M. M., Röhrnbauer, B., Feola, A., Deprest, J. & Mazza, E. Prosthetic meshes for repair of hernia and pelvic organ prolapse: Comparison of biomechanical properties. *Materials (Basel).* **8,** 2794–2808 (2015).

32. Feola, a *et al.* Deterioration in biomechanical properties of the vagina following implantation of a high-stiffness prolapse mesh. *BJOG* **120,** 224–32 (2013).

33. Andrew Jordan Feola. IMPACT OF VAGINAL SYNTHETIC PROLAPSE MESHES ON THE MECHANICS OF THE HOST TISSUE RESPONSE. *thesis* (2011).

34. Liang, R. *et al.* Vaginal degeneration following implantation of synthetic mesh with increased stiffness. *BJOG* **120,** 233–43 (2013).

35. Feola, A., Barone, W., Moalli, P. & Abramowitch, S. Characterizing the ex vivo textile and structural properties of synthetic prolapse mesh products. *Int. Urogynecol. J.* **24,** 559–64 (2013).

36. Falconer, C., Söderberg, M., Blomgren, B. & Ulmsten, U. Influence of different sling materials on connective tissue metabolism in stress urinary incontinent women. *Int. Urogynecol. J. Pelvic Floor Dysfunct.* **12,** (2001).

37. Pourdeyhimi, B. Porosity of surgical mesh fabrics: new technology. *J. Biomed. Mater. Res.* **23,** 145–152 (1989).

38. Boccaccio, A., Uva, A. E., Fiorentino, M., Lamberti, L. & Monno, G. A mechanobiology-based algorithm to optimize the microstructure geometry of bone tissue scaffolds. *Int. J. Biol. Sci.* **12,** 1–17 (2016).

39. Barone, W. R., Moalli, P. A. & Abramowitch, S. D. Textile Properties of Synthetic Prolapse Mesh In Response to Uniaxial Loading. *Am. J. Obstet. Gynecol.* 1–9 (2016). doi:10.1016/j.ajog.2016.03.023

40. Otto, J., Kaldenhoff, E., Kirschner-Hermanns, R., M??hl, T. & Klinge, U. Elongation of textile pelvic floor implants under load is related to complete loss of effective porosity, thereby favoring incorporation in scar plates. *J. Biomed. Mater. Res. - Part A* **102,** 1079–1084 (2014).

41. Klosterhalfen, B., Junge, K. & Klinge, U. The lightweight and large porous mesh concept for hernia repair. *Expert Rev. Med. Devices* **2,** 103–117 (2005).

42. Klinge, U. *et al.* Impact of polymer pore size on the interface scar formation in a rat model. *J. Surg. Res.* **103,** 208–14 (2002).

43. Orenstein, S. B., Saberski, E. R., Kreutzer, D. L. & Novitsky, Y. W. Comparative analysis

of histopathologic effects of synthetic meshes based on material, weight, and pore size in mice. *J. Surg. Res.* **176,** 423–429 (2012).

44. Deprest, J. *et al.* The biology behind fascial defects and the use of implants in pelvic organ prolapse repair. *Int. Urogynecol. J. Pelvic Floor Dysfunct.* **17 Suppl 1,** S16-25 (2006).

45. Norris, J. P., Breslin, D. S. & Staskin, D. R. Use of synthetic material in sling surgery: a minimally invasive approach. *J Endourol* **10,** 227–230 (1996).

46. Pascual, G. *et al.* The long-term behavior of lightweight and heavyweight meshes used to repair abdominal wall defects is determined by the host tissue repair process provoked by the mesh. *Surg. (United States)* **152,** 886–895 (2012).

47. Elmer, C., Blomgren, B., Falconer, C., Zhang, A. & Altman, D. Histological inflammatory response to transvaginal polypropylene mesh for pelvic reconstructive surgery. *J. Urol.* **181,** 1189–95 (2009).

48. Krause, H. G., Galloway, S. J., Khoo, S. K., Lourie, R. & Goh, J. T. W. Biocompatible properties of surgical mesh using an animal model. *Aust. New Zeal. J. Obstet. Gynaecol.* **46,** 42–45 (2006).

49. Pott, P. P. *et al.* Mechanical properties of mesh materials used for hernia repair and soft tissue augmentation. *PLoS One* **7,** e46978 (2012).

50. Dietz, H. P. *et al.* Mechanical properties of urogynecologic implant materials. *Int. Urogynecol. J. Pelvic Floor Dysfunct.* **14,** 239–43; discussion 243 (2003).

51. Rumian, a P., Draper, E. R. C., Wallace, a L. & Goodship, a E. The influence of the mechanical environment on remodelling of the patellar tendon. *J. Bone Joint Surg. Br.* **91,** 557–564 (2009).

52. Muellner, T. *et al.* Light and electron microscopic study of stress-shielding effects on rat patellar tendon. *Arch Orthop Trauma Surg* **121,** 561–565 (2001).

53. Eastwood, M., Mudera, V. C., McGrouther, D. A. & Brown, R. A. Effect of precise mechanical loading on fibroblast populated collagen lattices: Morphological changes. *Cell Motil. Cytoskeleton* **40,** 13–21 (1998).

54. Hinz, B., Mastrangelo, D., Iselin, C. E., Chaponnier, C. & Gabbiani, G. Mechanical tension controls granulation tissue contractile activity and myofibroblast differentiation. *Am. J. Pathol.* **159,** 1009–20 (2001).

55. Darby, I. A., Laverdet, B., Bont??, F. & Desmouli??re, A. Fibroblasts and myofibroblasts in wound healing. *Clin. Cosmet. Investig. Dermatol.* **7,** 301–311 (2014).

56. Van De Water, L., Varney, S. & Tomasek, J. J. Mechanoregulation of the Myofibroblast in Wound Contraction, Scarring, and Fibrosis: Opportunities for New Therapeutic Intervention. *Adv. wound care* **2,** 122–141 (2013).

57. Tomasek, J. J., Gabbiani, G., Hinz, B., Chaponnier, C. & Brown, R. a. Myofibroblasts and

mechano-regulation of connective tissue remodelling. *Nat. Rev. Mol. Cell Biol.* **3,** 349–63 (2002).

58. Lee, K. H., Kim, H. Y., Bang, H. J., Jung, Y. H. & Lee, S. G. The change of bead morphology formed on electrospun polystyrene fibers. *Polymer (Guildf).* **44,** 4029–4034 (2003).

59. Vashaghian, M., Zandieh, B., Roovers, J. P. & Smit, T. H. Electrospun matrices for pelvic floor repair: effect of fiber diameter on mechanical properties and cell behavior. *Tissue Eng. Part A* ten.TEA.2016.0194 (2016). doi:10.1089/ten.TEA.2016.0194

60. Huang, Z.-M., Zhang, Y.-Z., Kotaki, M. & Ramakrishna, S. A review on polymer nanofibers by electrospinning and their applications in nanocomposites. *Compos. Sci. Technol.* **63,** 2223–2253 (2003).

61. Li, W., Shanti, R. M. & Tuan, R. S. *Electrospinning Technology for Nanofibrous Scaffolds in Tissue Engineering*. **9,** (2006).

62. Vince Beachleya and Xuejun Wena,b,c, * aClemson–MUSC. Effect of electrospinning parameters on the nanofiber diameter and length. *Mater. Sci. Eng. C. Mater. Biol. Appl.* **29,** 663–668 (2009).

63. Kim, Y.-J., Ahn, C. H. & Choi, M. O. Effect of thermal treatment on the characteristics of electrospun PVDF−silica composite nanofibrous membrane. *Eur. Polym. J.* **46,** 1957–1965 (2010).

64. Lee, S. J. *et al.* The use of thermal treatments to enhance the mechanical properties of electrospun poly(epsilon-caprolactone) scaffolds. *Biomaterials* **29,** 1422–30 (2008).

65. Nezarati, R. M., Eifert, M. B. & Cosgriff-Hernandez, E. Effects of humidity and solution viscosity on electrospun fiber morphology. *Tissue Eng. Part C Methods* **19,** 810–819 (2013).

66. Stevens, M. M. & George, J. H. Exploring and engineering the cell surface interface. *Science* **310,** 1135–8 (2005).

67. Xie, J., MacEwan, M. R., Schwartz, A. G. & Xia, Y. Electrospun nanofibers for neural tissue engineering. *Nanoscale* **2,** 35–44 (2010).

68. Chang, P.-C. *et al.* Bone tissue engineering with novel rhBMP2-PLLA composite scaffolds. *J. Biomed. Mater. Res. A* **81,** 771–780 (2007).

69. Gomelsky, A., Penson, D. F. & Dmochowski, R. R. Pelvic organ prolapse (POP) surgery: the evidence for the repairs. *BJU Int.* **107,** 1704–19 (2011).

70. Roman Regueros, S. *et al.* Acute *in-vivo* response to an alternative implant for urogynecology. *Biomed Res. Int.* **2014,** 853610 (2014).

71. Karlovsky, M. E., Kushner, L. & Badlani, G. H. Synthetic biomaterials for pelvic floor reconstruction. *Curr. Urol. Rep.* **6,** 376–84 (2005).

72. Mistrangelo, E., Mancuso, S., Nadalini, C., Lijoi, D. & Costantini, S. Rising use of synthetic mesh in transvaginal pelvic reconstructive surgery: a review of the risk of vaginal erosion. *J. Minim. Invasive Gynecol.* **14,** 564–9 (2007).

73. Agarwal, S., Wendorff, J. H. & Greiner, A. Use of electrospinning technique for biomedical applications. *Polymer (Guildf).* **49,** 5603–5621 (2008).

74. Mangera, A., Bullock, A. J., Roman, S., Chapple, C. R. & MacNeil, S. Comparison of candidate scaffolds for tissue engineering for stress urinary incontinence and pelvic organ prolapse repair. *BJU Int.* **112,** 674–85 (2013).

75. Ruiz-Zapata, a. M. *et al.* Functional characteristics of vaginal fibroblastic cells from premenopausal women with pelvic organ prolapse. *Mol. Hum. Reprod.* **20,** 1135–1143 (2014).

76. Alarab, M., Kufaishi, H., Lye, S., Drutz, H. & Shynlova, O. Expression of extracellular matrix-remodeling proteins is altered in vaginal tissue of premenopausal women with severe pelvic organ prolapse. *Reprod. Sci.* **21,** 704–15 (2014).

77. Pant, H. R. & Kim, C. S. Electrospun gelatin/nylon-6 composite nanofibers for biomedical applications. *Polym. Int.* n/a-n/a (2012). doi:10.1002/pi.4380

78. Springer, I. N., Fleiner, B., Jepsen, S. & Acil, Y. Culture of cells gained from temporomandibular joint cartilage on non- absorbable scaffolds. *Biomaterials* **22,** 2569–2577 (2001).

79. Seyednejad, H., Ghassemi, A. H., Van Nostrum, C. F., Vermonden, T. & Hennink, W. E. Functional aliphatic polyesters for biomedical and pharmaceutical applications. *J. Control. Release* **152,** 168–176 (2011).

80. Franco, R. A., Nguyen, T. H. & Lee, B.-T. Preparation and characterization of electrospun PCL/PLGA membranes and chitosan/gelatin hydrogels for skin bioengineering applications. *J. Mater. Sci. Mater. Med.* **22,** 2207–18 (2011).

81. Zhang, Y., Ouyang, H., Lim, C. T., Ramakrishna, S. & Huang, Z.-M. Electrospinning of gelatin fibers and gelatin/PCL composite fibrous scaffolds. *J. Biomed. Mater. Res. B. Appl. Biomater.* **72,** 156–65 (2005).

82. Soliman, S. *et al.* Multiscale three-dimensional scaffolds for soft tissue engineering via multimodal electrospinning. *Acta Biomater.* **6,** 1227–37 (2010).

83. OPTICS11 Amsterdam, T. N. Measuring mechanical properties by nanoindentation. 1–5

84. Wang, S. *et al.* Bioactive and biodegradable silica biomaterial for bone regeneration. *Bone* **67,** 292–304 (2014).

85. Mattei, G., Gruca, G., Rijnveld, N. & Ahluwalia, a. The nano-epsilon dot method for strain rate viscoelastic characterisation of soft biomaterials by spherical nano-indentation. *J. Mech. Behav. Biomed. Mater.* **50,** 150–159 (2015).

86. Ruiz-Zapata, A. M. *et al.* Fibroblasts from women with pelvic organ prolapse show differential mechanoresponses depending on surface substrates. *Int. Urogynecol. J.* **24,** 1567–75 (2013).

87. de Tayrac, R., Deffieux, X., Gervaise, A., Chauveaud-Lambling, A. & Fernandez, H. Long-term anatomical and functional assessment of trans-vaginal cystocele repair using a tension-free polypropylene mesh. *Int. Urogynecol. J. Pelvic Floor Dysfunct.* **17,** 483–488 (2006).

88. Liang, R., Zong, W., Palcsey, S., Abramowitch, S. & Moalli, P. a. Impact of prolapse meshes on the metabolism of vaginal extracellular matrix in rhesus macaque. *Am. J. Obstet. Gynecol.* **212,** 174–176 (2014).

89. Jean-Charles, C. *et al.* Biomechanical properties of prolapsed or non-prolapsed vaginal tissue: impact on genital prolapse surgery. *Int. Urogynecol. J.* **21,** 1535–8 (2010).

90. Rubod, C. *et al.* Biomechanical properties of human pelvic organs. *Urology* **79,** 968.e17-22 (2012).

91. Guo, W., Frey, M. T., Burnham, N. a & Wang, Y. Substrate rigidity regulates the formation and maintenance of tissues. *Biophys. J.* **90,** 2213–20 (2006).

92. Chiquet, M., Renedo, A. S., Huber, F. & Flück, M. How do fibroblasts translate mechanical signals into changes in extracellular matrix production? *Matrix Biol.* **22,** 73–80 (2003).

93. Gautieri, A., Vesentini, S., Redaelli, A. & Buehler, M. J. Hierarchical structure and nanomechanics of collagen microfibrils from the atomistic scale up. *Nano Lett.* **11,** 757–766 (2011).

94. Wolfram, U., Wilke, H. J. & Zysset, P. K. Rehydration of vertebral trabecular bone: Influences on its anisotropy, its stiffness and the indentation work with a view to age, gender and vertebral level. *Bone* **46,** 348–354 (2010).

95. Pizzoferrato, a *et al.* Cell culture methods for testing biocompatibility. *Clin. Mater.* **15,** 173–190 (1994).

96. Walters, N. J. & Gentleman, E. Evolving insights in cell–matrix interactions: Elucidating how non-soluble properties of the extracellular niche direct stem cell fate. *Acta Biomater.* **11,** 3–16 (2015).

97. Raposo, G. & Stoorvogel, W. Extracellular vesicles: Exosomes, microvesicles, and friends. *J. Cell Biol.* **200,** 373–383 (2013).

98. Christopherson, G. T., Song, H. & Mao, H. Q. The influence of fiber diameter of electrospun substrates on neural stem cell differentiation and proliferation. *Biomaterials* **30,** 556–564 (2009).

99. Chen, M., Patra, P. K., Warner, S. B. & Bhowmick, S. Role of fiber diameter in adhesion and proliferation of NIH 3T3 fibroblast on electrospun polycaprolactone scaffolds. *Tissue Eng.* **13,** 579–587 (2007).

100. Mahshid Vashaghian, Alejandra M. Ruiz-Zapata, Manon H. Kerkhof, 3 Behrouz Zandieh-Doulabi, Arie Werner, Jan Paul Roovers, and T. H. S. Toward a New Generation of Pelvic Floor Implants With Electrospun Nanofibrous Matrices: A Feasibility Study. *Neurourol. Urodyn.* **34,** 224–230 (2016).

101. Ebersole, G. C. *et al.* Development of novel electrospun absorbable polycaprolactone (PCL) scaffolds for hernia repair applications. *Surg. Endosc.* **26,** 2717–28 (2012).

102. Hashizume, R. *et al.* Morphological and mechanical characteristics of the reconstructed rat abdominal wall following use of a wet electrospun biodegradable polyurethane elastomer scaffold. *Biomaterials* **31,** 3253–65 (2010).

103. Bashur, C. a, Dahlgren, L. a & Goldstein, A. S. Effect of fiber diameter and orientation on fibroblast morphology and proliferation on electrospun poly(D,L-lactic-co-glycolic acid) meshes. *Biomaterials* **27,** 5681–8 (2006).

104. Li, W.-J., Jiang, Y. J. & Tuan, R. S. Chondrocyte phenotype in engineered fibrous matrix is regulated by fiber size. *Tissue Eng.* **12,** 1775–1785 (2006).

105. Flemming, R. G., Murphy, C. J., Abrams, G. a., Goodman, S. L. & Nealey, P. F. Effects of synthetic micro- and nano-structured surfaces on cell behavior. *Biomaterials* **20,** 573–588 (1999).

106. Del Gaudio, C. *et al.* Evaluation of electrospun bioresorbable scaffolds for tissue-engineered urinary bladder augmentation. *Biomed. Mater.* **8,** 45013 (2013).

107. Hung, M.-J. *et al.* Tissue-engineered fascia from vaginal fibroblasts for patients needing reconstructive pelvic surgery. *Int. Urogynecol. J.* **21,** 1085–93 (2010).

108. Li, Q., Wang, J., Liu, H., Xie, B. & Wei, L. Tissue-engineered mesh for pelvic floor reconstruction fabricated from silk fibroin scaffold with adipose-derived mesenchymal stem cells. *Cell Tissue Res.* **354,** 471–80 (2013).

109. Pu, J., Yuan, F., Li, S. & Komvopoulos, K. Electrospun bilayer fibrous scaffolds for enhanced cell infiltration and vascularization *in-vivo*. *Acta Biomater.* **13,** 131–141 (2014).

110. Chan, S. *et al.* Tensile Stress-Strain Response of Small-diameter Electrospun Fibers. *Appl. Note* 1–4 (2012).

111. Balguid, A. *et al.* Tailoring Fiber Diameter in Electrospun Poly (e -Caprolactone) Scaffolds for Optimal Cellular Infiltration in Cardiovascular Tissue Engineering. **15,** (2009).

112. Moroni, L., Licht, R., de Boer, J., de Wijn, J. R. & van Blitterswijk, C. A. Fiber diameter and texture of electrospun PEOT/PBT scaffolds influence human mesenchymal stem cell proliferation and morphology, and the release of incorporated compounds. *Biomaterials* **27,** 4911–4922 (2006).

113. Joshi, V. S., Lei, N. Y., Walthers, C. M., Wu, B. & Dunn, J. C. Y. Macroporosity enhances vascularization of electrospun scaffolds. *J. Surg. Res.* **183,** 18–26 (2013).

114. Dong, Y., Liao, S., Ngiam, M., Chan, C. K. & Ramakrishna, S. Degradation behaviors of electrospun resorbable polyester nanofibers. *Tissue Eng. Part B. Rev.* **15,** 333–351 (2009).

115. Veleirinho, B., Rei, M. F. & Lopes-Da-Silva, J. A. Solvent and concentration effects on the properties of electrospun polyethylene terephthalate nanofiber mats. *J. Polym. Sci. Part B Polym. Phys.* **46,** 460–471 (2008).

116. Maleki, H., Gharehaghaji, a a, Moroni, L. & Dijkstra, P. J. Influence of the solvent type on the morphology and mechanical properties of electrospun PLLA yarns. *Biofabrication* **5,** 35014 (2013).

117. Saino, E. *et al.* Effect of electrospun fiber diameter and alignment on macrophage activation and secretion of proinflammatory cytokines and chemokines. *Biomacromolecules* **12,** 1900–1911 (2011).

118. Garg, K., Pullen, N. a., Oskeritzian, C. a., Ryan, J. J. & Bowlin, G. L. Macrophage functional polarization (M1/M2) in response to varying fiber and pore dimensions of electrospun scaffolds. *Biomaterials* **34,** 4439–4451 (2013).

119. Milleret, V., Hefti, T., Hall, H., Vogel, V. & Eberli, D. Influence of the fiber diameter and surface roughness of electrospun vascular grafts on blood activation. *Acta Biomater.* **8,** 4349–56 (2012).

120. Badami, A. S., Kreke, M. R., Thompson, M. S., Riffle, J. S. & Goldstein, A. S. Effect of fiber diameter on spreading, proliferation, and differentiation of osteoblastic cells on electrospun poly(lactic acid) substrates. *Biomaterials* **27,** 596–606 (2006).

121. Blaauboer, M. E. *et al.* Extracellular matrix proteins: A positive feedback loop in lung fibrosis? *Matrix Biol.* **34,** 2–10 (2013).

122. Rustad, K. C., Wong, V. W. & Gurtner, G. C. The role of focal adhesion complexes in fibroblast mechanotransduction during scar formation. *Differentiation* **86,** 87–91 (2013).

123. Levy-Mishali, M., Zoldan, J. & Levenberg, S. Effect of scaffold stiffness on myoblast differentiation. *Tissue Eng. Part A* **15,** 935–944 (2009).

124. Branco da Cunha, C. *et al.* Influence of the stiffness of three-dimensional alginate/collagen-I interpenetrating networks on fibroblast biology. *Biomaterials* **35,** 8927–8936 (2014).

125. Roman, S., Mangir, N., Bissoli, J., Chapple, C. R. & Macneil, S. Biodegradable scaffolds designed to mimic fascia-like properties for the treatment of pelvic organ prolapse and stress urinary incontinence. **30,** 1578–1588 (2016).

126. Yamamoto, N. *et al.* Effects of stress shielding on the mechanical properties of rabbit patellar tendon. *J. Biomech. Eng.* **115,** 23–8 (1993).

127. Nerurkar, N. L., Sen, S., Baker, B. M., Elliott, D. M. & Mauck, R. L. Dynamic Culture Enhances Stem Cell Infiltration and Modulates Extracellular Matrix Production on Aligned Electrospun Nanofibrous Scaffolds. **7,** 485–491 (2012).

128. Cardwell, R. D. *et al.* Static and Cyclic Mechanical Loading of Mesenchymal Stem Cells on Elastomeric, Electrospun Polyurethane Meshes. *J. Biomech. Eng.* **137,** 71010 (2015).

129. Berendsen, A. D. *et al.* Three-Dimensional Loading Model for Periodontal Ligament Regeneration *in-vitro*. *Tissue Eng. Part C. Methods* **15,** 1–10 (2009).

130. Chiquet, M. Regulation of extracellular matrix gene expression by mechanical stress. *Matrix Biol.* **18,** 417–426 (1999).

131. Kufaishi, H., Alarab, M., Drutz, H., Lye, S. & Shynlova, O. Static Mechanical Loading Influences the Expression of Extracellular Matrix and Cell Adhesion Proteins in Vaginal Cells Derived From Premenopausal Women With Severe Pelvic Organ Prolapse. *Reprod. Sci.* (2016). doi:10.1177/1933719115625844

132. Wazen, R. M. *et al.* Micromotion-induced strain fields influence early stages of repair at bone-implant interfaces. *Acta Biomater.* **9,** 6663–6674 (2013).

133. Tomasek, J. J., Gabbiani, G., Hinz, B., Chaponnier, C. & Brown, R. a. Myofibroblasts and mechano-regulation of connective tissue remodelling. *Nat. Rev. Mol. Cell Biol.* **3,** 349–363 (2002).

134. Lu, L., Oswald, S. J., Ngu, H. & Yin, F. C.-P. Mechanical properties of actin stress fibers in living cells. *Biophys. J.* **95,** 6060–71 (2008).

135. Tojkander, S., Gateva, G. & Lappalainen, P. Actin stress fibers - assembly, dynamics and biological roles. *J. Cell Sci.* **125,** 1855–1864 (2012).

136. Foolen, J., Deshpande, V. S., Kanters, F. M. W. & Baaijens, F. P. T. The influence of matrix integrity on stress-fiber remodeling in 3D. *Biomaterials* **33,** 7508–7518 (2012).

137. Wang, J. H. C., Thampatty, B. P., Lin, J. S. & Im, H. J. Mechanoregulation of gene expression in fibroblasts. *Gene* **391,** 1–15 (2007).

138. van Geemen, D., Driessen-Mol, A., Baaijens, F. P. T. & Bouten, C. V. C. Understanding strain-induced collagen matrix development in engineered cardiovascular tissues from gene expression profiles. *Cell Tissue Res.* **352,** 727–37 (2013).

139. Newby, A. C. Matrix metalloproteinases regulate migration, proliferation, and death of vascular smooth muscle cells by degrading matrix and non-matrix substrates. *Cardiovasc. Res.* **69,** 614–624 (2006).

140. Kim, B.-S., Nikolovski, J., Bonadio, J. & Mooney, D. J. Cyclic mechanical strain regulates the development of engineered smooth muscle tissue. *Nat. Biotechnol.* **17,** 979–983 (1999).

141. Gupta, V. & Grande-Allen, K. J. Effects of static and cyclic loading in regulating extracellular matrix synthesis by cardiovascular cells. *Cardiovascular Research* **72,** 375–383 (2006).

142. Junge, K. *et al.* Decreased collagen type I/III ratio in patients with recurring hernia after implantation of alloplastic prostheses. *Langenbeck's Arch. Surg.* **389,** 17–22 (2004).

143. Hinz, B. Tissue stiffness, latent TGF-β1 Activation, and mechanical signal transduction: Implications for the pathogenesis and treatment of fibrosis. *Current Rheumatology Reports* **11,** 120–126 (2009).

144. Wipff, P. J., Rifkin, D. B., Meister, J. J. & Hinz, B. \nMyofibroblast contraction activates latent TGF-beta1 from the extracellular matrix\n. *nJ Cell Biol*\n **\n179\n,** 123–1311 (2007).

145. Wipff, P.-J. & Hinz, B. Integrins and the activation of latent transforming growth factor beta1 - an intimate relationship. *Eur. J. Cell Biol.* **87,** 601–15 (2008).

146. Chaponnier, C. & Gabbiani, G. Tissue repair , contraction , and the myofibroblast factors involved in myofibroblastic. *Wound Repair Regen.* **13,** 7–12 (2005).

147. Ahmed, I. *et al.* Morphology, cytoskeletal organization, and myosin dynamics of mouse embryonic fibroblasts cultured on nanofibrillar surfaces. *Mol. Cell. Biochem.* **301,** 241–249 (2007).

148. Sheikh, Z., Brooks, P. J., Barzilay, O., Fine, N. & Glogauer, M. Macrophages, foreign body giant cells and their response to implantable biomaterials. *Materials (Basel).* **8,** 5671–5701 (2015).

149. Colaco, M., Mettu, J. & Badlani, G. The scientific basis for the use of biomaterials in SUI and POP. *BJU Int.* (2014). doi:10.1111/bju.12819

150. Yang, G., Im, H. J. & Wang, J. H. C. Repetitive mechanical stretching modulates IL-1beta induced COX-2, MMP-1 expression, and PGE2 production in human patellar tendon fibroblasts. *Gene* **363,** 166–172 (2005).

151. Chowdhury, T. T. *et al.* Dynamic compression counteracts IL-1beta induced inducible nitric oxide synthase and cyclo-oxygenase-2 expression in chondrocyte/agarose constructs. *Arthritis Res. Ther.* **10,** R35 (2008).

152. Tsuzaki, M. *et al.* ATP modulates load-inducible IL-1beta, COX 2, and MMP-3 gene expression in human tendon cells. *J. Cell. Biochem.* **89,** 556–562 (2003).

153. Sell, S. a. *et al.* The Use of Natural Polymers in Tissue Engineering: A Focus on Electrospun Extracellular Matrix Analogues. *Polymers (Basel).* **2,** 522–553 (2010).

154. Wang, S., Zhang, Z., Lü, D. & Xu, Q. Effects of Mechanical Stretching on the Morphology and Cytoskeleton of Vaginal Fibroblasts from Women with Pelvic Organ Prolapse. *Int. J. Mol. Sci.* 9406–9419 (2014). doi:10.3390/ijms16059406

155. Lee, C. H. *et al.* Nanofiber alignment and direction of mechanical strain affect the ECM production of human ACL fibroblast. *Biomaterials* **26,** 1261–1270 (2005).

156. Prodanov, L. *et al.* The interaction between nanoscale surface features and mechanical loading and its effect on osteoblast-like cells behavior. *Biomaterials* **31,** 7758–7765 (2010).

157. Bilsel, Y. & Abci, I. The search for ideal hernia repair; mesh materials and types. *Int. J. Surg.* **10,** 317–321 (2012).

158. Brown, C. N. & Finch, J. G. Which mesh for hernia repair? *Ann. R. Coll. Surg. Engl.* **92,** 272–8 (2010).

159. Greca, F. H. *et al.* The influence of porosity on the integration histology of two polypropylene meshes for the treatment of abdominal wall defects in dogs. *Hernia* **12,** 45–49 (2008).

160. Gao, Y., Liu, Z., Liu, F. & Furukawa, K. Mechanical shear contributes to granule formation resulting in quick start-up and stability of a hybrid anammox reactor. *Biodegradation* **23,** 363–372 (2012).

161. Katz, S., Izhar, M. & Mirelman, D. Bacterial adherence to surgical sutures. A possible factor in suture induced infection. *Ann. Surg.* **194,** 35–41 (1981).

162. Coughlin, R. W., Mullen, D., Brancieri, M., Rezman, V. & Vieth, R. F. Surface roughness enhances upward migration of bacteria on polymer fibers above liquid cultures. *J. Biomater. Sci. Polym. Ed.* **10,** 827–844 (1999).

163. Junge, K. *et al.* Elasticity of the anterior abdominal wall and impact for reparation of incisional hernias using mesh implants. *Hernia* **5,** 113–118 (2001).

164. Peña, E. *et al.* Mechanical characterization of the softening behavior of human vaginal tissue. *J. Mech. Behav. Biomed. Mater.* **4,** 275–83 (2011).

165. Gräbel, D., Prescher, A., Fitzek, S., Keyserlingk, D. G. V & Axer, H. Anisotropy of human linea alba: A biomechanical study. *J. Surg. Res.* **124,** 118–125 (2005).

166. Hernández, B. *et al.* Mechanical and histological characterization of the abdominal muscle. A previous step to modelling hernia surgery. *J. Mech. Behav. Biomed. Mater.* **4,** 392–404 (2011).

167. Hernández-Gascón, B. *et al.* Mechanical behaviour of synthetic surgical meshes: Finite element simulation of the herniated abdominal wall. *Acta Biomater.* **7,** 3905–3913 (2011).

168. Rubod, C. *et al.* Biomechanical properties of vaginal tissue: preliminary results. *Int. Urogynecol. J. Pelvic Floor Dysfunct.* **19,** 811–6 (2008).

169. Courtney, T., Sacks, M. S., Stankus, J., Guan, J. & Wagner, W. R. Design and analysis of tissue engineering scaffolds that mimic soft tissue mechanical anisotropy. *Biomaterials* **27,** 3631–8 (2006).

170. Ozog, Y. *et al.* Persistence of polypropylene mesh anisotropy after implantation: An experimental study. *BJOG An Int. J. Obstet. Gynaecol.* **118,** 1180–1185 (2011).

171. Zhu, L.-M., Schuster, P. & Klinge, U. Mesh implants: An overview of crucial mesh parameters. *World J. Gastrointest. Surg.* **7,** 226–36 (2015).

172. Klinge, U., Klosterhalfen, B., Müller, M., Ottinger, a P. & Schumpelick, V. Shrinking of polypropylene mesh *in-vivo*: an experimental study in dogs. *Eur. J. Surg.* **164,** 965–969 (1998).

173. Bergmeister, H. *et al.* Healing characteristics of electrospun polyurethane grafts with various porosities. *Acta Biomater.* **9,** 6032–40 (2013).

174. Massumi, M. *et al.* The Effect of Topography on Differentiation Fates of Matrigel-Coated Mouse Embryonic Stem Cells Cultured on PLGA Nanofibrous Scaffolds. **18,** (2012).

175. Pham, Q. P., Sharma, U. & Mikos, A. G. Electrospun poly(epsilon-caprolactone) microfiber and multilayer nanofiber/microfiber scaffolds: characterization of scaffolds and measurement of cellular infiltration. *Biomacromolecules* **7,** 2796–805 (2006).

176. Kwon, I. K., Kidoaki, S. & Matsuda, T. Electrospun nano- to microfiber fabrics made of biodegradable copolyesters: structural characteristics, mechanical properties and cell adhesion potential. *Biomaterials* **26,** 3929–39 (2005).

177. Bhardwaj, N. & Kundu, S. C. Electrospinning: a fascinating fiber fabrication technique. *Biotechnol. Adv.* **28,** 325–47 (2010).

178. Martins, a., Reis, R. L. & Neves, N. M. Electrospinning: processing technique for tissue engineering scaffolding. *Int. Mater. Rev.* **53,** 257–274 (2008).

179. Sill, T. J. & von Recum, H. a. Electrospinning: applications in drug delivery and tissue engineering. *Biomaterials* **29,** 1989–2006 (2008).

180. SY Chew1,2, Y Wen3, Y Dzenis3, and KW Leong1, *. The Role of Electrospinning in the Emerging Field of Nanomedicine. **12,** 4751–4770 (2008).

181. Liu, W., Thomopoulos, S. & Xia, Y. Electrospun Nanofibers for Regenerative Medicine. *Adv. Healthc. Mater.* **1,** 10–25 (2012).

182. Naderi, H., Matin, M. M. & Bahrami, A. R. Review paper: critical issues in tissue engineering: biomaterials, cell sources, angiogenesis, and drug delivery systems. *J. Biomater. Appl.* **26,** 383–417 (2011).

183. III, E. B. SOFTbank E-Book Center Tehran, Phone: 66403879, 66493070 For Educational Use. (1999).

184. Boyan, B. D., Hummert, T. W., Dean, D. D. & Schwartz, Z. Role of material surfaces in regulating bone and cartilage cell response. *Biomaterials* **17,** 137–146 (1996).

185. M. Alessandri a,1, G. Lizzo b,1, C. Gualandi c,d, C.Mangano b, A. Giuliani b,M.L. Focarete a,c, ∗,2,L. Calzà a,b,M. Alessandri a,1, G. Lizzo b,1, C. Gualandi c,d, C.Mangano b, A. Giuliani b,M.L. Focarete a,c, ∗,2,L. Calzà a,b. Influence of biological matrix and artificial electrospun scaffolds on proliferation, differentiation and trophic factor synthesis of rat embryonic stem cells.

186. Huang, L. *et al.* Improved mechanical properties and hydrophilicity of electrospun nanofiber membranes for filtration applications by dopamine modification. *J. Memb. Sci.* **460,** 241–249 (2014).

187. Baker, S. C. *et al.* Characterisation of electrospun polystyrene scaffolds for three-

dimensional *in-vitro* biological studies. *Biomaterials* **27,** 3136–46 (2006).

188. Woo, K. M., Chen, V. J. & Ma, P. X. Nano-fibrous scaffolding architecture selectively enhances protein adsorption contributing to cell attachment. *J. Biomed. Mater. Res. A* **67,** 531–537 (2003).

189. Matthews, J. a, Wnek, G. E., Simpson, D. G. & Bowlin, G. L. Electrospinning of collagen nanofibers. *Biomacromolecules* **3,** 232–8 (2002).

190. Mcmanus, M. C., Boland, E. D., Simpson, D. G., Barnes, C. P. & Bowlin, G. L. Electrospun fibrinogen : Feasibility as a tissue engineering scaffold in a rat cell culture model. (2006). doi:10.1002/jbm.a

191. Xie, M. *et al.* Evaluation of stretched electrospun silk fibroin matrices seeded with urothelial cells for urethra reconstruction. *J. Surg. Res.* **184,** 774–81 (2013).

192. Varanasi, V. ., Shiakolas, P. . & Aswath, P. . Optimizing strategies for electrospun silk fibroin tissue engineering scaffolds. *Biomaterials* **30,** 3058–3067 (2009).

193. Li, M. *et al.* Electrospun protein fibers as matrices for tissue engineering. *Biomaterials* **26,** 5999–6008 (2005).

194. Gomes, S. R. *et al. In-vitro* and *in-vivo* evaluation of electrospun nanofibers of PCL, chitosan and gelatin: A comparative study. *Mater. Sci. Eng. C* **46,** 348–358 (2015).

195. Schindler, M. *et al.* A synthetic nanofibrillar matrix promotes *in-vivo*-like organization and morphogenesis for cells in culture. *Biomaterials* **26,** 5624–31 (2005).

196. Ma, Z., Kotaki, M., Yong, T., He, W. & Ramakrishna, S. Surface engineering of electrospun polyethylene terephthalate (PET) nanofibers towards development of a new material for blood vessel engineering. *Biomaterials* **26,** 2527–36 (2005).

197. Alamein, M. A., Stephens, S., Liu, Q., Skabo, S. & Warnke, P. H. Mass Production of Nanofibrous Extracellular Matrix with Controlled 3D Morphology for Large-Scale Soft Tissue Regeneration. **19,** 458–473 (2013).

198. Webb, K. *et al.* Cyclic strain increases fibroblast proliferation, matrix accumulation, and elastic modulus of fibroblast-seeded polyurethane constructs. *J. Biomech.* **39,** 1136–44 (2006).

199. John J. Stankus1, 2, Donald O. Freytes2, 3, Stephen F. Badylak2, 3, 4, and W. R. & Wagner1, 2, 3, 4. Hybrid nanofibrous scaffolds from electrospinning of a synthetic biodegradable elastomer and urinary bladder matrix. **19,** 635–652 (2010).

200. Hong, Y., Ph, D., Takanari, K. & Amoroso, N. J. An Elastomeric Patch Electrospun from a Blended Solution of Dermal Extracellular Matrix and Biodegradable Polyurethane for Rat Abdominal Wall Repair. **18,** 122–132 (2012).

201. Tottey, S. *et al.* Extracellular matrix degradation products and low-oxygen conditions enhance the regenerative potential of perivascular stem cells. *Tissue Eng. Part A* **17,** 37–44

(2011).

202. Guarino, V., Alvarez-Perez, M., Cirillo, V. & Ambrosio, L. hMSC interaction with PCL and PCL/gelatin platforms: A comparative study on films and electrospun membranes. *J. Bioact. Compat. Polym.* **26,** 144–160 (2011).

203. McManus, M. C. *et al.* Electrospun Fibrinogen-Polydioxanone Composite Matrix: Potential for In Situ Urologic Tissue Engineering. *J. Eng. Fiber. Fabr.* **3,** 10 (2008).

204. Nair, R. P., Joseph, J., Harikrishnan, V. S., Krishnan, V. K. & Krishnan, L. Contribution of fibroblasts to the mechanical stability of *in-vitro* engineered dermal-like tissue through extracellular matrix deposition. *Biores. Open Access* **3,** 217–25 (2014).

205. Hiep, N. T. & Lee, B.-T. Electro-spinning of PLGA/PCL blends for tissue engineering and their biocompatibility. *J. Mater. Sci. Mater. Med.* **21,** 1969–78 (2010).

206. Selim, M., Bullock, A. J., Blackwood, K. a, Chapple, C. R. & MacNeil, S. Developing biodegradable scaffolds for tissue engineering of the urethra. *BJU Int.* **107,** 296–302 (2011).

207. Sun, T. *et al.* Self-organization of skin cells in three-dimensional electrospun polystyrene scaffolds. *Tissue Eng.* **11,** 1023–33 (2005).

208. McManus, M. *et al.* Electrospun nanofibre fibrinogen for urinary tract tissue reconstruction. *Biomed. Mater.* **2,** 257–62 (2007).

209. Maya, H. *et al.* Increased porosity of electrospun hybrid scaffolds improved bladder tissue regeneration. *J. Biomed. Mater. Res. A* 1–9 (2013). doi:10.1002/jbm.a.34889

210. Jeong, S. I. *et al.* Improved cell infiltration of highly porous 3D nanofibrous scaffolds formed by combined fiber–fiber charge repulsions and ultra-sonication. *J. Mater. Chem. B* **2,** 8116–8122 (2014).

211. Nam, J., Huang, Y., Agarwal, S. & Lannutti, J. Improved cellular infiltration in electrospun fiber via engineered porosity. *Tissue Eng.* **13,** 2249–57 (2007).

212. Nerurkar, N. L., Sen, S., Baker, B. M., Elliott, D. M. & Mauck, R. L. Dynamic culture enhances stem cell infiltration and modulates extracellular matrix production on aligned electrospun nanofibrous scaffolds. *Acta Biomater.* **7,** 485–91 (2011).

213. Lee, J. B., Yang, D. H. & Ph, D. Highly Porous Electrospun Nanofibers Enhanced by Ultrasonication for Improved Cellular Infiltration. **17,** (2011).

214. Zhong, S., Ph, D., Zhang, Y. & Lim, C. T. Fabrication of Large Pores in Electrospun Nanofibrous Scaffolds for Cellular Infiltration : A Review. **18,** (2012).

215. Baker, B. M. *et al.* The potential to improve cell infiltration in composite fiber-aligned electrospun scaffolds by the selective removal of sacrificial fibers. *Biomaterials* **29,** 2348–58 (2008).

216. Rnjak-Kovacina, J. & Weiss, A. S. Increasing the pore size of electrospun scaffolds. *Tissue Eng. Part B. Rev.* **17,** 365–72 (2011).

217. Wong, S.-C., Baji, A. & Leng, S. Effect of fiber diameter on tensile properties of electrospun poly(ε-caprolactone). *Polymer (Guildf).* **49,** 4713–4722 (2008).

218. Sell, S., Barnes, C., Simpson, D. & Bowlin, G. Scaffold permeability as a means to determine fiber diameter and pore size of electrospun fibrinogen. *J. Biomed. Mater. Res. - Part A* **85,** 115–126 (2008).

219. Ning Wanga, Krishna Burugapallia, Wenhui Songb, Justin Hallsa, Francis Moussya, Y. & Zhengc, Yanxuan Mac, Zhentao Wud, and K. L. Tailored fibro-porous structure of electrospun polyurethane membranes, their size-dependent properties and trans- membrane glucose diffusion. **4,** 207–217 (2011).

220. Youngstrom, D. W., Barrett, J. G., Jose, R. R. & Kaplan, D. L. Functional Characterization of Detergent-Decellularized Equine Tendon Extracellular Matrix for Tissue Engineering Applications. *PLoS One* **8,** (2013).

221. Hong, Y. *et al.* Mechanical properties and *in-vivo* behavior of a biodegradable synthetic polymer microfiber-extracellular matrix hydrogel biohybrid scaffold. *Biomaterials* **32,** 3387–94 (2011).

222. Abramowitch, S. D., Feola, A., Jallah, Z. & Moalli, P. a. Tissue mechanics, animal models, and pelvic organ prolapse: a review. *Eur. J. Obstet. Gynecol. Reprod. Biol.* **144 Suppl,** S146-58 (2009).

223. Veleirinho, B. *et al.* Foreign body reaction associated with PET and PET/chitosan electrospun nanofibrous abdominal meshes. *PLoS One* **9,** e95293 (2014).

224. Jaiswal, A. K., Dhumal, R. V., Bellare, J. R. & Vanage, G. R. *In-vivo* biocompatibility evaluation of electrospun composite scaffolds by subcutaneous implantation in rat. *Drug Deliv. Transl. Res.* **3,** 504–517 (2013).

225. Nasser Shakhssalim, 1 Mohammad Mehdi Dehghan, 2 Reza Moghadasali, 3 Moham- mad Hossein Soltani, 4 Iman Shabani, 5 Masoud Soleimani6. Bladder Tissue Engineering Using Biocompatible Nanofibrous Electrospun Constructs. *Cell. Mol. Urol.* (2011).

226. Leong, M. F., Chan, W. Y., Chian, K. S., Rasheed, M. Z. & Anderson, J. M. Fabrication and *in-vitro* and *in-vivo* cell infiltration study of a bilayered cryogenic electrospun poly(D,L-lactide) scaffold. *J. Biomed. Mater. Res. - Part A* **94,** 1141–1149 (2010).

227. Kim, M. S. *et al.* Highly porous 3D nanofibrous scaffolds processed with an electrospinning/laser process. *Curr. Appl. Phys.* **14,** 1–7 (2014).

228. Huang, L., Manickam, S. S. & McCutcheon, J. R. Increasing strength of electrospun nanofiber membranes for water filtration using solvent vapor. *J. Memb. Sci.* **436,** 213–220 (2013).

229. Xu, C., Yang, F., Wang, S. & Ramakrishna, S. *In-vitro* study of human vascular endothelial cell function on materials with various surface roughness. *J. Biomed. Mater. Res. A* **71,** 154–61 (2004).

230. Bullock, A. J., Roman, S., Osman, N., Chapple, C. & Macneil, S. Production of ascorbic acid releasing biomaterials for pelvic floor repair. (2015). doi:10.1016/j.actbio.2015.10.019

231. Chowdhury, M. & Stylios, G. Effect of experimental parameters on the morphology of electrospun Nylon6 fibres. *Int. J. Basic Appl. Sci.* **10,** 70–78 (2010).

232. Bruggeman, J. P. Biodegradable Polyol-Based Polymers A polymer pla ɳ orm for biomedical applica Ɵ ons.

233. Nijst, C. L. E. *et al.* NIH Public Access. **8,** 3067–3073 (2009).

234. Yang, D.-J., Chen, F., Xiong, Z.-C., Xiong, C.-D. & Wang, Y.-Z. Tissue anti-adhesion potential of biodegradable PELA electrospun membranes. *Acta Biomater.* **5,** 2467–74 (2009).

235. Lovett, M. *et al.* Tubular silk sca olds for small diameter vascular grafts. *Organogenesis* **6,** 217–224 (2010).

236. Han, D. & Gouma, P.-I. Electrospun bioscaffolds that mimic the topology of extracellular matrix. *Nanomedicine* **2,** 37–41 (2006).

237. Yang, X., Shah, J. D. & Wang, H. Nanofiber enabled layer-by-layer approach toward three-dimensional tissue formation. *Tissue Eng. Part A* **15,** 945–56 (2009).

238. Kundu, A. K., Gelman, J. & Tyson, D. R. Composite thin film and electrospun biomaterials for urologic tissue reconstruction. *Biotechnol. Bioeng.* **108,** 207–15 (2011).

239. Horan, R. L. *et al.* Biological and biomechanical assessment of a long-term bioresorbable silk-derived surgical mesh in an abdominal body wall defect model. *Hernia* **13,** 189–99 (2009).

240. Horst, M. *et al.* A bilayered hybrid microfibrous PLGA--acellular matrix scaffold for hollow organ tissue engineering. *Biomaterials* **34,** 1537–45 (2013).

241. Zhao, W. *et al.* Diaphragmatic muscle reconstruction with an aligned electrospun poly(ε-caprolactone)/collagen hybrid scaffold. *Biomaterials* **34,** 8235–40 (2013).

242. Merten, O.-W. Advances in cell culture: anchorage dependence. *Philos. Trans. R. Soc. Lond. B. Biol. Sci.* **370,** 20140040 (2015).

243. He, H. *et al.* Preclinical animal study and human clinical trial data of co-electrospun poly(L-lactide-co-caprolactone) and fibrinogen mesh for anterior pelvic floor reconstruction. *Int. J. Nanomedicine* 389 (2016). doi:10.2147/IJN.S88803

244. Boulanger, L., Boukerrou, M., Lambaudie, E., Defossez, A. & Cosson, M. Tissue integration and tolerance to meshes used in gynecologic surgery: an experimental study. *Eur. J. Obstet. Gynecol. Reprod. Biol.* **125,** 103–8 (2006).

245. Siniscalchi, R. T. *et al.* Highly purified collagen coating enhances tissue adherence and integration properties of monofilament polypropylene meshes. *Int. Urogynecol. J.* **24,** 1747–54 (2013).

246. Zhong, S., Zhang, Y. & Lim, C. T. Fabrication of Large Pores in Electrospun Nanofibrous Scaffolds for Cellular Infiltration: A Review. *Tissue Eng. Part B Rev.* **18,** 77–87 (2012).

247. Altaf Mangera, 1, 2* Anthony J. Bullock, 1 Christopher R. Chapple, 2 and Sheila MacNeil1. Are Biomechanical Properties Predictive of the Success of Prostheses Used in Stress Urinary Incontinence and Pelvic Organ Prolapse? A Systematic Review. *Neurourol. Urodyn.* **30,** 169–173 (2012).

248. Wang, K. *et al.* Enhanced Vascularization in Hybrid PCL/Gelatin Fibrous Scaffolds with Sustained Release of VEGF. *Biomed Res. Int.* **2015,** 11 (2014).

249. Drilling, S., Gaumer, J. & Lannutti, J. Fabrication of burst pressure competent vascular grafts via electrospinning: Effects of microstructure. *J. Biomed. Mater. Res. - Part A* **88,** 923–934 (2009).

250. Li, Y., Huang, Z. & Lü˘, Y. Electrospinning of nylon-6,66,1010 terpolymer. *Eur. Polym. J.* **42,** 1696–1704 (2006).

251. Risbud, M. V & Bhonde, R. R. Polyamide 6 composite membranes: properties and *in-vitro* biocompatibility evaluation. *J. Biomater. Sci. Polym. Ed.* **12,** 125–136 (2001).

252. Röhrnbauer, B. & Mazza, E. A non-biological model system to simulate the *in-vivo* mechanical behavior of prosthetic meshes. *J. Mech. Behav. Biomed. Mater.* **20,** 305–315 (2013).

253. Ruiz-Zapata, A. M. *et al.* Vaginal Fibroblastic Cells from Women with Pelvic Organ Prolapse Produce Matrices with Increased Stiffness and Collagen Content. *Sci. Rep.* **6,** 22971 (2016).

254. O'Callaghan, C. J. & Williams, B. Mechanical Strain-Induced Extracellular Matrix Production by Human Vascular Smooth Muscle Cells : Role of TGF- 1. *Hypertension* **36,** 319–324 (2000).

255. Ewies, A. A. A. *et al.* Changes in transcription profile and cytoskeleton morphology in pelvic ligament fibroblasts in response to stretch: The effects of estradiol and levormeloxifene. *Mol. Hum. Reprod.* **14,** 127–135 (2008).

256. Gigliobianco, G. *et al.* Biomaterials for Pelvic Floor Reconstructive Surgery: How Can We Do Better? *Biomed Res. Int.* **2015,** 1–20 (2015).

257. Winters, J. C., Fitzgerald, M. P. & Barber, M. D. The use of synthetic mesh in female pelvic reconstructive surgery. *BJU Int.* **98 Suppl 1,** 70–6; discussion 77 (2006).

258. De Keulenaer, B. L., De Waele, J. J., Powell, B. & Malbrain, M. L. N. G. What is normal intra-abdominal pressure and how is it affected by positioning, body mass and positive end-expiratory pressure? *Intensive Care Med.* **35,** 969–76 (2009).

259. Endo, M. *et al.* Cross-linked xenogenic collagen implantation in the sheep model for vaginal surgery. *Gynecol. Surg.* **12,** 113–122 (2015).

260. Deprest, J. & Feola, A. The need for preclinical research on pelvic floor reconstruction. *BJOG An Int. J. Obstet. Gynaecol.* **120,** 141–143 (2013).

261. Feola, A. *et al.* Host reaction to vaginally inserted collagen containing polypropylene implants in sheep. *Am. J. Obstet. Gynecol.* **212,** 474.e1-474.e8 (2015).

262. Chakroff, J., Kayuha, D., Henderson, M. & Johnson, J. Development and Characterization of Novel Electrospun Meshes for Hernia Repair. *SOJ Mater. Sci. Eng.* (2015).

263. Augustine, R. *et al.* Electrospun poly(ε-caprolactone)-based skin substitutes: *In-vivo* evaluation of wound healing and the mechanism of cell proliferation. *J. Biomed. Mater. Res. B. Appl. Biomater.* 1–10 (2014). doi:10.1002/jbm.b.33325

264. Alves da Silva, M. L. *et al.* Cartilage tissue engineering using electrospun PCL nanofiber meshes and MSCs. *Biomacromolecules* **11,** 3228–36 (2010).

265. Moroni, L., Schotel, R., Hamann, D., de Wijn, J. R. & van Blitterswijk, C. a. 3D Fiber-Deposited Electrospun Integrated Scaffolds Enhance Cartilage Tissue Formation. *Adv. Funct. Mater.* **18,** 53–60 (2008).

266. Ghasemi-Mobarakeh, L., Prabhakaran, M. P., Morshed, M., Nasr-Esfahani, M.-H. & Ramakrishna, S. Electrospun poly(epsilon-caprolactone)/gelatin nanofibrous scaffolds for nerve tissue engineering. *Biomaterials* **29,** 4532–9 (2008).

267. Wang, H. B. *et al.* Creation of highly aligned electrospun poly-L-lactic acid fibers for nerve regeneration applications. *J. Neural Eng.* **6,** 16001 (2009).

268. Sell, S. a, McClure, M. J., Garg, K., Wolfe, P. S. & Bowlin, G. L. Electrospinning of collagen/biopolymers for regenerative medicine and cardiovascular tissue engineering. *Adv. Drug Deliv. Rev.* **61,** 1007–19 (2009).

269. Chainani, A., Hippensteel, K. J., Kishan, A. & Garrigues, N. W. Multilayered Electrospun Scaffolds for Tendon Tissue Engineering 1, *. **0,** (2013).

270. Theisen, C. *et al.* Influence of nanofibers on growth and gene expression of human tendon derived fibroblast. *Biomed. Eng. Online* **9,** 9 (2010).

Acknowledgment:

Now that I am about to finish this chapter of my life and embark upon a new one, I know that I wouldn't stand here without the support of so many people who embraced me in different ways, and I want to thank as many of them as possible. Knowing the fact that in some years from now, I will be probably the only one reading this book, I want to write it the way I like, from the bottom of my heart so that I enjoy reading it all over again…

To my first promoter Prof. Theo Smit: dear Theo, I am so happy that I met you and had a chance to work with you. You have been a very open-minded, kind, and supportive supervisor to me and I appreciate the opportunity and the "believe" you had in me as I could not be able to go through all of this without you. During the past three years, you were more than just a supervisor to me, you were a true friend that I could trust and talk to, and be sure that he understood and cared. I am grateful for your encouraging words "always".

To my second promoter: Prof. Jan Paul Roovers: dear Jan-Paul, thanks for acknowledging my capabilities and knowledge, and giving me a chance to improve them. Working with you, I always had the confidence that I can do better. I admire your intelligence, ambitious attitude and your enthusiasm for getting this project further.

To my TEA-POP teammates: Dr. Manon Kerkhof, Dr. Alejandra Ruiz-Zapata, Prof. Bas Zaat, Dr. Marco Helder, Prof. Hans Bröllman, Chantal D., Payal S., Martijn R. and others. Thanks to all of you for encouraging me and supporting me during my PhD. I learnt a lot from every one of you. Good luck with your careers.

Dr. Behrouz Zandieh-Doulabi: thank you Agha Behrouz for always helping me, with "everything" from the lab experiments to my personal life. Thanks for having us always openly in your house, with your beautiful family and your wife Hedwig, and making us feel at home.

I would like to thank several people in ACTA who welcomed me openly and facilitated my PhD in many different ways. Prof. Gibbs, Prof. Everts, Prof. Klein-Nulend, Prof. Kleverlaan and Prof. Koostra: thanks for your support, comments and guidance. From the OCB-department: Jolanda, Cor, Ton, Teun, Drik-Jan, Ineke, Marion, Gang, Hans, Kamran, thanks for all your support, help, suggestions and your smiles whenever we met in the corridors. I am deeply grateful.

I got to know several nice, enthusiastic, intelligent and helpful PhD students in the past three years that made my path more fun and fruitful: Dongyun, Ceylin, Nawal, Francis, both Anna's, Carolijn, Ernst-Jan, Bas, Hessam, Patrick, and more: Great to know all of you. Ben and Mauenl, thank you for helping me with the microscope, and kindly helping everyone in the lab. Ben, thanks for encouraging me improving my Dutch, heel bedankt! Good luck with your chicken embryos!

I owe at least one paragraph to my roomies, my girls gang: Sara S., Beatriz B., Yixuan C. and Carolijn M.!! I love you sooo much girls! The PhD life would have been less fun without you! I am very grateful that I had the four of you to share my frustrations with, during the difficult times of my life in the past four years. I enjoyed our Friday after-work drinks as much as I did talking to each of you. Thank you girls! Good luck with the rest of your academic and romance life!

To my other, before and after-me, roomies, Thijs DJ., Angela B., Bernt-Jan, Jane, Hong W., Tijmen and Neda, thank you for our office times! Carolijn, thanks for the nice candies you always made for me! And Angela, thanks for helping me with my lab work. Thijs and Sara thanks for being such patient, kind and understanding teachers!! Jullie holp me veel om het Nederlandse taal te leren! Nu, ben Ik blij dat Ik Nederlands met jullie kan praten! Bedankt!

Thanks to my fellow Iranian students in ACTA: Sepanta F., Rozita J., Samaneh Gh., Hessam M., and Fereshteh M. I am glad that we had each other here to speak our language Farsi and share our difficulties to feel less home-sick. Good luck with the rest of your journey.

A special thanks goes to Arie Werner from the materials department of ACTA. Arie, I enjoyed every bit of our SEM sessions and the jokes we made to each other. You are absolutely a kind-hearted and nice man. Thanks for all your help with my SEM experiments.

Thanks to technical people in VUmc; Micha, Danny and Sjoerd for helping me with your technical support. Danny, I appreciate your creativity and responsibility in designing the experimental tools. Also thanks to Koen Van der Laan from Optics11 for helping me with the Piuma experiments.

I feel that I owe a big thank-you word to my former supervisors back in Iran; Dr. Yeganeh. And Dr. Karkhaneh, who always inspired me in my academic and personal life with their great attitudes and motivations. I will be grateful for the rest of my life, as this journey began with your inspirations.

Thanks to all my good friends in Iran, Mahboubeh E., Sara Gh., Nona F., Shadi M., Mojgan A., Mona K., Negar R., Reyhane M., Firoozeh S., Farzaneh M., Farshad H., Babak and Khosro F., and all the others who gave me their precious friendship.

During my life in the Netherlands, I met great people who made my new life happier; very special thanks to my best friends here Shiva S., Sara M., and Nasrin M., who always helped me figure out myself better and supported me all the time; thank you girls for befriending me! And thanks to: Nasim H., Fatima A., Azadeh A., Sepideh Gh., Hossein Kh., Alireza M., Elnaz S., Aida A., Farhad IN., Farzaneh Z., Hadi J., Armaghan, Poolad K. and Shekoofeh, Abdi M., Bahram & Bahar, Nastaran and Ehsan, my housemates Laura P., Gaida S., and Claudia S.; I am happy that we are/were friends.

Special thanks to Babak Loni; I am so lucky that I met you, Babak. Thank you for all your kindness, patience and support during the last years. You have made me a happier and stronger person, and I am deeply grateful for all of it.

This thesis belongs to my family more than it ever does to me, to whom words are certainly not enough!

Maman; my pretty chubby Mom, you are certainly the strongest woman I have ever known in my life. You are truly my everything and my best friend ever. I love you more than anything else in this world, Mom. Me, this book and any other dreams of mine would have never come true if it wasn't for you and your devotions. Thanks for standing by my side in every single step of life, and giving me your unconditional love, friendship and support! You made me the person I am today, Mom! Thanks for the pretty sound of life I experienced next to you!

Baba; thank you Babi for believing in me, trusting me and supporting me in every decision I made. Thanks for teaching me how to look at life, how to be strong and independent and how to not give up when things go rough! Thanks for many different conversations we had that after each, I got more profound and deep understanding of life! I will always be your little Mooshjana…Love you with all my heart Babi!

Jamshid; it's been a big part of my life hearing your voice that call me "Sanjab"!! Thanks for being around when I needed a shoulder to cry on, and loving me no matter what I do. You are the best

part of my childhood, and I will treasure it forever. I always enjoy talking to you, sharing my stories with you and above all, calling you my “best pal”. I am so proud of you!

My best friends, Roshanak Ch. and Yasi Z. Girls, you know how much I love you both! There are no words to say how much you mean to me! You both have always been like a sister to me; a sister I never wished for, as long as I had the two of you! I had the best times at school with you. Thank you for being there for me in the most difficult times of my life and supporting me. You never wanted anything but the best for me! Having you in my life, I always believed in “true friendships”.

Amoo Hasan, Saeed, va Reza, ame Kefayat va Masi, my little brother Arash, Daei Bijan, Behrouz, Behzad, my aunts Farzaneh, Faranak and Lisa! I am so lucky and grateful to have you, such an amazing family! Thank you for loving me, believing in me, forgiving me and making my life worth living! This thesis, beside my cheerful moments, would have never come true without you! And I memorialize my grandparents, Aziz and Aghajoon, who always loved us without asking anything in return. Rest in peace.

To anyone else, anywhere in this world, whom I might have been careless enough not to mention here, who helped me in this journey “life” for becoming the person I am today… a big THANK YOU! **Because me without you, is like a sky without the blue…**

و کلام آخر ....

اوقات خوش آن بود که با دوست به سر شد

باقی همه بی حاصلی و بی خبری بود

مهشید وشاقیان، خرداد ۱۳۹۶

Abbreviations list (alphabetical order):

ANOWA: one-way analysis of variance

α-SMA: alpha smooth muscle actin

COL: collagen

COX: cyclooxygenase

ECM: extracellular matrix

FDA: food and drug administration

HPRT: Hypoxanthine-guanine phosphoribosyltransferase

IL (I,8, β): interleukin

MMP: matrix metalloproteinase

PCL: Poly-caprolactone

PDMS: poly di-methyl siloxane

PET: poly ethylene terephthalate

PLA: poly lactic-acid

PLGA: poly lactic-*co*-glycolic acid

POP: pelvic organ prolapse

PU: poly urethane

RT-PCR: real-time polymerase chain reaction

SD: standard deviation

SEM (±): standard error of mean

SEM: scanning electron microscopy

SUI: stress urinary incontinence

TGF-β: transforming growth factor beta

TNF-α: tumor necrosis factor alpha

YWHAZ: tyrosine 3-monooxygenase/tryptophan 5-monooxygenase activation protein zeta

Publications list:

1. **Towards a new generation of pelvic floor implants with electrospinning: a feasibility study.**
   M.Vashaghian, A.M. Ruiz-Zapata, M. H. Kerkhof, M.N. Helder, J.P. Roovers, T. H. Smit.
   Journal of Neurourology and Urodynamics; published Feb 2016
2. **Electrospun matrices for pelvic floor repair: effect of fiber diameter on mechanical properties and cell behavior.**
   M.Vashaghian, B. Zandieh-Doulabi, J.P. Roovers, T. H. Smit.
   Journal of Tissue Engineering, Part A; published 2016
3. **Cyclic straining of human fibroblasts on electrospun scaffolds enhances their regenerative potential in a new model of pelvic floor loading**
   M. Vashaghian, Chantal M. Diedrich, B. Zandieh-Doulabi, A.Werner, Theodoor H. Smit, Jan-Paul Roovers
   Submitted Feb. 2017.
4. **Biomimetic matrices for pelvic floor repair: *review paper***
   M. Vashaghian, B. Zaat, T. H. Smit, J.P. Roovers
   Journal of Neurourology and Urodynamics; under revision Feb. 2017.
5. **Biocompatibility evaluation of Electrospun Nylon meshes for pelvic floor repair in an abdominal wall mice model**
   Chantal Diedrich, Martijn Riool, M. Vashaghian, T.H. Smit, J.P. Roovers, Bas Zaat.
   (in preparation)

Portfolio:

(Inter)national congresses and events

2013 -European Society of Biomaterials (ESB), Madrid, Spain (poster presentation).

-Annual Meeting of the Netherlands society for biomaterials and tissue engineering (NBTE), Lunteren, the Netherlands (poster presentation).

2014 -Annual Meeting of International Urogynecological Association (IUGA), Washington D.C., USA (poster presentation).

-European Society of Biomaterials (ESB), Liverpool, United Kingdom (oral presentation, best oral presentation award nominee).

-Annual meeting of the MOVE Research Institute Amsterdam, Amsterdam, The Netherlands (attendee).

2015 -Annual Meeting of the Netherlands society for biomaterials and tissue engineering (NBTE), Lunteren, the Netherlands (poster presentation).

-Electrospinning symposium, Geleen, the Netherlands (oral presentation).

-Annual Meeting of the Netherlands society for biomaterials and tissue engineering (NBTE), Lunteren, the Netherlands (attendee).

2016 -World congress of Biomaterials (WCB), Montreal, Canada (oral presentation).

-European Urogynecological Association (EUGA), Amsterdam, The Netherlands (oral presentation, best oral presentation award winner).

-Scientific visit to Tepha Inc., Boston Area, USA.

Awards

Best oral presentation award, EUGA 2016, Amsterdam.

Scientific courses

Characterization methods of biomaterials, TU Delft, 2012.

English Scientific Writing, ACTA, University of Amsterdam, 2015.

Author:

Mahshid Vashaghian was born on January 10th 1987 in Tehran, Iran; where she grew up and studied in the field of biomedical engineering. She graduated in 2008, by when she started her first job in biomedical industry and Iran Institute of Standards for Medical and Pharmaceuticals. In 2010, she moved to the Netherlands to do her master's degree in bioengineering and biotechnology in Technical University of Delft. She graduated in 2012, and shortly after started her PhD in Vrij Univeristy medical center of Amsterdam-Academic Medical Center of Amsterdam, under supervision of Prof. Theo H. Smit on 2013 April. Her PhD dissertation entitled "Nanofibrous matrices for pelvic floor repair" resulted in research publications in different scientific journals. She has presented her research in different national and international congresses and has collaborated with different academic institutes in the Netherlands. She partially worked with the medical device company Tepha Inc. Boston Area, as a scientist advisor for cell-biomaterials research and development. She is currently working in DEKRA-Certification Arnhem, as a medical device expert (auditor), where she pursues her passion about biomaterials and regenerative medicine.